Fushui Liu

CFD STUDY ON HYDROGEN ENGINE MIXTURE FORMATION AND COMBUSTION

Cuvillier Verlag Göttingen

CFD STUDY ON

HYDROGEN ENGINE MIXTURE FORMATION AND COMBUSTION

Master of Science

Fushui Liu

Brandenburgischen Technischen Universität Cottbus

Beijing Institute of Technology

Bibliografische Information Der Deutschen Bibliothek
Die Deutsche Bibliothek verzeichnet diese Publikation in der Deutschen Nationalbibliografie; detaillierte bibliografische Daten sind im Internet über http://dnb.ddb.de abrufbar.
1. Aufl. - Göttingen : Cuvillier, 2004
Zugl.: (TU) Cottbus, Univ., Diss., 2004
ISBN 3-86537-167-1

Nonnenstieg 8, 37075 Göttingen
Telefon: 0551-54724-0
Telefax: 0551-54724-21
www.cuvillier.de

1. Auflage, 2004
Gedruckt auf säurefreiem Papier

ISBN 3-86537-167-1

Preface

The impending worldwide energy crisis, most importantly the potential crisis of fossil fuels, and the ever increasing environmental impacts caused by automobiles have made it a great necessity to find a clean, regenerative energy form for the future. Hydrogen, the most abundant element in the universe, is being regarded as the most appropriate and promising energy carrier.

From this point of view, the German automaker BMW has chosen hydrogen engine as one of their research objects and has entrusted the author with research work on hydrogen injection and mixture formation in engine conditions.

Based on the BMW project, the author takes an ulterior step and lucubrates the combustion characteristics of hydrogen engine. Instead of the routine laboratory work, the whole process, including hydrogen injection, mixture formation, ignition and combustion, was studied by compute simulations with the help of well-known CFD Code AVL FIRE. In order to ensure the simulation results to be reliable, great effort has been put on verification and validation of the Code.

This six-part thesis focuses on the hydrogen direct injection engine and tries to find some general principles to optimize its performance.

Part I analyzes the present problems related to the traditional internal combustion engine, puts forward the hydrogen economy and shows the necessity to develop hydrogen engine.

Part II deals with the Verification and Validation of Fire Code, and proves that FIRE is capable of simulating the supersonic flow in Hydrogen direct injection engine.

Part III studies the influence of many factors on hydrogen injection and mixture formation, and reveals the detailed behavior of the mixture formation process in Hydrogen engine.

Part IV gives detailed analysis of all the available combustion models in FIRE version 8, and concludes that only TFSC model is capable of calculating hydrogen laminar combustion.

Part V investigates the combustion performance on Hydrogen engine at different conditions and gives the general concepts for optimization of NO emission and thermal efficiency.

Part VI makes a summary of the thesis and gives the main conclusions.

Contents

List of Figures and Tables

Part I: Introduction

The invention of the automobile is a critical element of the social, economic, and cultural evolution of human civilization. The most important effect of the automobile's discovery is the fact that the automobile, and other means of transportation which have the combustion engine, increased the speed with which people and goods could be moved over land. This one consequence has led to a dramatic change in automobile economics and style over the course of the twentieth century and reflects the changing trends and scientific knowledge in the automobile industry.

Today … transportation is an essential component of health care, education, employment, recreation, culture, maintenance of ties with family and friends, and all that makes life worthwhile. Transportation is what enables individuals to become full-fledged, participating, contributing members of society and what enables communities to work the way they could and should. In this day and age, and in this society, transportation is a necessity[1].

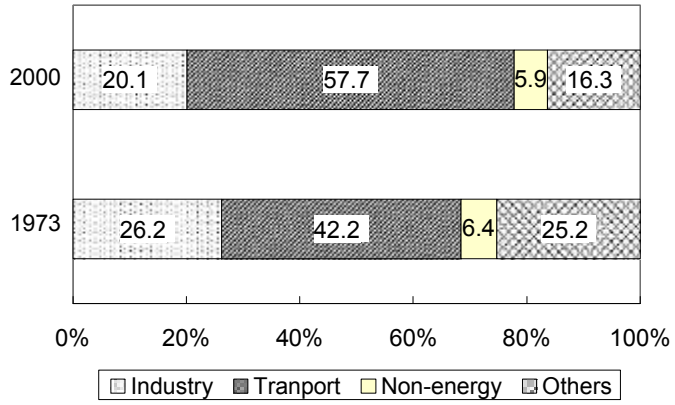

Figure 1-1. Oil Energy Consumption by Sectors in OECD countries

The modern society is to a great extent dependent on combustion. 90% of the world's primary energy comes from combustion of fossil fuels - coal, oil and natural gas[2]. While more than half of the oil is consumed by transportation sectors (figure 1-1).[3] What an important role the transportation is playing for the energy consumption in the whole world!

Engine is the heart of a vehicle. Since almost all transportation modes depend on the internal combustion engine, either fueled with gasoline, or diesel, or kerosene (jet planes), internal combustion engine actually plays the key role in energy consumption and social activities.

1.1 Crisis of traditional Internal Combustion Engines

Over the years, ever since the boom of the industrial age, the advancement in vehicles and automobiles has been tremendous. From the slow and noisy open-air automobiles to the space-aged electric hybrid cars, the advancement of

technology has inspired us to have better and faster engines.

Unfortunately, the traditional internal combustion is facing more and more difficulties.

1.1.1 Pollutions and Greenhouse effect

"Plants and animals that lived ages ago have returned to haunt us with a vengeance. Their incinerated remains pollute both land and sea, and clog the air we breathe. Life from the past now threatens life of the present"4.

In the course of a century, the world's consumption of fossil fuels has grown at an exponential rate, increasing by a factor of 20[5]. This has led to a series of environmental problems such as local air pollution, acid rain, the risk of climatic changes and the release of polluting effluents to the soil and water.

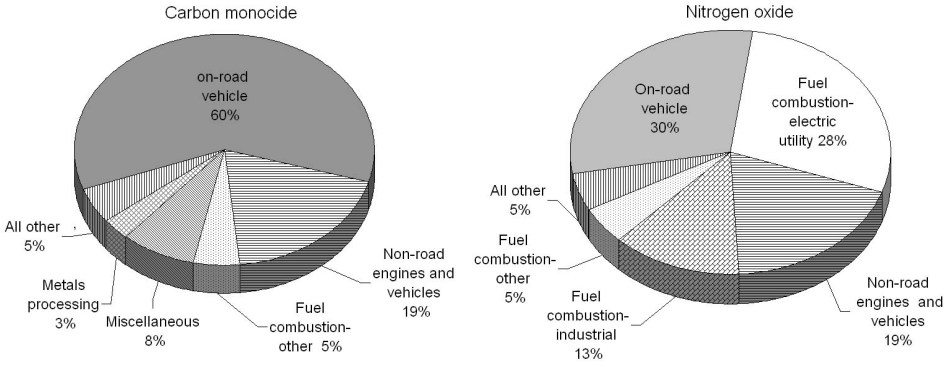

Figure 1-2. General description of sources of the human-caused air pollution

Figure 1-2 gives the general description of sources of the human-caused air pollution[6]. Around 80% of carbon monoxide pollution is produced by combustion engines (including the engines in on-road vehicles and non-road vehicles) and 95% of nitrogen oxide is caused by fuel combustion in all type of engines. It can be concluded that engine is the main source of air pollution.

With the development of engine technology, the injurious pollutant from IC engine might be controlled. But CO_2 emission, which is the fundamental product from fossil oil combustion, could never be significantly reduced in traditional engine. It is just the CO_2 that contributes the most to the greenhouse effect of the earth.

According to research by IPCC (The United Nations Intergovernmental Panel on Climate Change)[7], the concentration of greenhouse gases, especially CO_2, has increased substantially since the beginning of the industrial revolution (Figure 1-3[8]), which leads to the continuous increase of the surface temperature of the earth because the greenhouse gases prevent significant amount of radiation and heat from escaping into space. An increase of 0.6°C of the surface temperature of the earth has been observed over the past 100 years (figure 1-4[9]).

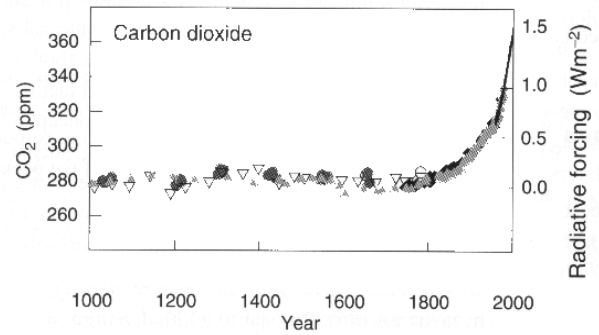

CO_2 concentration in the atmosphere measured in icecores from Antarctic.
(Source: IPCC 2002)

Figure 1-3. Variation of Carbon Dioxide concentration in atmosphere

With global warming emerging, it has led to several chain events such as sea level rising, depletion of the ozone, and having too much radiation in the atmosphere. If the emission of greenhouse gases is not effectively controlled, the problems will be more and more serious.

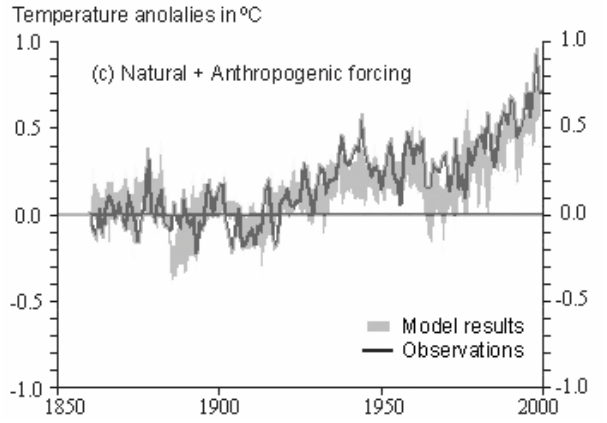

Figure 1-4. Earth's temperature variation in the last century

The world now faces tremendous challenges associated with greenhouse gas emissions, climatic change, and the need for a sustainable development. IPCC has been studying these problems for over 13 years, and a general consensus has been achieved between researchers, industry leaders and politicians that dramatic reductions in greenhouse gas emissions must be achieved in order to prevent man-made climatic changes.

1.1.2 Legislations, cost and taxes

In order to reduce the pollution, the European Union and the EPA in the US have set increasingly demanding standards on the allowable emissions for new vehicles since 1970. Figure 1-5 gives a general impression of the intensity of legislations in European, US and Japan[10].

In order to meet the stricter and stricter legislations, the carmakers must develop more and more new technologies, such as MPI/EGR/GDI/Catalyst for SI Engine,

to reduce the emissions. The application of new technologies has really helped a lot for the reducing of harmful gas emissions.

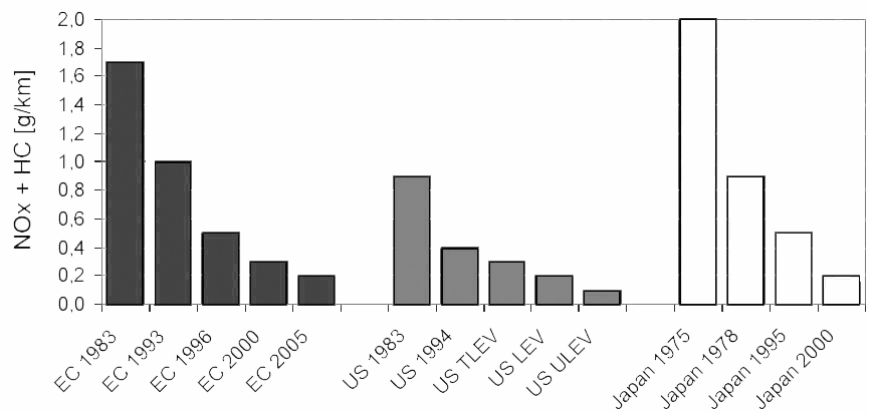

Figure 1-5. Emission Limits in Europe, US and Japan

Since 1987 the level of allowable hydrocarbons emitted is down by 90% with the level of nitrogen oxides decreased by 83% and the level of carbon monoxide decreased by 80%. This significant level of change is expected to continue in future years as public opinion and environmental needs force technology and car design to improve[11].

But the introduction of new technologies also makes the car cost becomes higher and higher. Figure 1-6[12] presents the variation of new car expenditure in USA in the recent 30 years. It gives a very clear impression that the normal consumers are going to carry heavier and heavier burden.

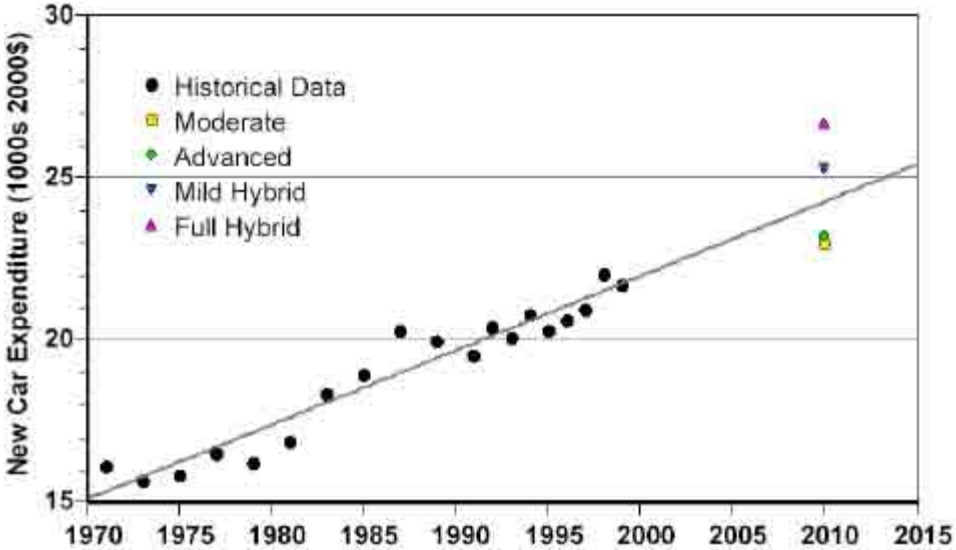

Figure 1-6. Variation of new car expenditure in USA

Although the by-product emissions have been reduced significantly with the development of technology, the amount of carbon dioxide, which is the main cause of greenhouse effect, emitted worldwide has continued to increase. Carbon dioxide is a product of combustion and therefore only is reduced by better fuel consumption, or fuels the engine with carbon-free fuels.

The threatened environmental catastrophe can be avoided only by significant reductions in vehicle-miles, (which people will not accept), or by significantly improved miles/g of carbon dioxide (which fossil fuel technologies are unable to deliver). Only the development of low and zero emission vehicles offer a solution to this logjam and they are required in both the long and the short term.

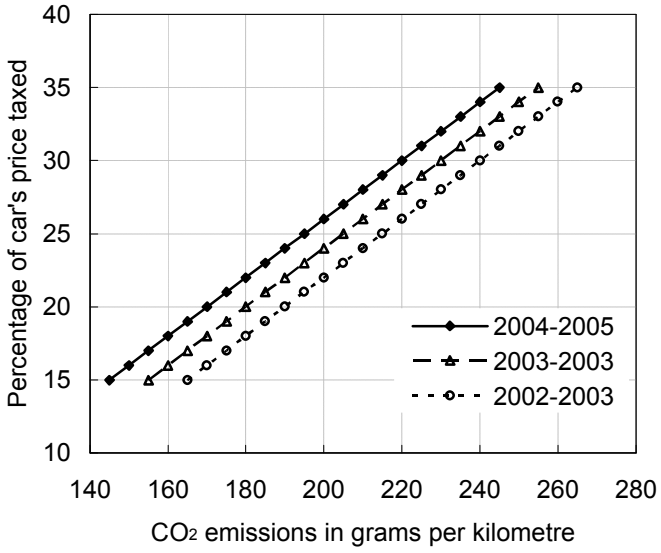

Figure 1-7. Car benefit charges based on carbon dioxide emissions in UK

Two ways are adopted by the developed countries to force both the customer and producer to accept the environmental protect concept:

- To exact CO_2 emission tax. UK is an example country, which has executed this policy since July 2002. Up to 35% of the car price will be taxed for the CO_2 producer (refer to figure 1-7[13]), and the tax will be higher and higher. This policy adds an even heavier burden on normal consumer.
- To force the carmaker to produce CO_2-free products. Table 1-1[14] lists the requirements for manufacturer's fleet sales, which is constituted by California Air Resources Board (CARB). This policy is disgusted by the manufacturers, but will lead the automobile industry into a new phase.

Table 1-1. CARB requirements for manufacturer's fleet sales

Model Year	Conventional vehicle	TLEV	LEV	ULEV	ZEV
1994	90	10			
1995	85	15			
1996	80	20			
1997	73		25	2	
1998-2000	48		48	2	2
2001-2002			90	5	5
2003			75	15	10

1.1.3 Limit of fossil oil

Aside from problems relating to pollution, the limiting supply of natural resources has also come to attention – particularly the oil supply.

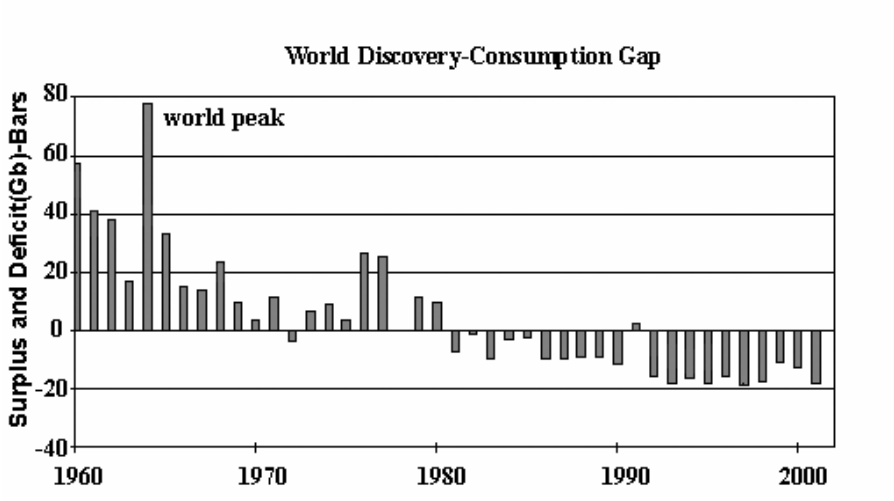

Figure 1-8. World discovery and consumption gap of fossil oil

It appears that total oil discovery in 2001 was about 8 Gb including deepwater oil, and NGL. The world's oil account has been running a deficit since 1981, as it continues to eat into its inheritance from past discovery (figure 1-8[15])

According to the investigations, the ultimate oil production (conventional) in the world is around 1750Gb[16]. If there is no new energy resource, the world's endowment of oil will be depleted in 50-100 years (figure 1-9[17]). Consequently, the oil supply shortfall will trigger the third and permanent radical rise in oil prices.

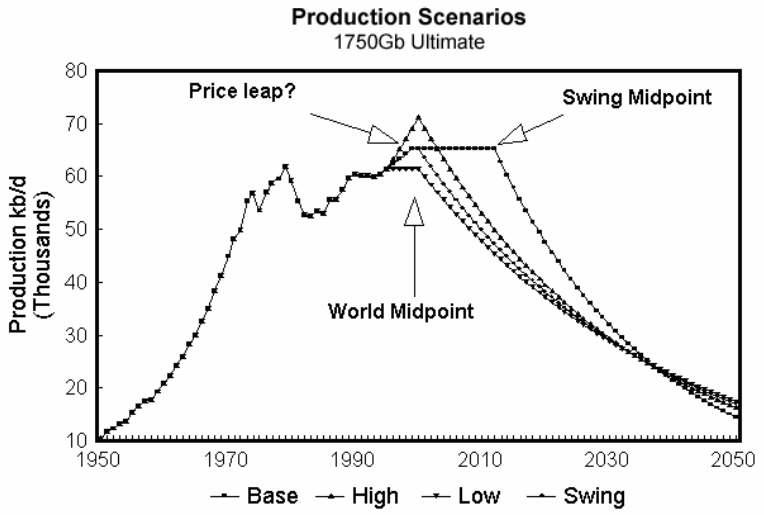

Figure 1-9. The Global Hubbert Peak Forecast of Future Global Oil Output

Summarizing the above three aspects, it can be imaged that that traditional automobile industry is surrounded by so many fatal problems:

- Serious pollution, and consequentially be restricted by
- Strict legislations, which will lead the automobiles become more and more complicated and expensive
- The carmaker and consumer will carry more and more burden of cost and tax.

- The oil resource will be depleted.

Where will the automobile industry go?

1.2 Hydrogen economy

"I believe that one day hydrogen and oxygen, which together form water, will be used either alone or together as an inexhaustible source of heat and light."(From "The Mysterious Island" by Jules Verne, 1874)

Hydrogen is the most plentiful element in the universe, but it is not easily accessible on the earth. Hydrogen is a neutral energy carrier. This means that the environmental benefit of using hydrogen depends upon how the hydrogen is produced. A renewable energy system using hydrogen as a carrier or for energy storage does not result in harmful pollutants being released to the natural environment. It is possible to eliminate the release of pollutants from mobile combustion. If we are to overcome the climatic challenges we now face, the introduction of hydrogen as an energy carrier must surely be a clear presupposition.

1.2.1 Zero emission

The most significant and obvious advantage hydrogen engines have is that it has no negative environmental impact. The government of California considers the hydrogen vehicle as a ZEV or a zero emissions. This means that any vehicle powered by hydrogen fuel has very low or negligible emissions. The only by-products are de-mineralized water, heat, and energy; therefore this may dramatically reduce the problems of urban pollution. When hydrogen is burned the resulting emission has no unburned hydrocarbons, no smoke, no carbon monoxide or carbon dioxide. With this fact, it is obvious that hydrogen cars produce fewer "system-wide" releases of greenhouse gases. From water to mater, Hydrogen can help us to complete a real clean cycle.

1.2.2 Wide Range of Flammability

Hydrogen has a wide flammability range in comparison with all other fuels. As a result, hydrogen can be combusted in an internal combustion engine over a wide range of fuel-air mixtures. A significant advantage of this is that hydrogen can run on a lean mixture. This is why it is fairly easy to get an engine to start on hydrogen.

Generally, fuel economy is greater and the combustion reaction is more complete when a vehicle is run on a lean mixture. Additionally, the final combustion temperature is generally lower, reducing the amount of pollutants, such as nitrogen oxides, emitted in the exhaust.

1.2.3 Recycled Fuel

Hydrogen is found in large amounts on earth bound in organic material and in

water. Over 70% of the earth is covered with water. The percent of hydrogen in water measured by weight is 11.2%. There is definitely an abundant supply. The advantage in using hydrogen as fuel is that, during combustion, it binds itself to the oxygen in the air, and creates water. Hydrogen is therefore totally renewable.

Breaking down water to hydrogen and oxygen is a process that requires energy. If renewable energy is used, the resulting hydrogen will also be a clean and renewable energy carrier. Once obtained, though, hydrogen is an ideal energy carrier—similar to electricity, but more easily stored—and unlike fossil fuels, we will never run out of hydrogen.

Many forms of renewable energy sources such as solar power, tidal waters and wind power cannot provide stability in energy production, and there is often a disparity between the time of production and desired time that the energy is used. Energy systems that are based on these kinds of sources consequently require a means of storing energy, and hydrogen is an ideal energy carrier, especially for automobiles.

1.2.4 High heating value

Pound for pound, hydrogen contains nearly three times more energy than gasoline – that's one of the reasons why it's a superior fuel.

Table 1-2. Comparison of heating values of hydrogen, natural gas and gasoline[18]

Characteristic	Hydrogen	Natural gas	Gasoline
Low Heating value (kJ/g)	120	50	44.5

When Hydrogen is used in airplane as fuel, its advantage is significant. Hydrogen's high heating value reduces the fuel weight by a factor of 2.8, which allows for smaller motors and makes the plane lighter and less noisy.

The world is moving towards a new solar-powered, hydrogen-based economy.

1.3 Application of Hydrogen as Fuel

Hydrogen can be used as a fuel in either Fuel Cells or Internal Combustion Engines.

1.3.1 Fuel Cell

Fuel cell technology had been patented in 1839. It was considered a curiosity by the general public right until the time that it was utilized in space in the 1960s.

Fuel cells have the potential to revolutionize the energy and transportation sectors. In combination with renewable energy, an energy and transportation system could be developed with much less environmental impact than the present day system:

1.3.1.1 Advantages

1). Zero Emission

Hydrogen fuel cell vehicle is considered as a Zero Emission Vehicle (ZEV).

The only by-products from hydrogen fuel cell are de-mineralized water, heat, and electricity; therefore this may dramatically reduce the problems of urban pollution. When hydrogen is burned in the fuel cell (in a flameless process), the resulting emission has no unburned hydrocarbons, no smoke, no carbon monoxide or carbon dioxide.

2). High efficiency

Another advantage is its high fuel efficiency. Fuel cells "extract more power out of the same quantity of fuel when compared to traditional combustion power of gasoline" making it 30% - 90% more efficient than regular gasoline. Peter Hoffman, an editor and publisher of The Hydrogen and Fuel Cell Letter and author of several hydrogen fuel cell related books, argues that the hydrogen fuel cell engines can become more than twice as efficient as internal-combustion engines.

3). Simple structure

Hydrogen fuel cells are also simple in design. They do not contain any moving parts compared to the internal combustion engine.

General Motors unveiled the Autonomy last January 7, 2002, consisting of no pedals and no dashboard. Though investing for the research of the best hydrogen fuel cell vehicle is a hard and risky role, this company took the stand and premiered its first prototype at the Detroit Motor show. It included a "low-slung chassis platform with four wheels attached to it" which gave the skateboard look. Software provides the car with a drive-by-wire control system, which is controlled by the driver from a single control stalk rising from the floor of the car. This eliminates the need for mechanical systems of wires and valves traditionally used to steer, power, and brake, which allows the driver to now sit wherever he or she wants (even the back seat.) It also eliminates the need of an engine compartment in the front since all the vehicle's power train is found in the wheel area. Without these mechanical parts, there is no need to buy motor oil, brake fluids, or transmission fluids[19].

Because of this Simple structure, it allows hydrogen fuel cell cars to have a simpler design, higher reliability, and quiet operation, which is most likely not going to fail.

4). Fast refueling

Hydrogen fuel cell automobiles are more likely considered "advancement to battery powered cars". They may have the advantages of a battery-powered car, but they differ from them because they have the ability to refuel quickly and go

longer between refueling.

1.3.1.2 Present problems

Even though Hydrogen Fuel Cell is very attractive and prospective, there are still some obstacles which will block its wide application in transportation area in near future:

1). High cost

The high cost of fuel cell has been a barrier to further advance in the use of hydrogen fuel cell. The cost of the internal combustion engine is $50 per kilowatt of capacity. The hydrogen fuel cell, however, costs about $1500 – $3000 per kilowatt![20] Hydrogen fuel cells will have to be much cheaper in order for it to be placed into the commercial vehicles.

2). Lack of infrastructure

The lack of infrastructure is another major objection to the use of hydrogen fuel cell vehicles. The absence of "hydrogen filling stations" on every corner would present a problem for the use of fuel cell vehicles. The introduction of hydrogen as a propellant fuel on a larger scale and for the use in private automobiles would require an established infrastructure.

3). Technical problems

There are several types of fuel cells with different characteristics and uses. But, when the detailed techniques are investigated, there are still lots of work to do before Fuel Cell is competitive with the internal combustion engines in the transportation sector. For examples[21]:

- Alkaline fuel cells (AFC) are very sensitive to CO_2. Due to CO_2 is everywhere on the earth, alkaline fuel cells can't be used in vehicle if the shortcoming is not overcame.
- The electrical efficiency of Phosphoric acid fuel cells (PAFC) is relatively low, around 35-45%.
- The Solid oxide fuel cells (SOFC) must operate at temperatures close to 1,000°C in order to achieve enough conductivity. There have been considerable difficulties with materials at this high temperature. Research is being done both to develop new, more stable materials for these temperatures, and to decrease the operational temperature.
- Proton exchange membrane (PEM) fuel cell is considered to be the most prospective, but there are still lots of work to do in order to increase the efficiency, output/weight and output/volume ratios.

Because of the above disadvantages and problems, fuel cells are generally considered to be the ideal device for future transportation, but not today. Then, what should we do now? Should we just sit back and waiting for the

development of fuel cell?

1.3.2 Hydrogen Engine

The extensive development of the IC engines, and the existence of repair and maintenance industries associated with piston engines provide strong incentives to remain with this technology until fuel cells are proven reliable and cost competitive.

In addition, while the fuel cell enjoys high public relations appeal, the present fuel cells seem not offer significant efficiency advantages relative to an optimized combustion system. There are many reasons which will make the Hydrogen Engine much more competent than Fuel cell:

1). Existing industries

Internal Combustion engines have been produced for well over a century, and currently have an established base of sales and service outlets worldwide to efficiently support this technology.

Manufacturers have continually invested in efficiency and reliability gains over this time, and more recently focused on reducing emissions in response to customer demands for a cleaner environment.

The engine industries have been well developed and widely spread all over the world since the first internal combustion engine. From parts manufacture to engine production, from research to repair, vast systems are well established.

The existing industries have a great inertia to keep on combustion engine production. The hydrogen engine gives the engine industries a good opportunity to have a new life.

2). Fuel adaptability

Since there are not enough refueling infrastructures, the application of Hydrogen fuel should start regionally. Hydrogen engine, which is possible to use gasoline fuel, presents a great advantage for the development of hydrogen economy.

The German automaker BMW has equipped their first hydrogen cars with tanks for both hydrogen and gasoline such that the engine automatically changes over from hydrogen to gasoline in the event that the hydrogen tank should run dry. This characteristic makes the hydrogen engine more acceptable than fuel cell to the end user.

3). Low cost

Due to the well-developed IC engine technology and industrial foundations, the hydrogen engine has much more cost competent oven fuel cell, at least in the near future.

4). High thermal efficiency

The theoretical thermodynamic efficiency of an Otto cycle engine is based on

the compression ratio of the engine and the specific-heat ratio of the mixture as shown in the equation[22]:

$$h_{th} = 1 - \frac{1}{(v1/v2)^{g}}$$

Where:

$v1/v2$ = the compression ratio

γ = specific heat ratio of the mixture

η_{th}= theoretical thermodynamic efficiency

The higher the compression ratio and/or the specific-heat ratio, the higher the indicated thermodynamic efficiency of the engine. The compression ratio limit of an engine is based on the fuel's resistance to knock. A lean hydrogen mixture is less susceptible to knock than conventional gasoline and therefore can tolerate higher compression ratios.

The specific-heat ratio is related to the mixture's molecular structure. The less complex the molecular structure, the higher the specific-heat ratio. Hydrogen has a much simpler molecular structure than gasoline and therefore the specific-heat ratio of hydrogen-air mixture is higher (γ = 1.4) than that of conventional gasoline-air mixture (γ= 1.1).

Ford has unveiled a direct-hydrogen ICE concept car, which it plans to introduce by 2006. This concept-vehicle, the P2000 H21CE, is equipped with a version of the Ford Focus 2.0-liter Zetec gasoline-engine that has been modified to use hydrogen. Ford says that hydrogen improves the internal combustion engine's efficiency by 25 to 30 percent[23]. This value shows the similar efficiency as that of fuel cells.

5). Extreme Low emission

Theoretically, the only by-product emission from the Hydrogen engine is NOx. But the NOx emission can be tremendously reduced by lean combustion. Considering part of the lubricating oil will be burned, there will be a little COx or particles in the exhaust gas. With careful design, the harmful gas emission can be neglectable.

The Ford Model U Concept is propelled by an internal combustion engine (ICE) that's optimized to run on hydrogen fuel instead of gasoline. The engine is supercharged and inter-cooled for maximum efficiency, power and range. Its emission of all pollutants, including carbon dioxide, is nearly zero[24].

Therefore, Hydrogen engine, with both the advantage of clean-recycle fuel and advantage of well-established industrial foundations, will have a great vitality and will be a big competitor to the fuel cell in the near future.

1.4 Object of the Thesis

There are existing theories for the design and modification of traditional engines. But, due to the special performance of Hydrogen fuel and the short period of development, there still not be complete theory for the optimum design of Hydrogen engine. It is necessary to study the general characteristics of hydrogen engine in order to get the best performance with least emission.

Based on the above situations, this thesis will focus on the Hydrogen Direct Injection Engine, with the help of CFD tool-ALV FIRE, research the mixture formation, ignition and combustion process in order to find some clues to optimize the mixture formation and combustion process.

---

[1] *Transportation and Society - The Role of Values, http://www.druglibrary.org/schaffer/Misc/driving/s1p4.htm.*

[2] *World energy outlook 2000, http://library.iea.org/dbtw-wpd/textbase/nppdf/free/2000/weo2000.pdf*

[3] *Transportation and Energy, http://people.hofstra.edu/geotrans/eng/ch8en/conc8en/ch8c2en.html#1*

[4] *http://gtalumni.org/StayInformed/magazine/fall91/hydrogen.html*

[5] *Bellona Report 2002 Hydrogen-Status and possibilities.*

[6] http://geography.uoregon.edu/shinker/geog101/lectures/lec02/lec02_figs/human-caused-air-pollution-and-sources-fig3-10.gif

[7] *Climate Change 2001, IPCC Third Assessment Report, 2001.*

[8] *Climate Change and Biodiversity, Intergovernmental Panel on Climate Change, 2002.*

[9] *Climate Change 2001, IPCC Third Assessment Report, 2001.*

[10] *Horst Preschern and Kurt Engeljehringer, 2001.*

[11] *http://students.bath.ac.uk/en1wros/Government.htm*

[12] *John M. DeCicco, 2003.*

[13] *Data for this graph come from Tax Issues - Reform of Company Car Tax, www.ovl.co.uk/tax_company2.htm*

[14] *René Kemp, 2002.*

[15] *The Coming Global Oil Crisis, http://www.oilcrisis.com/*

[16] *C. J. Campbell, 1996.*

[17] *The Coming Global Oil Crisis, http://www.oilcrisis.com/*

[18] *Bellona Report 2002 Hydrogen-Status and possibilities.*

[19] *Forsythia Igot, 2002.*

[20] *Forsythia Igot, 2002*

[21] *Bellona Report 2002 Hydrogen-Status and possibilities.*

[22] *Andre Lanz, et al., 2001. The orignal book gives the definition "g = specific heat ratio of the fuel". Here, the definition is modified to "g = specific heat ratio of the* ***mixture****" by the author.*

[23] *Thammy Evans and Peter Light, 2001.*

[24] *http://www.ford.com/en/innovation/engineFuelTechnology/hydrogen-Internal- Combustion.htm*

Part II: Basic Research on FIRE Simulation

2.1 Introduction

In order to optimize combustion processes, engine designers have traditionally undertaken manual engine modifications, conducted testing, and analyzed the results. This iterative process is painstakingly slow and costly and does not lend itself to identifying the optimal engine design specifications.

In response, scientists have developed several Computational Fluid Dynamics (CFD) modeling codes that can simulate the in-cylinder processes of heat engines. AVL FIRE is one of the most outstanding codes, which is specially developed for IC engine simulation.

The majority of the research work in this thesis is accomplished with the help of AVL FIRE.

Most of the CFD simulations are carried out in three steps: Pre-processing, Number crunching and post-processing. Figure 4-1 gives a general explanation of an entire simulation process with AVL FIRE.

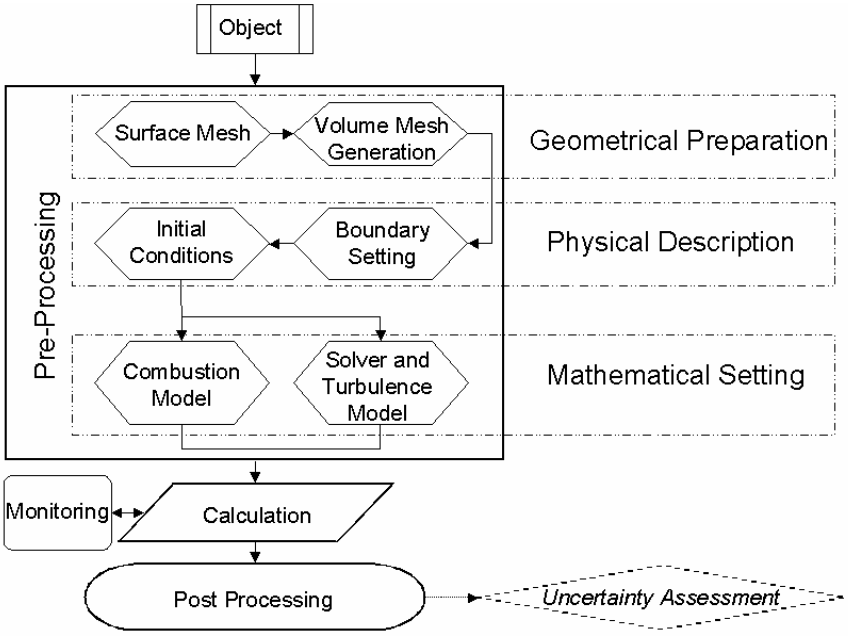

Figure 2-1. General Simulation Flowchart for IC Engines with AVL Fire

Pre-processing is normally the most important portion in CFD process, which determines the reliability of the simulation result.

- **Mesh generation** (including mesh movement information) will be the most time consuming step. The Mesh/Grid distribution will significantly influence the calculated flow distribution as well as the calculation time.
- **Initial and boundary conditions** should be described according to the

real situation of the researching object, which will directly influence the final result, especially for reaction flow.

- There are several **turbulence models** available in FIRE version 8, such as k-ε model, RSM, AVL-HTM. Theoretically, different turbulence models are suitable for different situations, but to find a suitable turbulence model for a specific problem is really a tough question and need lots of experience.
- **Combustion model** selection is very important for reaction flow simulation. Different combustion has different property. The selection of combustion model is definitely lying on one's understanding of the models.

It has to be kept in mind that a single, minor mistake in the above steps may cause significant error. "It is easy to make a simulation, but difficult to get reliable result"!

This chapter will discuss some of the main issues, which may influence the reliability of the simulation result. The discussion is largely based on FIRE application, but is also referential to other CFD Codes.

Corresponding experiments have been adapted to validate the reliability of the simulation results.

2.2 General approach to reliable simulation

Computational Fluid Dynamics has already demonstrated its capability to produce solutions of various complex flows of practical interest. Nowadays, the question is not so much: can a numerical simulation of this flow be made, but rather: is the solution reliable enough? Therefore CFD has reached a stage where it is important to be able to quantify the uncertainty of the predictions, or to make sure that they can be used with sufficient confidence.

Error quantification in CFD involves two stages: Verification and Validation (V&V). The AIAA definitions of Verification and Validation[1], are:

- Verification: The process of determining that a model implementation accurately represents the developer's conceptual description of the model and the solution to the model.
- Validation: The process of determining the degree to which a model is an accurate representation of the real world from the perspective of the intended uses of the model.

There are lots of theories to deal with the verification and validation in CFD applications, and the methodology is almost completely established. Therefore, this thesis will not study the detailed Verification and Validation theory, but discuss some fundamental techniques in FIRE application in order to ensure that the simulation results be reliable.

To make efficient error assessment is greatly dependent on the experience as well as the knowledge of the user. Generally, FIRE simulation result should be assessed in the following steps:

(1). Grid convergence study

As the grid is refined (grid cells become smaller and the number of cells in the flow domain increase) the spatial discretization errors should asymptotically approach zero, excluding computer round-off error.

There is a balance of result accuracy and time consumption. The available computer capability will also limit the balance. How fine the grid will be should be dependent on the focus of the task. Therefore, the result of the balance should be that the mesh should have the minimum number of cells but ensure acceptable accuracy.

(2). Y plus

Y plus or Y^+ is a special CFD scalar, which reflects the turbulent intensity and length scale near a physical wall. CFD results are dubious where the local y^+ parameter varies outside of the range 30 to 1000[2].

Ideally the height of wall elements should be adjusted so that y^+ is kept as close as possible to 300, but this is not possible without knowing the results of the simulation a priori. An ideal model would involve adaptive meshing, where wall element thickness would be adjusted during the solution of the problem. Unfortunately there is no such function in present FIRE Versions. Therefore, the mesh should be modified manually when the y^+ is too high or too low.

(3). Temporal Convergence study

Time-accurate simulations involve taking discrete time steps. One must examine the sensitivity of the simulation results to the magnitude of the time step. The effects and possible errors are usually related to the time filtering of various time scales existing in the unsteady flow field.

Fire simulation result is, to some extent, dependent on the time increment for transient flow, especially for reaction flow. Therefore, the comparison calculations must base on the same time increment.

Generally, smaller time increment will help the convergence of a calculation. But too small time increment will not only significantly increase the calculation time consumption, but may also increase the round-off error.

The practical method is to choose the maximum time increment, which should be able to reflect the interested variation of the flow.

(4). Iterative Convergence

Convergence of the segregated solver is measured by the relative difference from iteration to iteration. A relative error of velocity $||u_i-u_{i-1}||/||u_i||$ is assessed at each outer iteration for each field variable u_i (u, v, w, p, k, e). Notation $||u_i||$ indicates the magnitude or norm of a particular field variable vector. Normally,

all field variables should converge below the given criteria before the maximum Iterations.

The default convergence criterion in FIRE version 8 is 1e-4 and the default maximum iteration is 1000. Some of the convergence criterions, such as momentum and pressure, should be smaller for very sensitive situations. Normally, all calculations will get converged before 1000 iterations. Therefore, there is no necessity to change this number.

Occasionally unconverged (the residual oscillates in certain range, neither converge to the given value nor diverge) steps may be acceptable at the starting of the calculation. An unconverged step during the calculation will cause significant accumulated error, which will lead to wrong result even calculation diverged.

(5). Observation and analysis

The mid-term results should be observed and analyzed according to one's knowledge and experience. For example, the flow in a duct should maintain mass conservation through the duct. Further total pressure recovery in an inlet should stay constant or decrease through the duct.

(6). Validation by Benchmark experiment data

To validate the simulation result with benchmark experiment data is the most effective method. In fact, it is the most frequently used method in IC engine simulations.

Either the initial/boundary conditions or/and turbulence/combustion models or control parameters should be adjusted according to the validation result.

(7). Examination with present theory

All the calculation results should be accordant with the present theories. Unreasonable phenomenon must be analyzed with great care.

For some extreme conditions, it is not possible to make benchmark experiment. The calculation result can only be checked with theoretical analysis.

2.3 FIRE V&V study on supersonic gas injection

Since in cylinder hydrogen injection is a typical supersonic process, the supersonic flow simulation must be discussed in order to correctly describe the mixture formation process in a hydrogen engine.

Some of the basic V&V steps will be studied in detail in this section to ensure the accuracy of later simulations.

2.3.1 A supersonic air-injection experiment

The experiment[3] condition is described in Figure 2-2a, and the schlieren density graduate of the flow field is shown in figure 2-2b.

The shock surfaces and the flow contour are clearly shown in the picture. This

information will be used for the validations in the following parts.

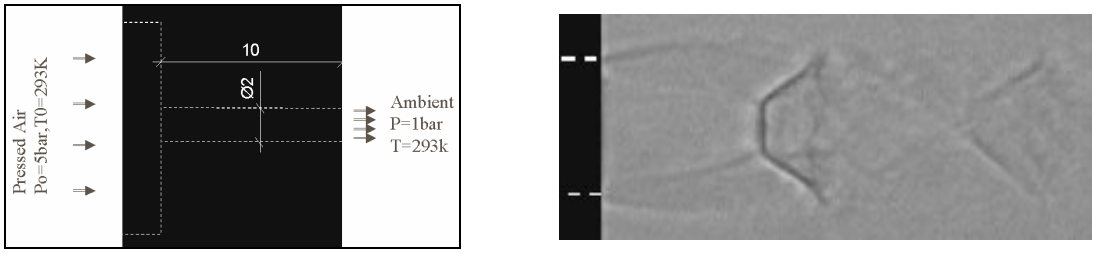

(a) Experiment condition (b) Density graduate

Figure 2-2. Supersonic air-injection experiment setting and result

2.3.2 Spatial discretization

Three meshes (figure 2-3) are generated to simulate the example model:

- *Fine mesh:* with round about 10,000 cells and extreme fine grid near the outlet port, this mesh can capture the shock position as well as contour exactly.
- *Rough mesh:* with round about 3000 cells, the grids are relative equally distributed.
- *Medium mesh:* with almost the same number of cells as the rough mesh, but the grids are much finer near the outlet port, and the boundary layers are also refined.

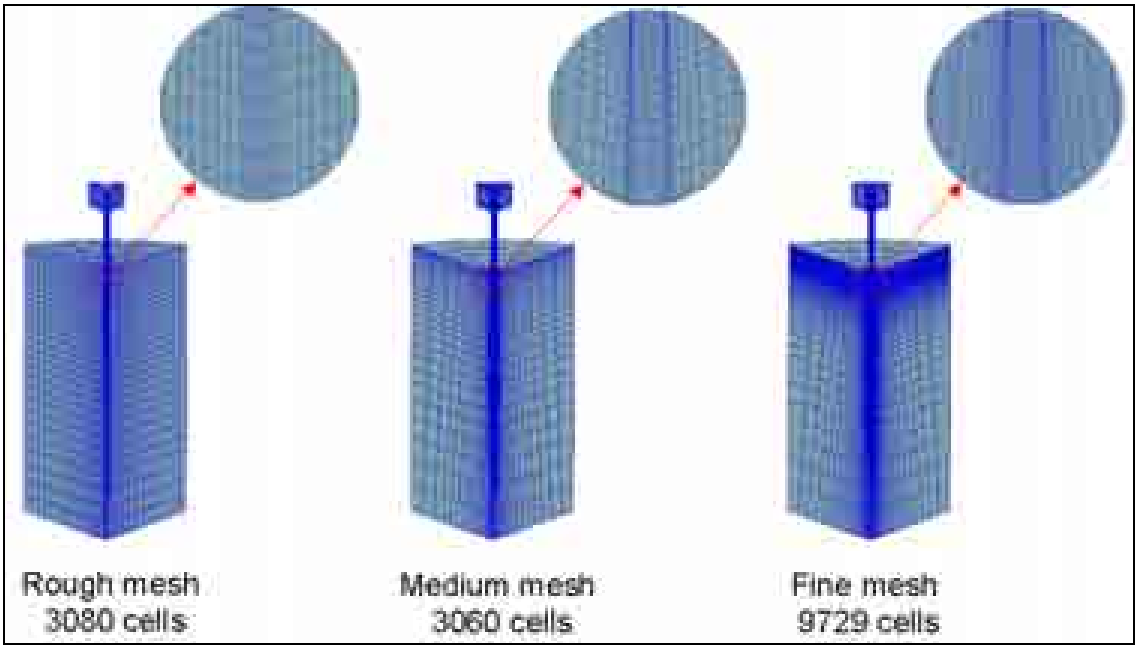

Figure 2-3. Meshes for grid convergence study

Figure 2-4 shows the comparison of the calculated velocity fields with the three meshes. The rough mesh can neither capture the shock nor simulate the right flow contour, while the medium mesh, with the same number of cells as the rough mesh, can get the similar flow contour as the fine mesh and be able to capture the first shock surface.

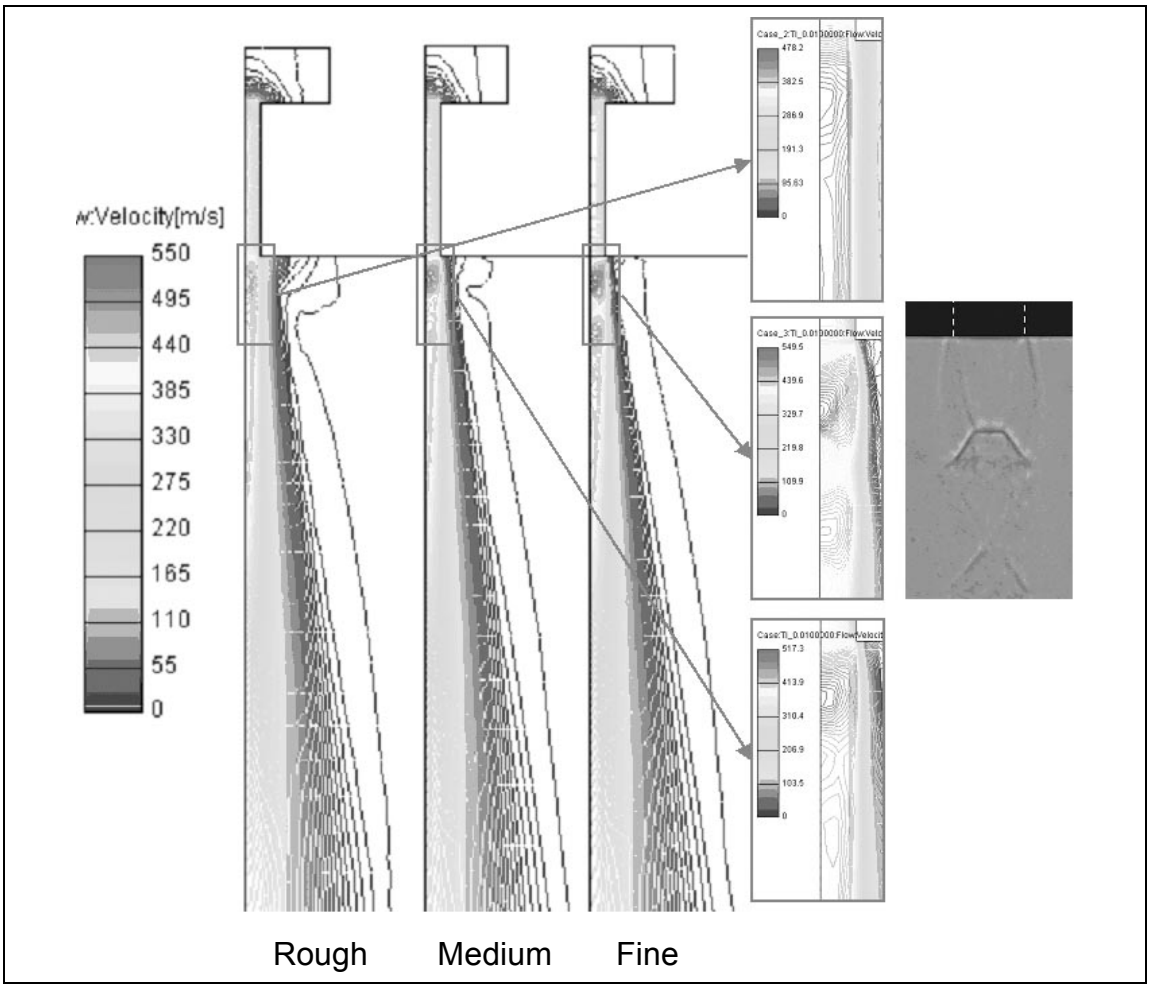

Figure 2-4. Comparison of the calculated velocity fields with different meshes

Figure 2-5 presents the variation curves of inlet mass flow and mean turbulence kinetic energy of the three models respectively. Table 2-1 gives the comparison at 5 ms. Both figure 2-5 and table 2-1 show that the medium mesh will get the similar result as the fine mesh, but the rough mesh will cause non-negligible error.

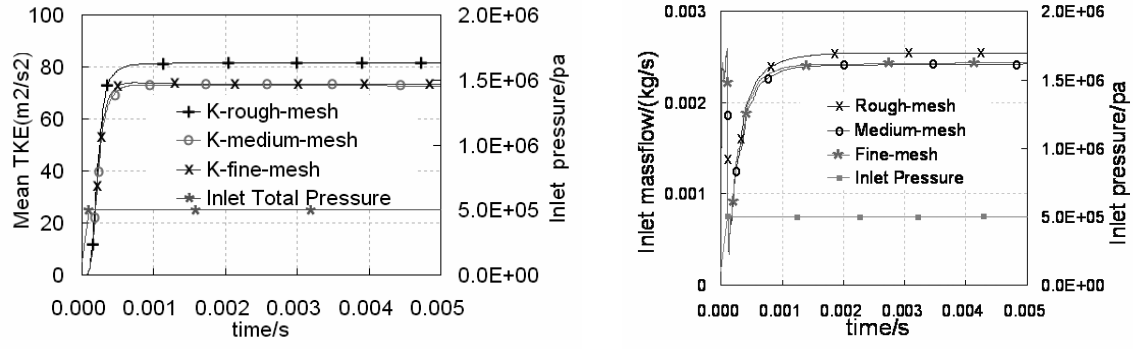

(a). Mean TKE (b). Inlet mass flow

Figure 2-5 Variation of Mean TKE and inlet mass flow with different meshes

Since the inlet mass flow and the stream contour are the most important characteristics in the mixture formation process in a hydrogen engine, the

medium mesh will be suitable for hydrogen engine simulation.

Table 2-1. Comparison of inlet mass flow and mean TKE in different meshes

	Fine mesh		Rough mesh		Medium mesh	
	Value	Error/%	Value	Error/%	Value	Error/%
Inlet mass flow/(kg/s)	0.00244317	-	0.002545	4.2	0.002425	-0.7
Mean TKE	73.2463	-	81.6022	11.4	72.704	-0.7

Notes: (1). The values are compared at 5 ms.

(2).”Error” means the difference from the value of the fine mesh.

In addition, this study gives the idea that the grid near the outlet port should be very fine, while in other area can be relatively rough, according to the gradient of the characteristic parameter, in order to reduce the number of cells.

2.3.3 Time increment

Time Increment selection is the headmost question for time-marching problems. Generally, the smaller the time increment is, the easier the calculation get converged, but the more calculation time will be consumed. This part will discuss the influence of time increment in detail.

The inlet boundary is set to be total pressure, which will increase linearly from 100 kpa to 500 kpa during 0 to 0.1 ms, then keep to be 500 kpa (refer to figure 2-6). Therefore, it is a typical time-marching problem during 0 to 0.1 ms. The flow will converge to steady state gradually after 0.1 ms.

With the medium mesh, the temporal effect is studied with different time increment (2e-8s, 5e-8, 1e-7s, 5e-7s, 2e-6s, 5e-6s, 1e-5s, 2e-5s). Here will only compare the results from the last 4 cases (2e-6s, 5e-6s, 1e-5s, 2e-5s) in order to simplify the analysis.

2.3.3.1 Influence on final result of a steady flow

Table 2-2 gives the comparison of maximum velocity and the minimum temperature in the whole domain at 10 ms, when the flow has almost converged to steady state. The differences among all calculations are less than 0.3%. This table gives a strong impression that time increment has very little influence on the final results.

Table 2-2. Comparison of maximum velocity and the minimum temperature at 10 ms

dt/s	2e-6s		5e-06s		1e-05s		2e-05s	
	Value	Error/%	Value	Error/%	Value	Error/%	Value	Error/%
Max. Velocity/(m/s)	516.71	-	517.04	0.06	517.33	0.12	517.58	0.17
Min. Temperature/K	160.62	-	160.45	-0.11	160.3	-0.20	160.17	-0.28

Notes: (1). The values are compared at 10 ms.

(2). “Error” means the difference from the value with dt=2e-6s.

2.3.3.2 Influence on dynamic performance of a transient flow

When the transient behavior is analyzed, the difference emerges. Figure 2-6 shows the calculated mean pressure during the development of the flow. It gives a clear trend that the bigger the time step is, the more dynamic information will be filtered. Therefore, when the dynamic performance of a time-marching problem is focused, the time increment must be small enough.

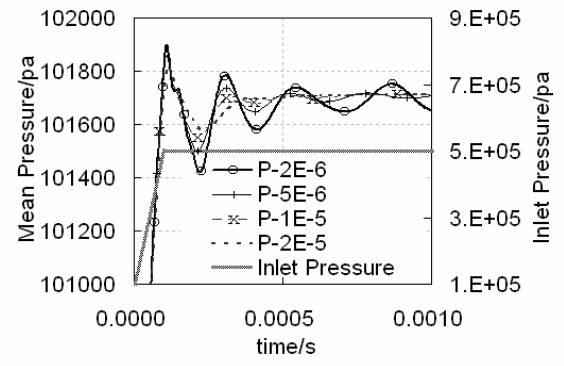

Figure 2-6. Variation of Mean Pressure in transient flow

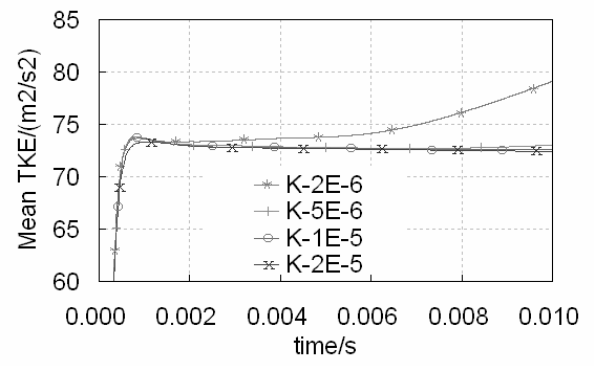

Figure 2-7. Variation of Mean TKE in transient flow

2.3.3.3 Influence on Turbulence kinetic Energy

Figure 2-7 shows the simulated variations of mean Turbulence Kinetic Energy with different time increments. It gives strong evidence that the final TKE magnitude is dependent on the time increment, rather than the boundary conditions. It will be discussed later that TKE influences the reaction process of a reaction flow significantly (refer to PART IV). Therefore, one must pay much attention to select a proper time increment for reaction flow simulation.

2.3.4.4 Influence on Calculation time

Figure 2-8 gives a comparison of the normalized calculation time with different time increment.

Figure 2-8(b) compares the consumed CPU time and I/O time up to 50 ms, when the flow has converged to steady state and all of the main parameters have almost converged to fixed values. This figure gives a rough idea that the bigger the time increment is, the less time will be consumed. But too bigger time increment, say bigger than 2e-5s, will no more same time consumption since it needs more internal iterations to converge to the given Convergence Criterion. The analysis of figure 2-8a helps to explain this phenomenon.

Figure 2-8(a) compares the consumed CPU time and accumulated iterations from 0 to 0.2 ms, during which the flow behaves as typical dynamic process. Since the smaller the time increment is, the easier the calculation get converged in every time step, the accumulated CPU time and Iterations are almost the same for the calculation of this violently dynamic process.

Furthermore, the underrelaxation factors must be carefully adjusted to avoid divergence when the time increment is too big.

Summarizing the above analysis, it can be concluded that:

- Smaller time increment, say 2e-6s or even smaller, should be selected for dynamic process simulation in order to get better convergence and capture the transient behavior.
- Bigger time increment, say 1e-5s or bigger, can be adopted for the simulation of steady flow or relatively gentle dynamic flow in order to save CPU time as well as disc space.

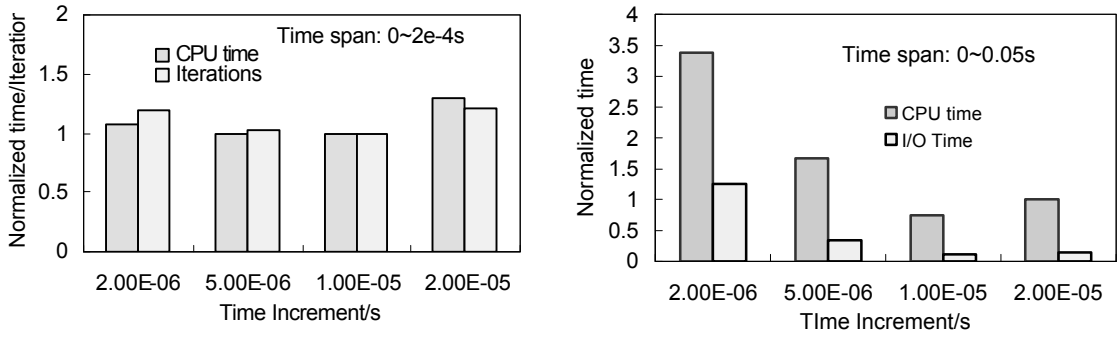

(a). Transient flow (b). Steady flow

Figure 2-8. Comparison of CPU time and iterations under different time increments

It is always efficient to used different time increments, smaller at the beginning and bigger after, for a time-marching problem.

2.3.4 Convergence Criterion

The default setting of Convergence Criterion in FIRE version 8 is 1e-4 for all parameters. It is acceptable for steady flow simulation. But the Criterion should be stricter for transient flow simulations.

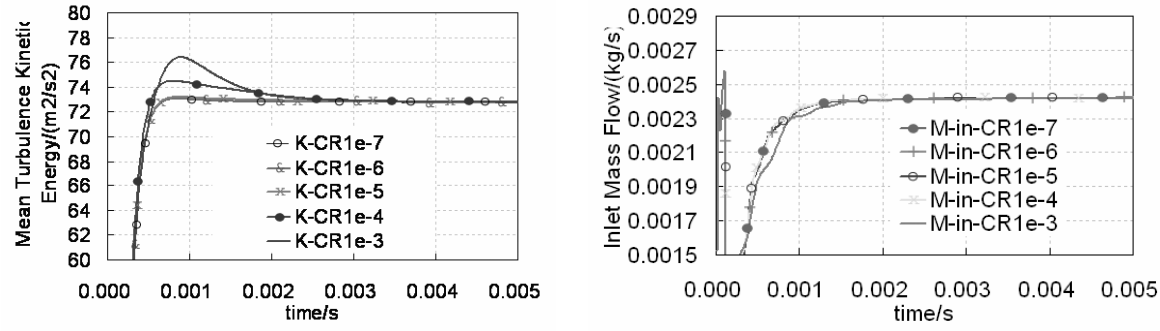

(a). Mean TKE (b). Total inlet mass flow

Figure 2-9. Comparison of flow performances under different convergence criterions

Figure 2-9 gives the comparison of the TKE and mass flow with different convergence criterions. All of the cases are calculated with the same time

increment of 1e-5s.

During the dynamic phase (0-2ms), most of the parameters, especially mean TKE and mass flow, have obvious difference when the convergence criterion is bigger than 1e-5. When the criterion is less than 1e-5, the results are almost the same. That is to say, it is necessary to set the convergence criterion to be 1e-5 or less for transient flow simulation.

After 2ms, all parameters will converge to fixed values no matter how much the convergence criterions are. In other words, the convergence criterion can be relaxed for steady flow simulation.

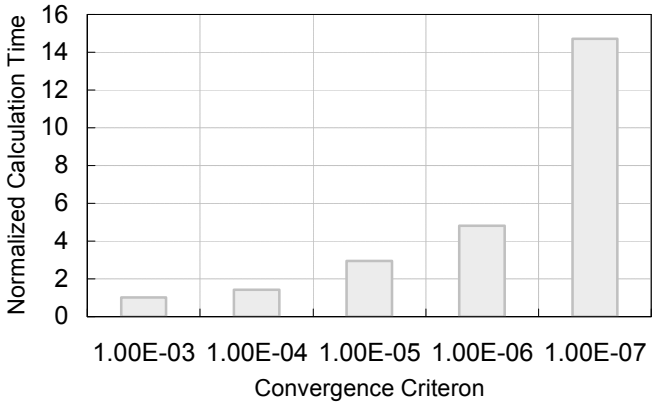

Figure 2-10. Comparison CPU times under different convergence criterion

The normalized calculation times are shown in figure 2-10. The consumed CPU time will increase sharply with de decrease of the value of Convergence Criterion.

Therefore, when convergence criterion is set to be around 1e-5, the calculation will get accurate result with relatively less CPU time. This value will be used for transient and reaction flow calculations in the following studies.

2.3.5 Turbulence Model

There are several turbulence models available in Fire version 8, such as k-ε, AVL-HTM and RSM.

The k-ε model is the most widely used first order, two-equation turbulence model. It is numerically robust and has been tested in a broad variety of flows, including heat transfer, combustion, free surface and two-phase flows. It is generally accepted that the k-ε model usually yields reasonably realistic predictions of major mean-flow features in most situations. It is particularly recommended for a quick preliminary estimation of the flow field, or in situations where modeling other physical phenomena, such as chemical reactions, combustion, radiation, multi-phase interactions.[4]

The RSM (Reynolds Stress Model) belongs to second order models, which offer opportunities to better capture the physics of various turbulence

interactions

Figure 2-11 compares the velocity fields, which are calculated with k-ε model, HTM model and RSM model separately. Both HTM model and RSM can capture the separation phenomena reasonably, but there is not so clear separation when k-ε is used.

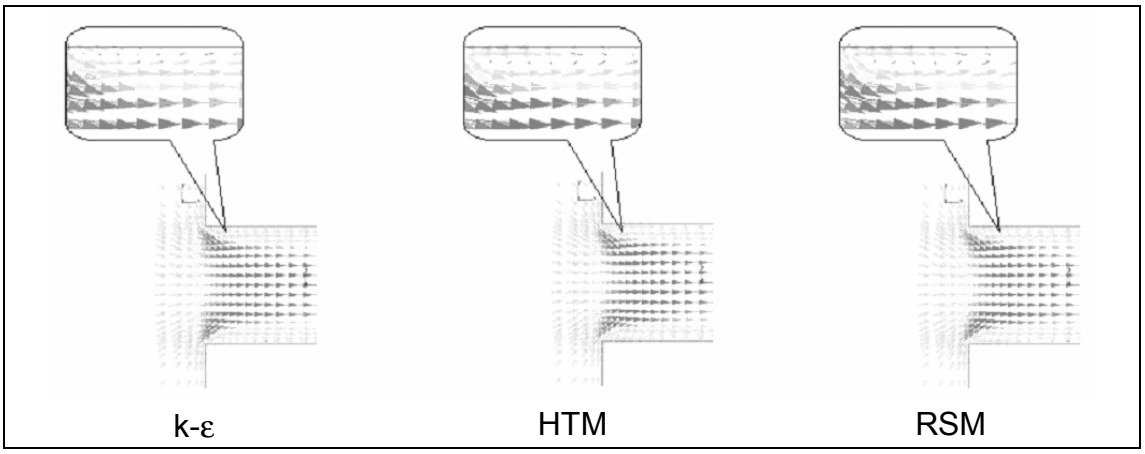

Figure 2-11. Comparison of velocity fields with different turbulence models

However, the second order models do not always show an indisputable superiority over k-ε model. One of the reasons is that more terms need to be modeled. The advantages may be annulled if some of the terms are modeled inaccurately.

Figure 2-12 gives an example that the RSM models are possible to converge to a wrong result, and finally lead to the calculation diverged. Since RSM model have very high requirement to the mesh quality and to the calculation setting, it is not recommended to use this model unless it is necessary.

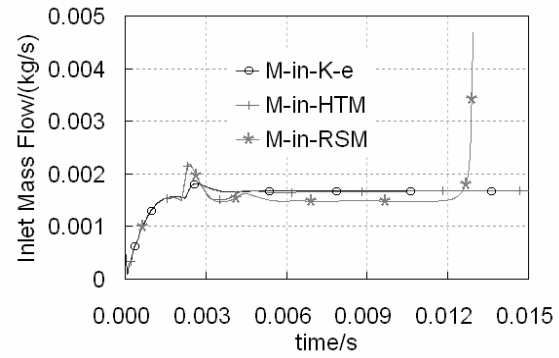

Figure 2-12. Comparison of stability of different turbulence models

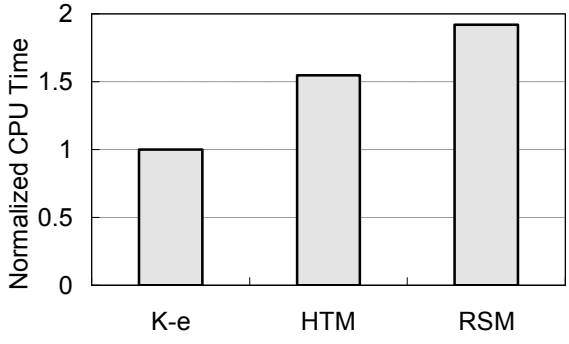

Figure 2-13. Comparison of CPU time of different turbulence models

The AVL-HTM is a hybrid of k-ε model and RSM model. The hybrid turbulence model (HTM) greatly improves results compared to its standard k-ε counterpart (figure 2-12). On the other hand, this approach improves significantly the convergence rate in comparison to the Reynolds-stress model (figure 2-13).

The use of RSM and AVL-HTM models put higher demands on computing resources. Figure 2-13 gives a rough impression that the RSM will consume roughly twice the CPU time as the k-ε model. The HTM models rank in the middle.

In addition, neither RSM nor HTM turbulence model can be used from the beginning of the calculation, because it needs some solution to calculate further. The only way is to activate k-ε model for the first few time steps and then restart with RSM/HTM turbulence model.

Based on the above analysis, k-ε will be used for most of the calculations in order to reduce CPU time and get stable calculation. HTM model will be used in the case, where dynamic performance of the flow is focused.

2.4 FIRE Validation with hydrogen injection experiments

In order to successfully simulate the mixture formation process in the Hydrogen Engine, a series experiments have been done to validate FIRE capability on Hydrogen injection[5]. Correspondingly, all of the experiments have been simulated with AVL FIRE. The simulation results show very good agreement with the experiment results.

2.4.1 Experiment on H2 Injection

With the help of Schlieren technique, the whole Hydrogen injection process is photographed at different time. A group of pictures will reflect the stream contour, penetration and mixture density distribution at different time.

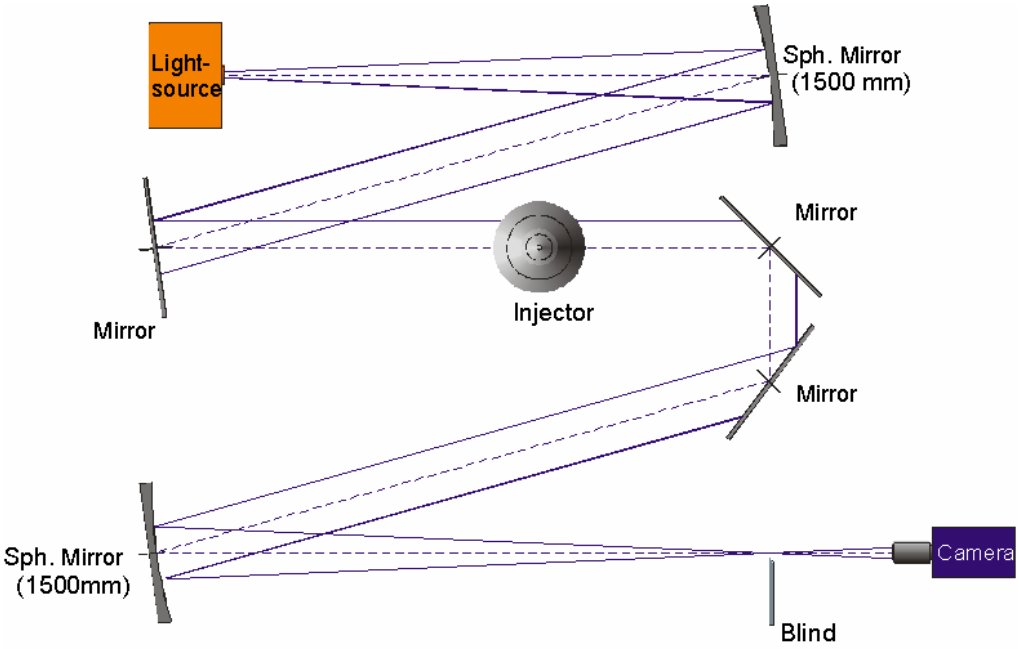

Figure 2-14. Illustration of hydrogen injection measurement system

The measurement system is illustrated in figure 2-14. The radial Light from flashlight is collimated by a spherical mirror. The parallel ray paths through

the Injection zone and be refracted by the Hydrogen stream. Focused by another spherical mirror, the image is received by a CCD Camera. By synchronizing the flash and shutter timing, series of images is photographed at setting time.

(2) Research Objects

Three injectors are used to make the experiment. They are name:

(a). One-hole without tube

(b). One-hole with tube

(c). Ten-holes with tube

Figure 2-15 shows the diagrams of the injectors.

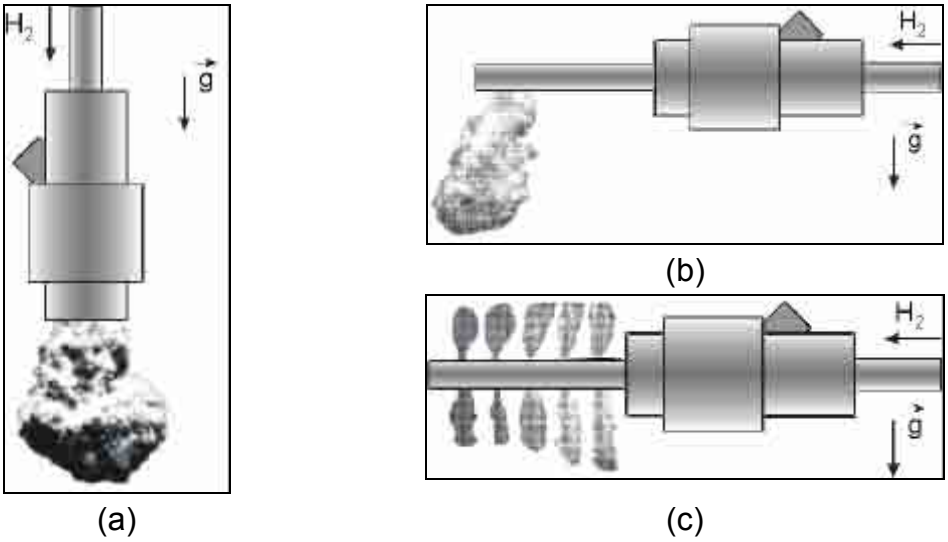

(a) (b) (c)

Figure 2-15. Diagrams of injectors in the experiments

(3) Parameters Setting

Table 2-3 lists the experiment setting: the valve rises to wide-open position in around 2.3ms, then keeps wide open till 6.3/6.4ms. All of the picture are photographed during the opening and wide-open period. Hydrogen is supplied from a 3-bar source.

(4) Measurement Results

The measurement results are series of Schlieren photographs, which reflect the density gradients at specific time. The dynamic injection processes are clearly recorded in these pictures.

Table 2-3. Parameter setting in experiment

Type	Without-tube			One-hole with tube			Ten-holes with tube		
Timing /ms	Open	Close	Temp./K	Open	Close	Temp./K	Open	Close	Temp./K
	2.30	6.34	294	2.28	6.46	294	2.30	6.44	294

2.4.2 FIRE Simulations

With the given boundary conditions, the three experiments are simulated with AVL FIRE version 8.2.

2.4.2.1 Simulation setting

All the simulations are modeled with the same setting:

- Convergence Criterion: 1e-5
- Time increment: 2e-7s x 50 steps, 5e-7s x 40 steps, 2e-6s x 40 steps, then 1e-5s
- Turbulence Model: k-ε
- Mesh: similar as the above medium mesh

2.4.2.2. Result and comparison

(1). One-hole without tube

Figure 2-16 shows the simulated hydrogen distribution at the beginning of the injection, while the stream varies the most seriously. The Schlieren photos at corresponding moment are also presented for comparison. The simulation results show very good agreement with the measurement ones.

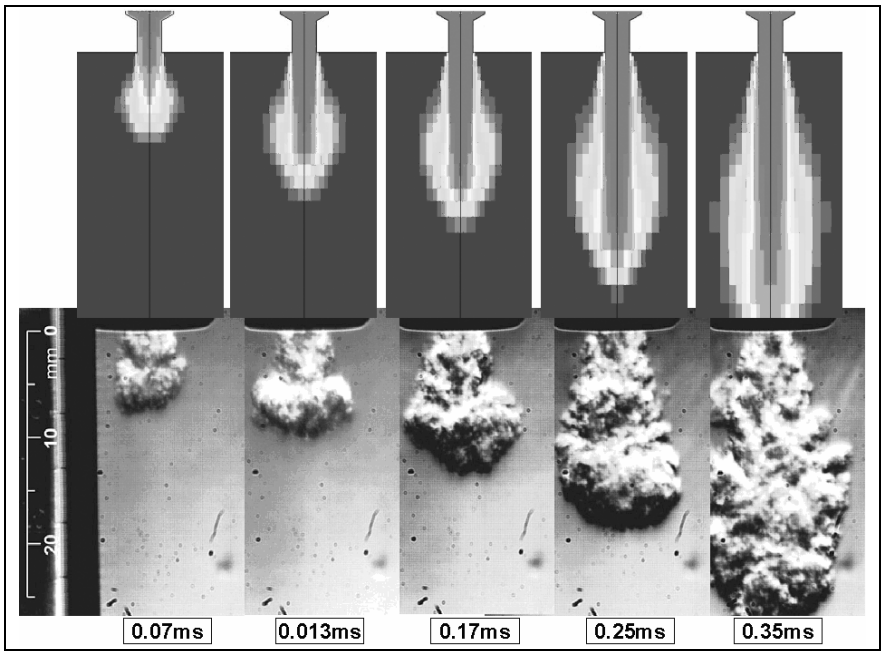

Figure 2-16. Comparison of simulated and experimental density gradients for One-hole-without-tube injector

Figure 2-17 and table 2-4 gives detailed comparison of Hydrogen streams, from the points of view of stream angle and stream penetration, at typical moments (0.4ms and 1.20 ms). The comparison shows that the differences are less than 5%.

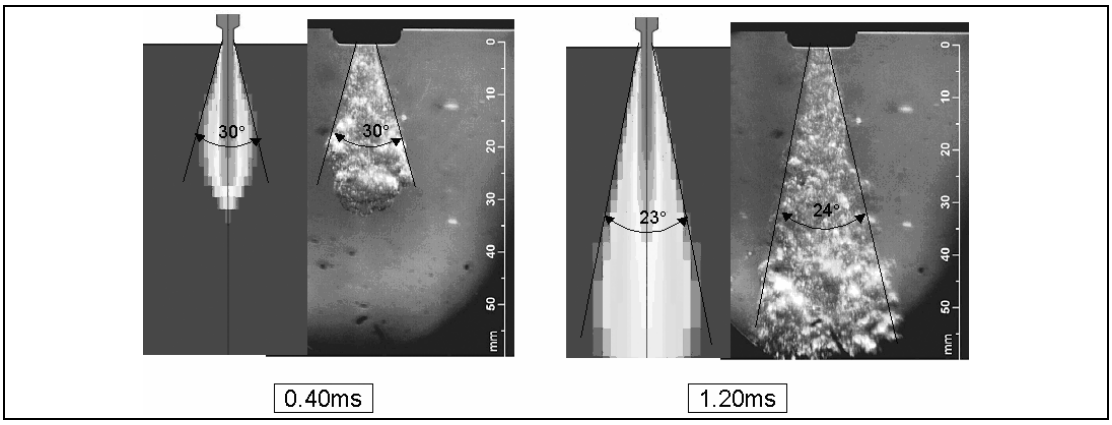

Figure 2-17. Comparison of simulated hydrogen streams and Schlieren Photos with respect to stream angle and stream penetration

Table 2-4. Quantitive Comparison of simulated results and Schlieren Photos for one-hole-without-tube injector

	Penetration/mm			Stream Angle/deg		
time/ms	Experiment	Simulation	Difference/%	Experiment	Simulation	Difference/%
0.4	32.0	31.0	-3.1	30.0	30.0	0.0
1.2	85.0	85.0	0.0	24.0	23.0	-4.2

(2). One-hole with tube

Figure 2-18 gives a visual comparison of the density gradients at specific time (under part, Simulation; up part, Schlieren). This comparison shows that the simulated results are very close to measurement ones, from the point of views of stream penetration, injection angle and stream trend. The only difference is that the simulated streams are thinner than the measured results.

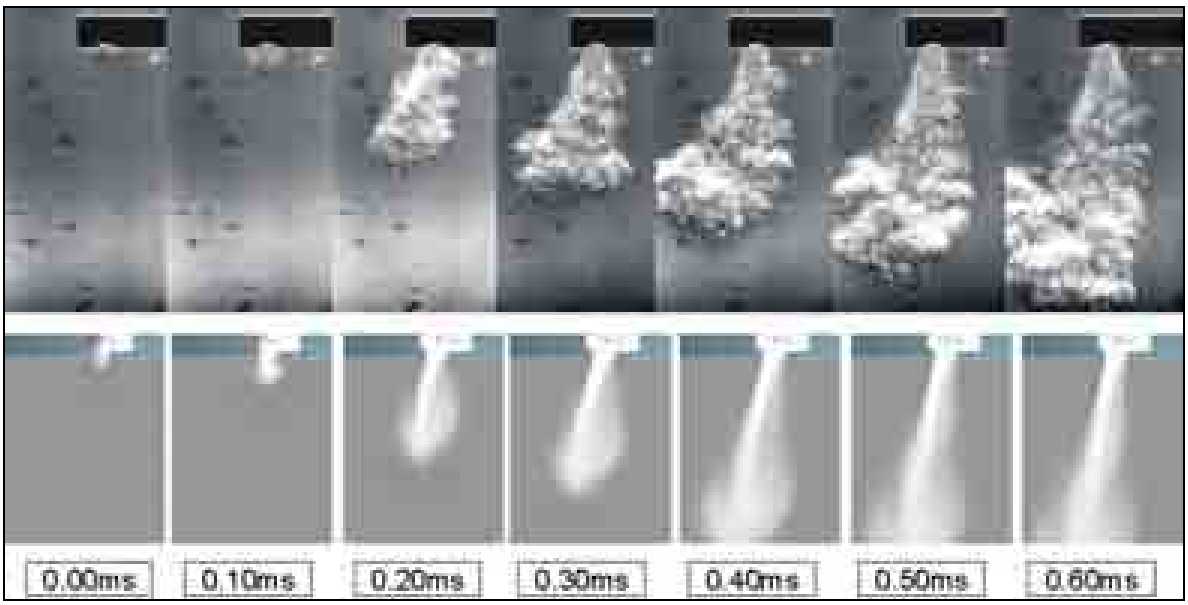

Figure 2-18. Comparison of simulated and experimental density gradients for one-hole-with-tube injector

Table 2-5. Comparison of penetrations of simulated and measured results

Time/ms	0.00	0.10	0.20	0.30	0.40	0.50	0.60
x-Measurement	0.0	3.7	16.8	22.0	28.0	35.1	38.8
x-Simulation	0.0	3.7	15.4	20.5	27.1	35.1	39.5
Difference/%	0.0	0.0	-8.7	-6.7	-3.2	0.0	1.9

Table 2-5 and figure 2-19 gives detailed comparison of penetrations at different time. The maximum difference appears during 0.20~0.30 ms, and then becomes the same as the measurement results. The difference is less than 10% in the whole time domain.

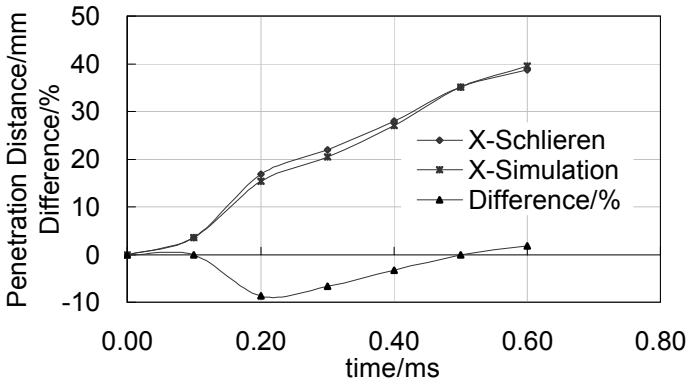

Figure 2-19. Comparison of penetrations of simulated and measured results for One-hole-with-tube injector

(3). Ten-holes with tube

This example is the most complicated model, which will test the FIRE capability of simulating multi-hole Hydrogen Injection problem.

Since this simulation needs a very big mesh and very much time consuming, only the beginning of the injection process, up to 0.5 ms, is simulated. The typical simulated density distributions are shown in Figure 2-20 (middle). The injection process is also described in Figure 2-20(under part).

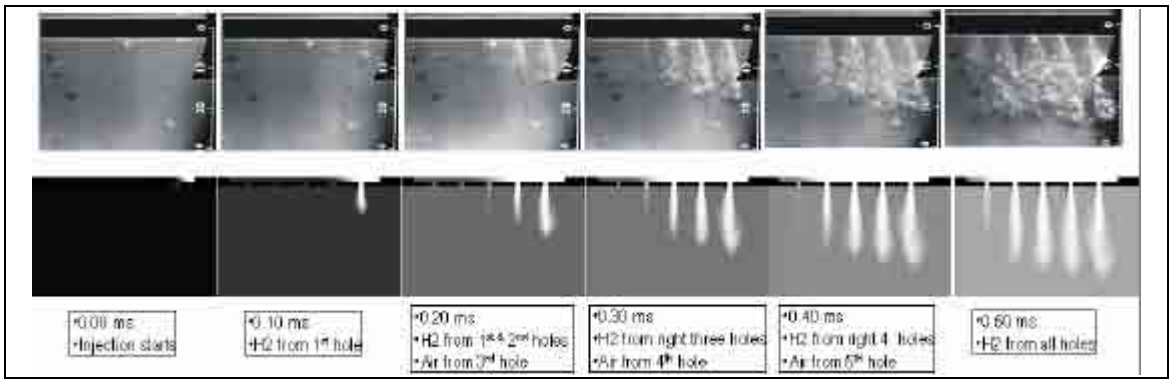

Figure 2-20. Comparison of simulated and experimental density distributions for ten-hole injector

Table 2-6 gives detailed comparison of injection procedure, stream penetration,

injection angle and stream contour, respectively. The comparison shows good agreement between simulation and measurement results.

Table 2-6. Comparison of injection procedure, stream penetration, injection angle and stream contour for ten-hole injector

Item	Schlieren	Simulation	Consistency
Procedure	Described in figure 2-20	Same as Schieren	Excellent
Penetration	Left hole has better penetration at beginning, then becomes the same	Same as Schieren	Excellent
Angle	acute angle (backward)	Similar as Schieren, but with less rake	Acceptable
Contour	Similar as one hole injection (without tube)	Same as Schieren, but thinner	Acceptable

2.4.3 Error Analysis and Comments

The difference between the simulation and measurement results could be caused by the following aspects:

(1). The inlet boundary is set to be total pressure, which increase linearly form 0 to 2.3 ms. In fact, the injector valves are lifted by electromagnet. Since there is no information about the valve lift curve as well as the pressure variation curve during the experiment, the linear pressure increase may not represent the real condition.

(2). Every experiment has been done for several rounds. The graphs are selected from all of the pictures. In other words, one group of pictures may not be from one experiment round.

(3). The surface roughness is not considered in the simulations and all of the edges are treated as sharp ones. This will more or less influence the stream contour.

(4). Grid convergence study shows that the grid dimension influence the stream contour as well as penetration significantly. Finer grid will get better result but with penalty of significant increase of calculation time and resource requirement.

The above validation shows that simulated results have good agreement with the experiment ones with accuracy of higher than 90% in all cases. Therefore, it can be concluded that FIRE version 8 is capable to simulate the supersonic hydrogen injection process with good accuracy.

2.5 Brief summary

CFD simulation is an effective tool for hydrogen engine performance study. The problem is how to make reliable simulations with present CFD codes.

Verification and Validation are fatally important to carry out valuable CFD

research. All the relative effects, such as grid convergence and Iterative Convergence, should be carefully studied before practical simulations.

FIRE is proved to be an effective tool for supersonic flow calculation and be capable to simulate hydrogen injection and mixture formation process in hydrogen engine with satisfied accuracy.

---

[1] *AIAA, 1998.*

[2] *Eric L. Peterson, 1999.*

[3] *The experiment was carried out in the Chair of thermodynamics TU-Munich and provided by BMW.*

[4] *AVL Fire, 2003. Theory, Version 8.*

[5] *The experiments are carried out by the Thermotec Engineering Services GmbH and provided by BMW*

Part III: Simulation of Hydrogen Injection and Mixture Formation

3.1 Introduction

Hydrogen fuel delivery system can be broken down into three main types[1]:

- Central injection (or "carbureted")
- Port injection
- Direct injection.

3.1.1 Central Injection

The simplest method of delivering fuel to a hydrogen engine is by way of a carburetor or central injection system. This system has advantages for a hydrogen engine. Firstly, central injection does not require the hydrogen supply pressure to be as high as for other methods. Secondly, central injection or carburetors are used on gasoline engines, making it easy to convert a standard gasoline engine to hydrogen or gasoline/hydrogen engine.

The disadvantage of central injection is that:

It is more susceptible to irregular combustion due to pre-ignition and backfire.

Due to the long distance between injector/carburetor and cylinder, there will be response delay. There might also be concentration difference in different cylinders if the intake manifold is not well designed.

Since hydrogen will displace much of the combustion chamber, the maximum theoretical power will be reduced. (Figure 3-1)

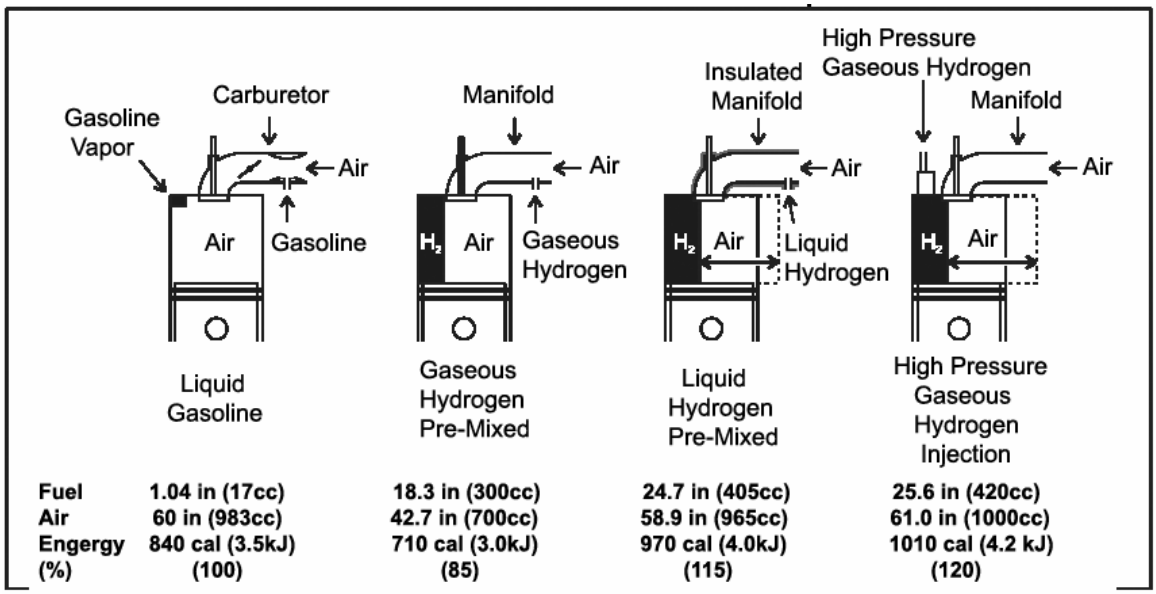

Figure 3-1. Comparison of combustion chamber volumes and energy content for gasoline and hydrogen fueled engines.

3.1.2 Port Injection Systems

The port injection fuel delivery system injects fuel directly into the intake manifold at each intake port, rather than drawing fuel in at a central point. Typically, the hydrogen is injected into the manifold after the beginning of the intake stroke. In this case, the backfire problem can be avoided and the probability for premature ignition is reduced.

In port injection, the air is injected separately at the beginning of the intake stroke to dilute the hot residual gases and cool any hot spots. Since less gas (hydrogen or air) is in the manifold at any one time, any pre-ignition is less severe. The inlet supply pressure for port injection tends to be higher than for carbureted or central injection systems, but less than for direct injection systems.

3.1.3 Direct Injection Systems

More sophisticated hydrogen engines use direct hydrogen injection into the combustion cylinder during the compression stroke. In direct injection, the intake valve is closed when the fuel is injected, completely avoiding premature ignition during the intake stroke. Consequently the engine cannot backfire into the intake manifold.

Direct injection system requires higher fuel rail pressure than the other methods, but in compensation for better acceleration and much higher power output. The power output of a direct injected hydrogen engine is 20% higher than for a gasoline engine and 42% higher than a hydrogen engine using a carburetor.

Due to the reduced mixing time of the air and fuel in a direct injection engine, the air/fuel mixture can be non-homogenous, which will bring up the difficulties on combustion process organization. Consequently, NOx emissions could be higher and thermal efficiency lower than the non-direct injection systems. In other words, the mixture formation process is the key point in the design of a direct injection engine.

Therefore, this part will focus on the injection and mixture formation of hydrogen engine. With the help of FIRE Code, the detailed phenomenon and its influence on combustion will be discussed to find a general idea to optimize the mixture formation in a direct injection Hydrogen engine.

3.2 Characteristics of Hydrogen Injection

3.2.1 Stoichiometric Air/Fuel ratio

The theoretical or stoichiometric combustion of hydrogen and oxygen is given as:

$$2H_2 + O_2 = 2H_2O$$

That is to say, 32 grams of Oxygen is needed to burn 4 grams of Hydrogen completely.

Under normal condition, Oxygen mass friction in air is considered to be 23.2%. Therefore, the stoichiometric or chemically correct Air/Fuel ratio for the complete combustion of hydrogen in air is about 34.5:1 by mass.

It is known that the mole weight of Hydrogen is 2 and the mole weight of air is approximate 28.9, the stoichiometric Air/Hydrogen ratio by volume can be deduced as approximately 2.4:1 according to Avogadro's law.

3.2.2 Injection Characteristics

Converting the Stoichiometric Air/Hydrogen volume ratio into engine conditions, it can be figured out that: great volume of Hydrogen, which will take more than 40% of cylinder volume, will be injected into the cylinder in every cycle to compose stoichiometric mixture.

Normally, the diameter of injection hole is less than 1 mm, and the injection duration is less than 90° crank angle (after intake valve closure and before ignition begin). Therefore, the injection speed must be extremely high.

Normally, the Hydrogen injection process has the following characteristics:

(1). High injection pressure

The injection pressure could be higher than 100 bar. The big pressure difference in the cylinder will cause tremendous pressure gradient around the injector, which makes the calculation be easy to diverge. Therefore, the underrelaxation factors and convergence criterions should be carefully adjusted.

(2) Very High speed

The maximum injection speed could be up to 2000m/s (Mach number close to 2). To calculate such a supersonic flow, the time increment must be small enough and Consequently, the calculation is very much time consuming.

(3). Intensive variation of the characteristic parameters in the domain

During the injection, all the characteristic parameters (pressure, temperature, density, TKE, velocity, etc) have intensive gradients near the injector and around the stream. In order to correctly simulate the gradients, the mesh must be fine enough in the corresponding zone.

According to this characteristic, the mesh could be generated in such a way: the grid is fine enough near the injector and around the stream, but relatively rough in other area in order to reduce the number of cells.

All the calculation meshes in this thesis are built manually in order to reduce the number of cells and accelerate the calculation.

3.2.3 Criterion for mixture formation

Detailed study shows that the mixture could never become homogenous in direct inject engine due to the limited time for mixture formation. Three criterions are given here to judge the mixture state in order to compare the mixture formation

processes in different cases:

- Hydrogen "cloud" should be continuous in the whole cylinder in order not to intermit flame propagation.
- Hydrogen is equally distributed in the "cloud". The less the concentration difference is, the better the mixture is formed.
- The higher the volume percentage of the hydrogen "cloud" is, the better the mixture is formed.

3.3 Influence of engine speed

Comparison calculations, with moving mesh and fixed mesh separately, are carried out to find the influence of engine speed. With a 6-hole injector, 1/6 of the cylinder mesh is used for the calculations. The maximum inlet mass flow is set to be 0.6 g/s with the same injection timing (figure 3-2) in both cases.

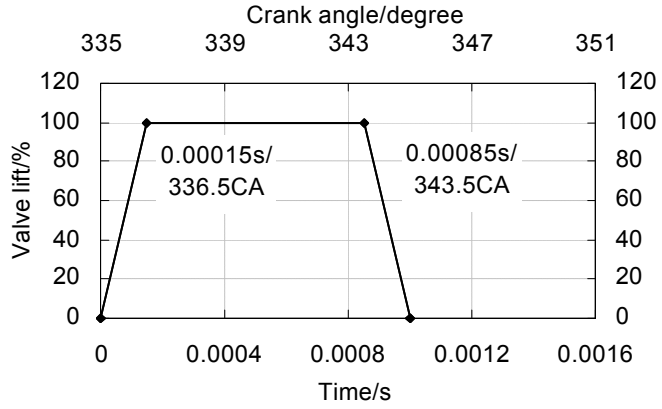

Figure 3-2. Illustration of injection timing

The engine speed is set to be 1667 r/min in the "moving" calculation. The boundary conditions are the same in both of the calculations.

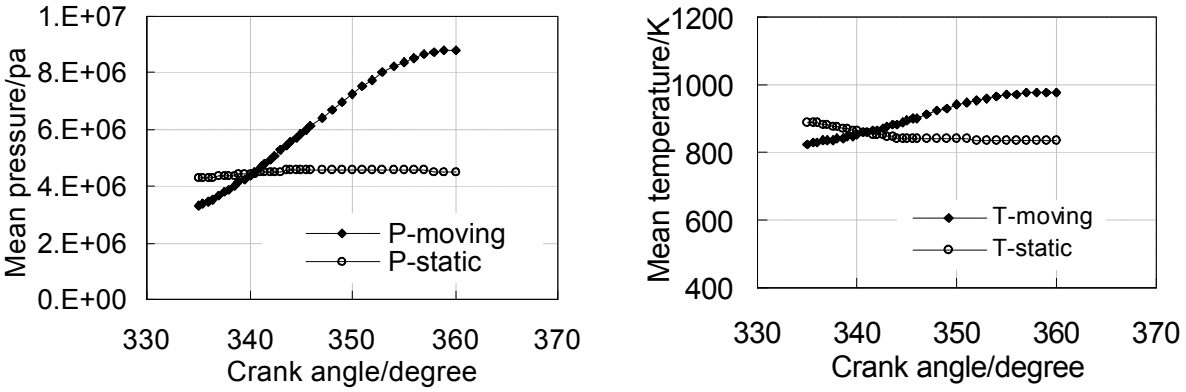

(a). Mean pressure (b). Mean temperature

Figure 3-3 Comparison of pressure and temperature with moving and steady meshes

The initial conditions are adjusted to make the mean pressure and mean temperature the same at 340°CA (middle of injection process) in both cases

(figure 3-3).

Table 3 shows a comparison of the hydrogen distributions at different time/degrees.

Table 3-1. Comparison of the hydrogen distributions at different time/degree

Angle	Moving	Static	Angle	Moving	Static
337°	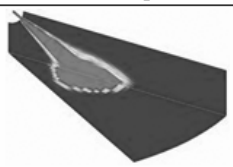	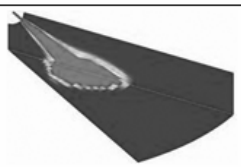	350°	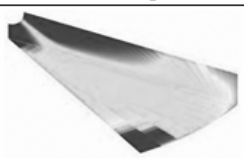	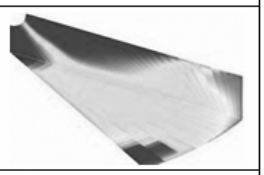
340°	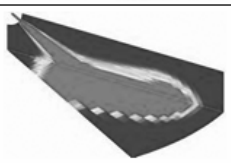	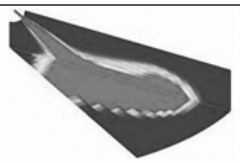	360°		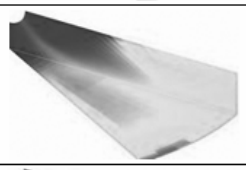
345°	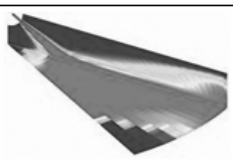	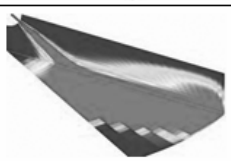	370°		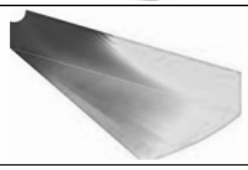

It shows that both the steam penetration and Hydrogen distribution have not much difference in the two cases despite of the volume variation in moving case. In other word, piston moving has little influence on the variation of hydrogen distribution in the cylinder domain.

This phenomenon can be easily understood when the high injection speed is considered. The maximum injection speed is approximately 1800 m/s in these calculations, while the mean piston speed is less than 10 m/s in most engines. The huge velocity difference makes the mixture formation process be governed mainly by the injection performance rather than the piston movement.

Based on the above analysis, the mixture formation process in Hydrogen injection engine can be studied with fixed mesh in order to simplify the calculation.

3.4 Influence of Injector Construction

Since injector is the key part, this part will study the influence of injector structure on Hydrogen injection and mixture formation process.

(a). 6-hole Injector (b). 12-hole Injector

Figure 3-4. Diagrams of 6-hole and 12-hole Injector

Two injectors, with different number of holes but the same total section area, are studied in order to find the influence of hole number. The two injectors are illustrated in figure 3-4.

Table 3-2 lists the setting of the two calculations. Both the two cases have the same injection timing as show in figure 3-2.

Table 3-2. Parameter setting of calculations based on the two injectors

Models	Hole Diameter	Mass flow/ (g/s)	Cylinder Pressure/bar	Cylinder Temperature/K
6 hole	0.54mm	0.732×6	32	800
12 hole	0.38mm	0.366×12	32	800

Since the holes are equally distributed, simple meshes (figure 3-5) with one hole are built to reduce calculation time.

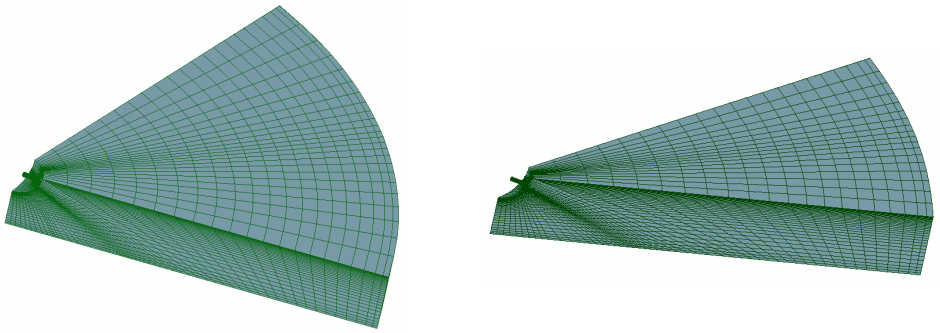

(a). Mesh for 6-hole injector (b). Mesh for 12-hole injector

Figure 3-5. Diagram of meshes for hydrogen injection simulation

Table 3-3 compares the hydrogen distributions (hydrogen mass fraction) at the representative time for the two cases.

Table 3-3. Comparison of hydrogen distribution of two injectors

Time/ms	0.2	0.5	1.0	1.5
6-hole	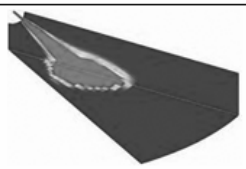	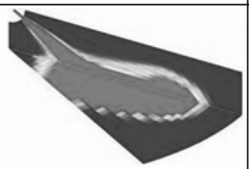	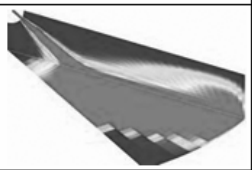	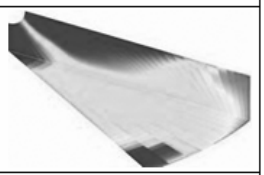
12-hole	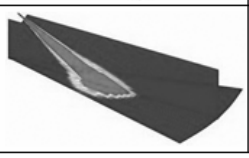	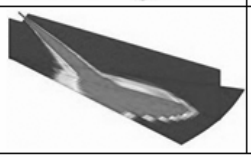	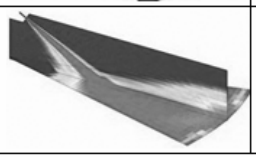	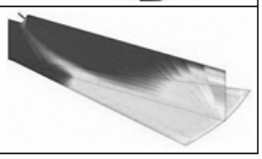

Note: all pictures have the same scale of 0(blue) to 0.04 (red).

Even though the hydrogen distribution shows the similar trend at the same time, there are many differences between the two cases:

(1). During injection, the hydrogen stream from 6-hole injector is much thicker than that from 12-hole injector due to the bigger hole diameter.

(2). Since the thicker stream is more difficult to be broken, it has more inertia. Therefore, the stream head in 6-hole case is faster than that in 12-hole

case (1ms, 1.5ms).

(3). When injection is finished (1.0 ms), hydrogen has pervaded out and covered almost the whole piston surface in 12-hole case. But there is still no hydrogen at the corners in 6-hole case.

(4). At 1.5 ms, there is a rich zone at the up corner opposite to the hole in 6-hole case, but hydrogen has no covered the whole piston surface. There is much better hydrogen distribution in 12-hole case at the same time.

Later study will show that higher hydrogen concentration will get higher combustion temperature, more NO emission and lower thermal efficiency. Therefore, faster mixture formation is propitious to optimize engine combustion. The 12-hole case has better mixture formation performance than the 6-hole case according the criterions in 3.2.3. Speaking generally, the more the hole number, the better the mixture formation.

Table 3-4. Hydrogen distribution with and without initial swirl for the 12-hole injector

Time/ms	No swirl	Swirl 10 m/s	Swirl 20 m/s
0.1			
0.3			
0.5	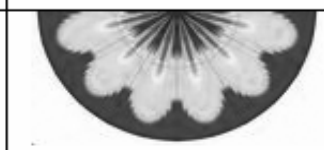		
0.7	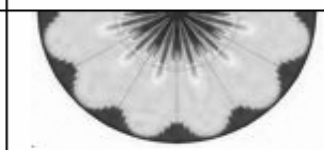		
0.9	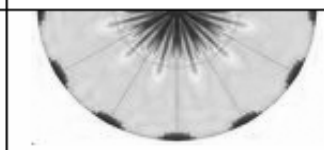	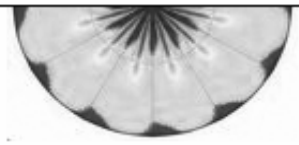	
1.0			
1.5	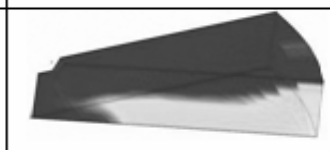		
2.0	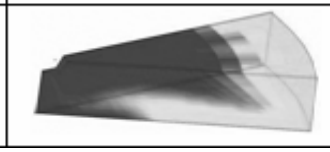	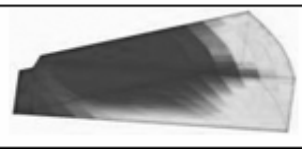	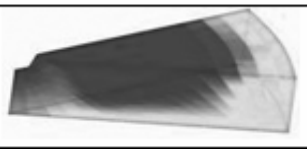

3.5 Influence of initial swirl

The influence of initial swirl is studied with a 12-hole injector by given different initial swirls before injection starts. The injection timings are the same for all of the three cases (as shown in figure 3-2). The maximum inlet mass flow is set to be 0.6 g/s in every hole. Therefore, the final mean hydrogen equivalent ratio is approximately 0.3 for all the three cases.

Table 3-4 shows the hydrogen distribution at different time. The value of initial swirl means the initial swirl flow speed near the cylinder liner. The swirl speed 20 m/s is corresponding to Ricardo swirl ratio of 2.25 when engine speed is 2000 r/min.

The following opinions can be gotten from table 3-3:

(1). During the injection process, swirl has little influence on hydrogen distribution. This phenomenon can be explained by the huge difference between injection speed and swirl speed.

(2). Hydrogen can reach the cylinder liner when the injection finishes, and almost equally distributed along the swirl direction with 12-hole injector. Therefore,

(3). Swirl has little influence on mixture formation for 12-hole injector engine.

3.6 Mixture formation process analysis[2]

A real engine geometry is adopted to study detailed mixture formation. Figure 3-6 shows the geometry of the research object.

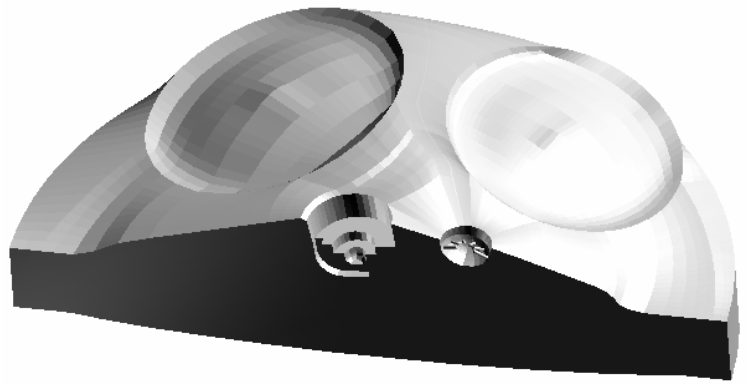

Figure 3-6. Geometry of the research object

A 12-hole injector is equipped on the cylinder head. A spark plug in installed in the middle of the cylinder. Comparison simulations have been carried out to see the influence of injector installation.

Case 1: One hole subtends to the spark plug directly (figure 3-7a)

Case 2: the injector is rotated with 15°, the spark plug is in the middle of two injecting streams (figure 3-7 b)

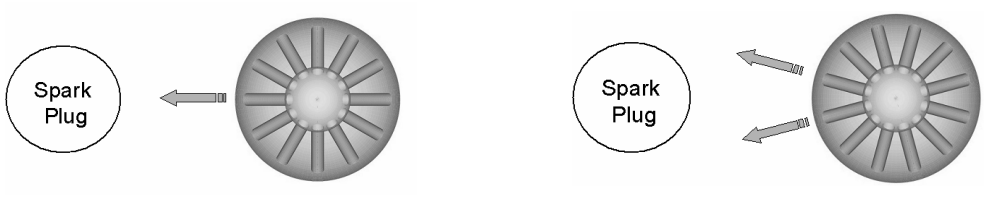

(a) (b)

Figure 3-7. Illustration of injector orientation

Table 3-5 lists the injection setting and the initial conditions. Both cases have the same injection timing as shown in figure 3-8.

Table 3-5. Parameter setting and initial conditions for injection

	Hole Diameter	Mass flow/ (g/s)	Cylinder Pressure/bar	Cylinder Temperature/K
Case 1	0.38mm	4.5×2	32	800
Case 2	0.38mm	4.5×2	32	800

3.6.1 Case 1 analysis

Figure 3-8 shows the injection and mixture formation process from the beginning of injection to 13 ms (12 ms after injection finished).

The stream from the opposite-spark-plug hole will be blocked by the spark plug during the injection phase. After injection is finished, the hydrogen cloud leaves the spark plug and moves to the cylinder wall slowly.

Other streams have the same behavior that hydrogen is injected to the piston surface, then reflected to the cylinder wall, and then move slowly to the cylinder center along the inner surface of cylinder head.

Since the injector is eccentric installed, the streams on the right side reach to the piston surface first.

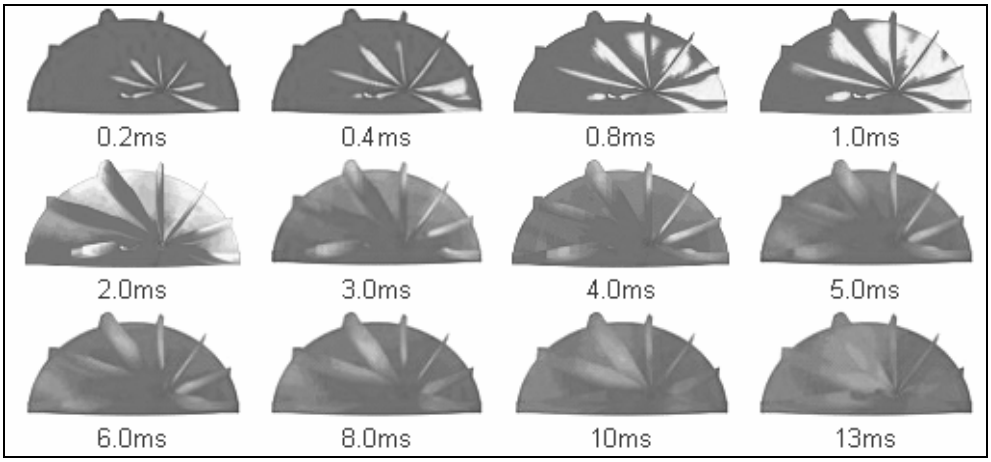

Figure 3-8. Injection and mixture formation in case I

When the hydrogen concentration in the spark plug gap is analyzed, very surprising phenomenon will be observed (figure 3-9):

During the injection process, there is very high hydrogen concentration (Figure

3-9a).

After the injection finished, the hydrogen concentration reduces rapidly because the hydrogen cloud moves away from the spark plug to cylinder wall due to inertia effect. It will reduce to less than 0.1 at around 2.5ms (1.5 ms after injection finished), and then keep the low value for approximate 7ms (figure 3-9b). 9 ms after the injection finished, hydrogen cloud, which is injected from adjacent holes, moves back to the spark plug gap, and make the hydrogen concentration increase again.

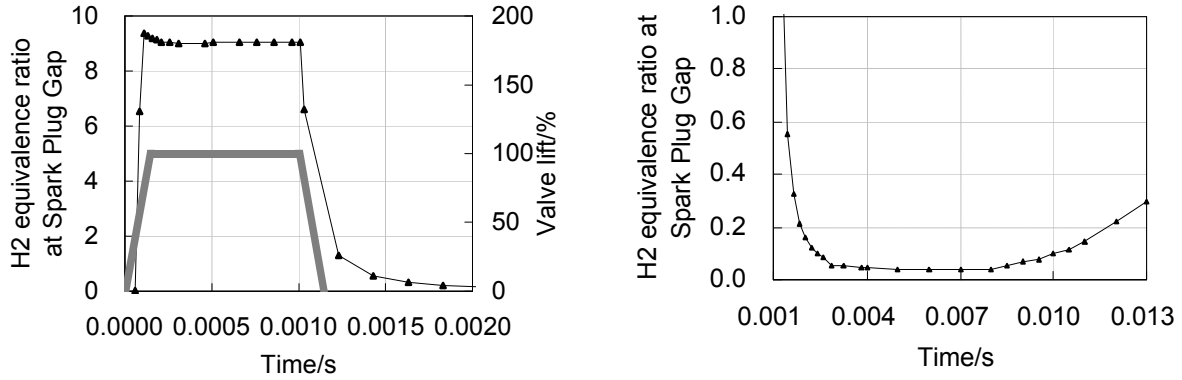

(a). During injection (b). After injection

Figure 3-9 Variation of hydrogen concentration in Spark Plug Gap in Case I

3.6.2 Case 2 analysis

Figure 3-10 shows the injection and mixture formation process of case 2.

Since no stream is injected to spark plug directly, there is no block effect in case 2. All the streams have the similar behavior as described in previous section. The only difference, which is caused by the eccentric installation of injector, is that the streams reach the cylinder wall and be reflected back at different time, which causes asymmetrical hydrogen distribution in the cylinder.

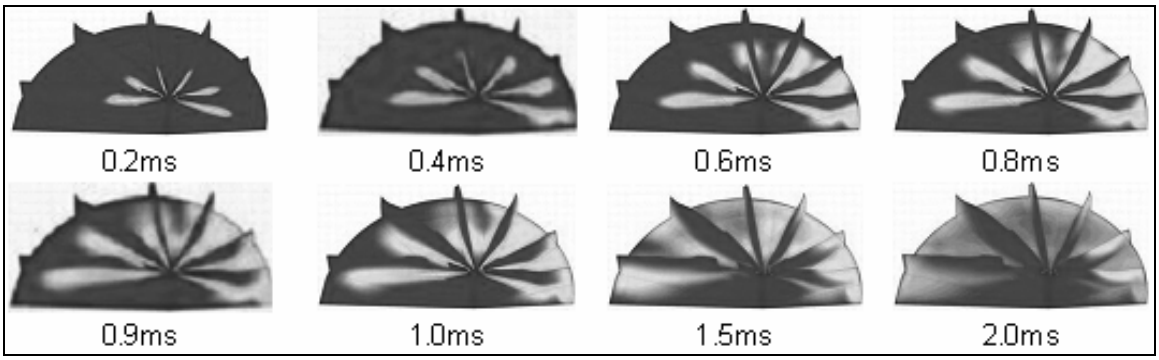

Figure 3-10. Injection and mixture formation in case II

Comparing figure 3-10 with figure 3-8, it can be seen that hydrogen is better mixed with air in case 2 than that in case 1. It gives an idea that the injector should be installed in the way that no hole subtends to any protuberant part in cylinder in order the stream not to be blocked.

When the hydrogen concentration in spark plug gap is observed, it can be seen that the variation curve has the similar trend as that in case 1, but the value is much smaller during the injection period (dot-and-dash line in figure 3-12).

Figure 3-12 also gives the variation curves of hydrogen concentration at other two points, which are on the symmetric section and at the up-left and up-right corners in the cylinder (as shown in figure 3-11).

Figure 3-11 Indication of monitoring points

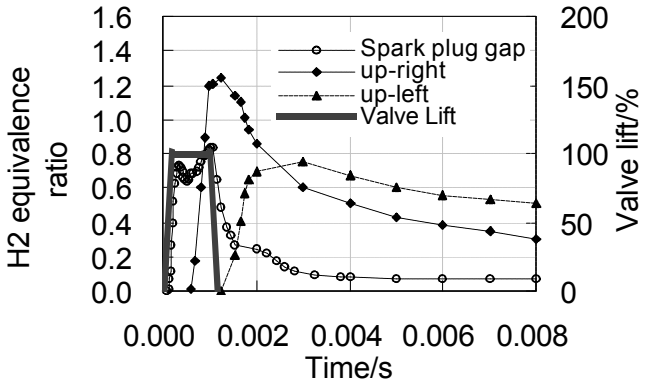

Figure 3-12. Variation of Hydrogen concentration at different position in Case II

At up-right point, hydrogen concentration reaches its peak valve (ϕ=1.24) at 1.5ms, and then reduces gradually (solid line in figure 3-12). The hydrogen equivalence ratio is still bigger than 0.3 at 8ms (7 ms after injection finished).

At up-left point, the maximum hydrogen concentration appears approximate 1.5 ms later than that at up-right point (dashed line in figure 3-12) due to the far distance from injector. The peak hydrogen concentration is approximately 2/3 of that at up-right point. Since the hydrogen stream is better mixed with air and the flow velocity becomes slower, the high concentration cloud takes much longer time to move across up-left point and makes the hydrogen concentration keep high value for relatively longer period.

3.6.3 Discuss on mixture flammability

3.6.3.1 Lean flammability limit in engine condition

Isadore Drell and Frank Belles had detailed analysis of the flammability limits of Hydrogen-Air mixture[3]. They concluded that the lean limit occurs at lower concentration as the mixture temperature increase with a linear relationship, while the pressure effect appears to be small.

They gave the lean limit up to 400°C (673.15K) mixture temperature. Since this temperature range is not enough to cover the ignition temperature in engine condition, the lean limit line is extended up to 700°C (973.15K) and plotted in figure 3-13.

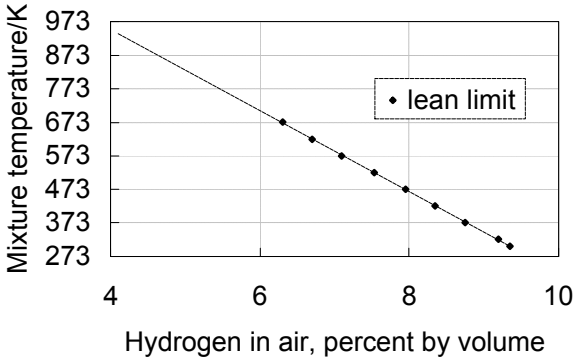

Figure 3-13. Influence of temperature on hydrogen lean flammability limit

The self-ignition temperature of hydrogen is 585°C (858.15K). Therefore, the ignition temperature should not be higher than this value. That is to say, the lean flammability limit should be higher than 4%, which approximately equals to hydrogen equivalence ratio of 0.1, in engine condition.

3.6.3.2 Ignition timing

10ms will correspond to 120°CA when engine runs at 2000r/min, or, 180°CA at 3000 r/min. Considering the delay of inlet value closure and advance of ignition, the time difference between injection start and ignition should be less than 10 ms in normal condition.

Back to figure 3-9 and figure 3-12, it is obvious that the possible ignition range is only 1.5 ms (from 1ms to 2.5 ms, or 0-1.5 ms after injection finished), which corresponds to 18°CA when engine runs at 2000r/min.

Considering the variation of ignition advance and injection duration at different work conditions, this kind of design, as shown in figure 3-6, will make the control of injection timing to be very complicated.

More over, since this ignition arrangement gives very short time for mixture formation, there must be big concentration difference in the whole cylinder domain. This will take the risk of ignition failure, which will efface the advantage of the stratified combustion for extra lean mixture. If the flame can successfully propagate, the NO emission is bound to increase due to the high combustion temperature at rich zone, which will abate the advantage of the lean combustion.

3.6.3.3 Ignition points

Figure 3-12 gives a new clue for the arrangement of ignition position.

When the spark plug is installed far away from the cylinder center, at least two advantages can be expected:

(1). Long period of high concentration gives much freedom for injection timing as well as ignition timing.

(2). The spark plug will no longer block any stream. Therefore, it is not necessary for injector orientation.

Naturally, it is suggested that the spark plug should be installed away from the center of the cylinder in order to organize successful ignition.

3.7 Brief summary

Hydrogen direct injection engine, with its good safety and high power output, is the most sophisticated type among all types of hydrogen engines.

Injector is the most important part for mixture formation process in the cylinder. With the same injection pressure and the same total injection section area, more holes will accelerate the mixture formation process and give better mixture distribution.

Since the injection speed is very high, engine speed and initial swirl have little influence on the injection and mixture formation process.

Due to non-homogenous distribution, ignition position and ignition timing should be carefully designed in order to organize successful ignition and stable flame propagation. Side located spark plug shows obvious advantages over central located one from the points of view of stream blockage and flammability of the charge.

---

[1] *Andre Lanz, et al., 2001.*

2 This part is from the technical report for "FIRE Simulation of Hydrogen Injection Project" sponsored by BMW in 2002. Author: Fushui Liu.

3 Isadore L. Drell and Frank E. Belles, 1958.

Part IV: Validation of Different Combustion Models in FIRE

4.1 Introduction

With the development of CFD technology, a number of combustion models have been developed over the last decade. Some of them have been implemented into various commercial CFD codes to simulate the combustion process in IC engine.

Since most of the combustion models are base on some hypothesis, every combustion model has its special characteristics and is suitable for some situations. In other words, not all of the combustion models are universal. It's true that there are many successful simulations, which show reasonable agreement with measurement results. But it is really a big challenge for a new hand to get satisfied result. To have a good understanding of the characteristics of the combustion models will always be the first step to start IC engine combustion simulation.

Further more, almost all of the combustion models are developed mainly for gasoline/diesel engine. There is very little information about their application in hydrogen engine. Therefore, it is necessary to study and validate the available combustion models in order to make reliable simulations for Hydrogen engine combustion research.

4.1.1 Analysis of current approach

In the manuals of the commercial CFD codes, the most suitable combustion models are recommended for specific situations. The users can simply follow the procedure, as shown in figure 4-1, to carry out their own simulations.

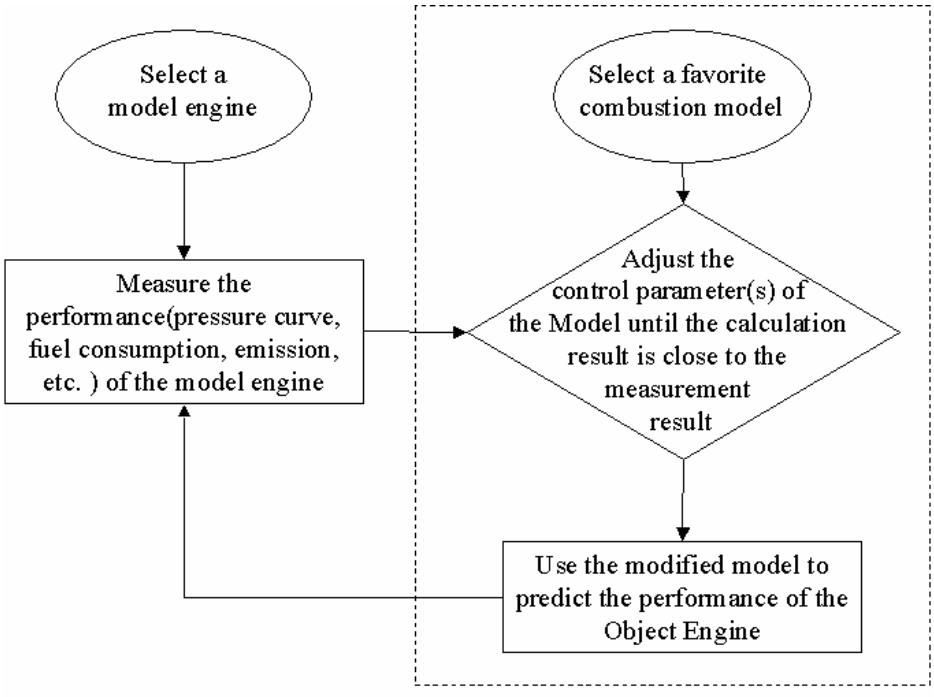

Figure 4-1. Normal approach for engine combustion simulation

Based on lots of fundamental researches by the Code developer, this simple approach can get satisfied results for most of the simulations on traditional engines.

When there is no ready-made recommendation for the simulation of a new fuel engine, or there is no model engine, there must be many difficulties to adopt this approach. The user has to choose the suitable model himself according to his understanding of the available combustion models. Due to lack of reference data, the selection of the control parameters in the model will be also a bewildering problem.

4.1.2 “Robot” approach for Hydrogen engine study

This thesis is going to study the general performance of Hydrogen combustion and find the basic principles to organize optimum Hydrogen combustion, rather than a specific engine. Therefore, the above routine is not suitable for the study.

A general approach, or a “Robot-simulation approach”, will be researched in this thesis in order to make the hydrogen engine combustion simulation be more reliable and more flexible.

Before the “robot” approach is promoted, it is necessary to review the combustion process in a SI engine.

Many pioneers did the detailed research on the ignition[123], flame development and propagation process in the SI engines. The research shows that the burning of a premixed charge in SI engine can be divided into the following phrases:

(1). Spark ignition.

(2). Laminar flame growth and transition to turbulent combustion

(3). Turbulent flame development and propagation

(4). Near-wall combustion and after burning

The first phase is accomplished by the ignition system of the engine. In the CFD codes, this phase is normally simulated by given fixed heat release and reaction progress in the ignition zone, which can hardly be changed by the user.

The second phase is purely influenced by the performance of the charge, and plays an important role in the development of the third phase, and, consequently, influences the whole reaction progress. The laminar flame speed of the charge should be the main focus during CFD simulation. Unfortunately, this phase is ignored in many combustion models.

The third phase lies on two aspects: (1) characteristics of the charge and (2) turbulence condition. Theoretically, turbulence will mainly increase the flame surface, but not change the flame speed. In other words, this phase is essentially influenced by the laminar flame speed of the charge and accelerated by turbulence. Most of the combustion models are developed by focusing on this phase. Unfortunately, many combustion models pay too much attention to the

turbulence behavior, but neglect the laminar performance of the charge.

Phase 4 is mainly influenced by quench effect. It has significant influence on hydrocarbon emission in gasoline engines, but little influence on the combustion process in Hydrogen engine due to the very small quench distance of Hydrogen fuel.

From the above analysis, it can be seen that laminar combustion characteristics of the fuel is the kernel of the combustion performance in a SI engine.

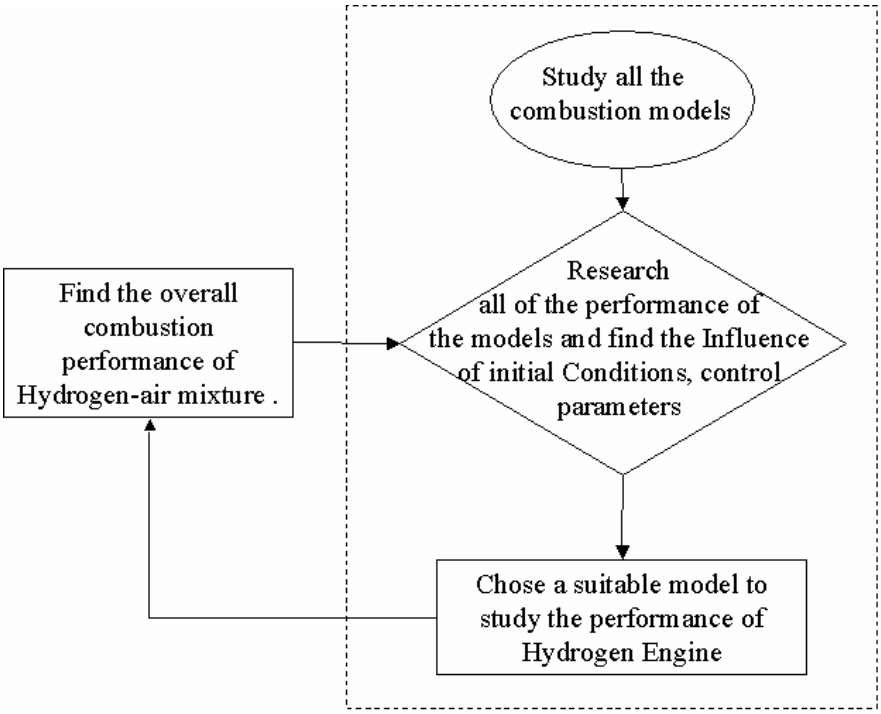

Figure 4-2. New simulation approach based on laminar flame speed

Based on laminar flame speed, a new approach is promoted, as shown in figure 4-2. The kernel of the approach is to find a suitable combustion model, which can reflect the overall laminar combustion performance of the Hydrogen fuel.

The only risk of this approach is that the turbulence effect might not be exactly reflected due to lack of validation. But, it will give reasonable result when it is used for multi-case comparison and finding the general conceptions to optimize the engine performance, due to the following reasons:

(1). Turbulence condition is independent of fuel and is only influenced by geometrical and mechanical performance of the engine (cylinder geometry, engine speed, fuel injection process, etc). When the working condition is fixed, the turbulence condition should be the same at the same angle in the same engine.

(2). Even though some combustion models have not the function to simulate laminar flame performance, but all have consideration of turbulence effect.

(3). The laminar combustion speed of Hydrogen-air mixture is almost an

order higher than gasoline-air mixture. Laminar performance plays much more important role in Hydrogen engine combustion than that in gasoline engine.

It is well known that simulation can never replace experiment, but extend the experiments. In other words, the function of simulation is to give guidance to the design and modification of an engine, and reduce experimental work. From this point of view, this approach will give a "robot" solution for Hydrogen engine performance study and can be also used for other SI engine research.

4.1.3 Reference data for the validation

4.1.3.1 Hydrogen laminar flame speed

Laminar flame speed is a function of temperature, pressure and mixture concentration. Many experts have done lots of experiments to determine the Laminar flame speed of Hydrogen-Air mixture. Sebastian Verhelst and Roger Sierens summarized predecessor's achievements and give the laminar flame speed under engine conditions, which cover the entire operating range of hydrogen fuelled spark-ignition engines.

Table 4-1 gives the Hydrogen laminar speed at different conditions[4]. If there is not special explanation, all of the validation in this PART will use these data as reference.

Table 4-1. Hydrogen laminar speed at different conditions

T (K)	P (bar)	λ	Sl (cm/s)	T (K)	P (bar)	λ	Sl (cm/s)	T (K)	p (bar)	λ	Sl (cm/s)	T (K)	p (bar)	λ	Sl (cm/s)
300	1	1.00	217.3	300	4.75	3.000	2.98	300	14	1.00	205	500	12	1.00	517.1
300	1	2.00	66.97	300	5	1.000	229	300	16	1.00	199.8	500	16	1.00	500
300	1	2.50	27.27	300	6	1.000	226.8	300	16	2.00	17.7	500	16	1.75	137.9
300	1	3.00	10.7	300	8	1.000	221.6	300	16	2.50	3.65	500	16	2.50	29.29
300	2	1.00	228.2	300	8	1.500	87.5	300	16	3.00	0.42	700	1	1.00	860.7
300	3	1.00	230.8	300	8	2.000	27.2	500	1	1.00	483.1	700	1	1.50	712.7
300	4	1.00	230.5	300	8	2.500	7.74	500	1	1.50	356	700	1	2.00	578.8
300	4	1.50	109.6	300	8	3.030	1.12	500	1	2.00	242.7	700	1	2.50	463.4
300	4	2.00	39	300	10	1.000	216	500	1	2.50	149.6	700	2	1.00	938.4
300	4	2.50	13.1	300	12	1.000	210.4	500	2	1.00	517.9	700	8	1.00	1020
300	4	3.03	3.36	300	12.25	1.300	116.5	500	4	1.00	536.8	700	16	1.00	995.4
300	4.75	1.30	149.4	300	12.25	2.150	14.34	500	6	1.00	537.2	700	16	1.75	432.7
300	4.75	2.15	25.7	300	12.25	3.000	0.6	500	8	1.00	532.3	700	16	2.50	141.9

4.1.3.2 A typical Laminar flame characteristic in a spherical vessel

The spherical vessel method is accepted to be the most reliable method to measure the flame speed of a given charge in wide range of initial condition[5].

Figure 4-3 gives a typical trend of Laminar Flame Radius in a spherical vessel,

which is used for the Determination of Burning Speed for Methane-Oxidizer-Diluent Mixtures, measured by Faranak Rahim[6]. From this diagram, it is obvious that the increase of Laminar Flame Radius is linear during the early stage of the combustion.

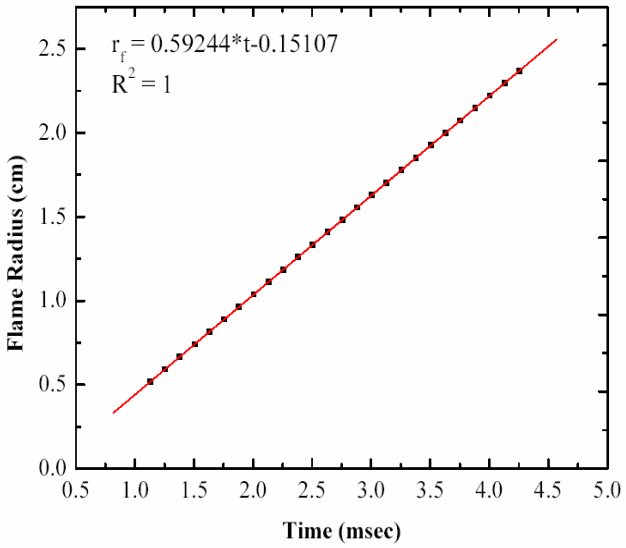

Figure 4-3.Variationof flame radius in spherical vessel for Methane combustion

Hydrogen flame propagation should behavior in the same way. Therefore, figure 4-3 can be used as a typical reference to analyze the flame propagation process of hydrogen combustion.

4.1.4 Pre-description of model validation

4.1.4.1 Validation criterions

In order to find a suitable model fro hydrogen engine combustion study, all of the four available combustion models in FIRE version 8 are validated in this part. The validation will focus on the following performances:

(1). Turbulence effect

The flame speed should converge to a fixed value, the laminar flame speed, when turbulence kinetic energy tends to become zero. Otherwise, the model is proven not able to simulate laminar combustion performance, and can’t be used for Hydrogen engine study.

(2). Range of flame speed

Hydrogen-Air mixture has a wide range of laminar flame speed. At 300K/ambient pressure, the flame speed is as high as 2.17 m/s for stoichiometric mixture. Since some models are developed for gasoline engine, them cannot simulate the high flame speed, and can’t be used for hydrogen engine study.

(3). Temperature effect

The flame speed will become higher when the initial temperature increases

(refer to table 3-1). If the simulated flame speed does not have such positive temperature effect, the model can't be used for hydrogen engine study.

(4). Concentration effect

When the mixture is leaner than stoichiometric, it has the performance that: the leaner the mixture is, the lower the flame speed will be. Since hydrogen can burn with wide range of concentration, this performance is very important for engine performance study. If the model can't simulate this concentration effect, the model can't be used for hydrogen engine study.

Only when the model can simulate all of the above four performances, it will be considered to be the suitable model and be used for hydrogen engine study in the next part of the thesis.

4.1.4.2 Research objects

Three geometries are used to simulate Hydrogen combustion Properties. They are Rectangular pyramid, Cake and Rectangle to simulate flame propagation in 3-dimensional, 2-dimensional and 1-dimensional separately (Figure 4-4):

1). Spherical Vessel method is the typical method to measure Laminar Flame Speed. In order to match the experiment condition, a pyramid mesh is built for most of the calculations. Ignition will take place at the tip of the pyramid (center of the ball).

If there is no extra explanation, the calculation will use pyramid mesh in this part.

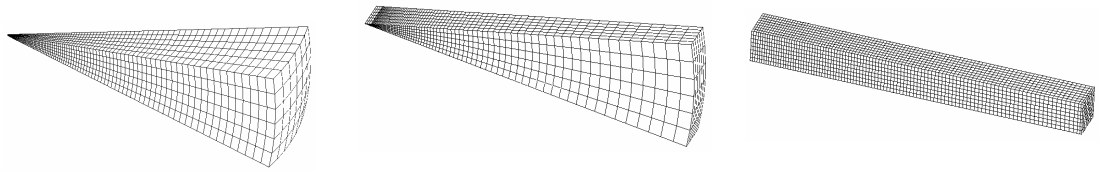

a) Pyramid (3D) b) Cake (2D) c) Rectangle (1D)

Figure 4-4. Three geometries for hydrogen combustion simulation

2). Cake mesh is used to generate cylindrical (2-dimention) flame surface, which is used as a reference to see the influence of geometry on simulated flame speed. The simulated flame speed should be independent of the geometry. Otherwise the result is doubtful. Ignition points are placed along the sharp edge (axis of the cylinder) in this case.

3). Since the one-dimensional flame propagation directly corresponds to the definition of laminar flame speed, the rectangle mesh is used to simulate one-dimensional flame. Five (or more) ignition points are placed on one end surface to generate plane flame surface.

All of the geometries have the same length/radius of 0.05m.

The calculation of flame speed for all of the three cases is described in Appendix

I.

4.2 Validation of Eddy Breakup model

This model is also named as Magnussen Model. The model assumes that in premixed turbulent flames, the reactants (fuel and oxygen) are contained in the same eddies and are separated from eddies containing hot combustion products. The chemical reactions usually have time scales that are very short compared to the characteristics of the turbulent transport processes. Thus, it can be assumed that the rate of combustion is determined by the rate of intermixing on a molecular scale of the eddies containing reactants and those containing hot products, in other words by the rate of dissipation of these eddies.

The mean reaction rate $\overline{rr_{fu}}$ can thus be written in accordance with Magnussen and Hjertager[7]:

$$\overline{rr_{fu}} = \frac{C_{fu}}{t_R}\,\bar{r}\,\min\left(\bar{y}_{fu}, \frac{\bar{y}_{Ox}}{S}, \frac{C_{Pr}\cdot\bar{y}_{Pr}}{1+S}\right) \qquad (4\text{-}1)$$

C_{fu} , C_{Pr} : empirical coefficients

τ_R: turbulent mixing time scale for reaction.

y_{fu}: fuel mass fraction;

y_{Ox}: Oxygen mass fraction;

y_{Pr}: Products mass fraction;

The first two terms of the “minimum value” of operator “min(...)” simply determine whether fuel or oxygen is present in limiting quantity, and the third term is a reaction probability which ensures that the flame is not spread in the absence of hot products.

4.2.1 Example calculation

An example, with the Pyramid mesh, is carried out to get the general understanding of simulated combustion process with Eddy breakup model. The calculation assumes that the initial turbulence kinetic energy is $0.1 m^2/s^2$ with length scale of 1e-6m. The vessel in charged with stoichiometric hydrogen/air mixture at initial temperature of 300K, and initial pressure of 1 atm. Constant A is set to be 10 in Eddy Breakup Model.

Figure 4-5 shows the distribution of Normalized Reaction Rate and Absolute Pressure at 1ms separately. From figure 4-5, the following ideas can be achieved:

- The pressure distribution picture gives very clear evidence that there is not much pressure difference in the vessel.
- The flame will propagate radially. But the flame surface is quite thick. It is obvious that it is a turbulence reaction flow, but appears a

quasi-laminar phenomenon.

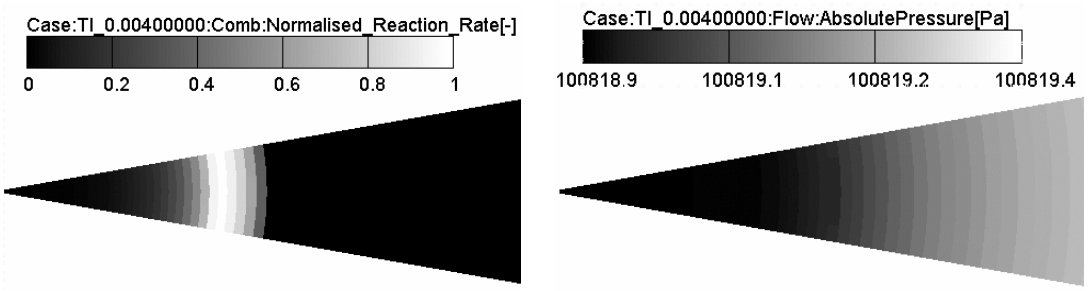

(a). Normalized reaction rate (b) Absolute pressure

Figure 4-5 Example distributions with Magnussen model

Figure 4-6 shows the calculated results of flame surface and flame speed. The variation of flame surface shows a quasi-linear increase (figure 4-6a) when r is less than 0.02m (r/R=40%). The flame speed curve is quite flat when the flame radius is around 0.02m (0.010s in time domain). Taking the flame speed in this flat range as the presentative flame speed, all of the effects will be validated in the later sections.

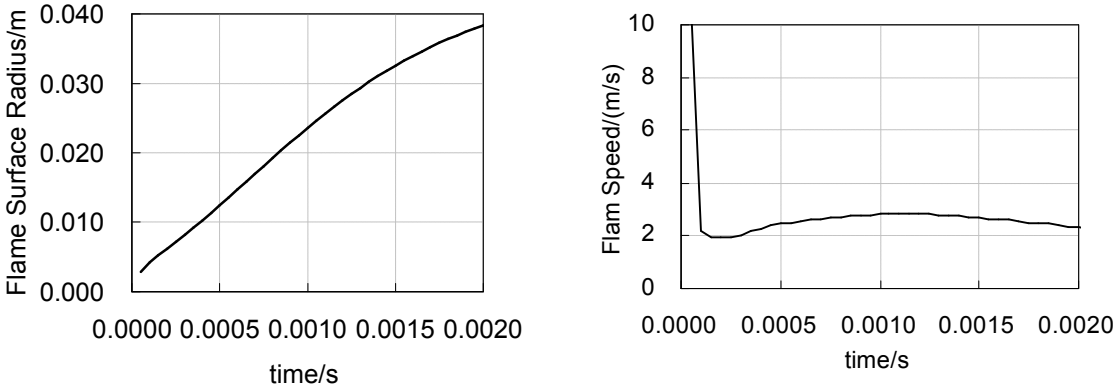

(a) (b)

Figure 4-6. Typical curves of flame surface and flame speed with Magnussen model

4.2.2 Temperature effect

With the same setting as in the example calculation but initial length scale of 2e-6m, the variation of flame speed with different initial temperature is simulated and analyzed in this section.

Figure 4-7 compares the calculated flame speed versus the reference laminar flame speed. It can be seen that there is big difference between the two curves. In other words, the temperature effect in Eddy Breakup Model is far less than expected one.

Back to formula 4-1, no temperature effect can be found in all of the three terms. That is to say, the temperature effect was not considered in the basic theory in Eddy Breakup Model. The calculated temperature effect is not the result of the

density difference due to different initial temperature.

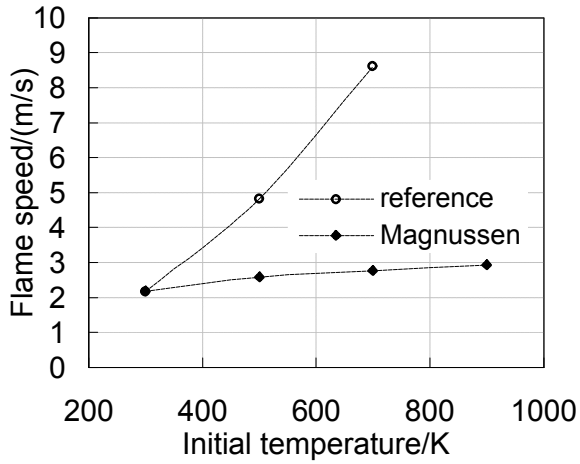

Figure 4-7. Comparison of simulated temperature effect on flame speed with Magnussen Model versus reference data

Therefore, It can be concluded that Eddy Breakup Model cannot simulate the Temperature Performance of Hydrogen Combustion.

4.2.3 Concentration effect

With the same setting as in the example calculation but initial length scale of 2e-6m, the variation of flame speed with different mixture concentration (ϕ=0.3, 0.5, 0.75, 1.0) is simulated and analyzed in this section.

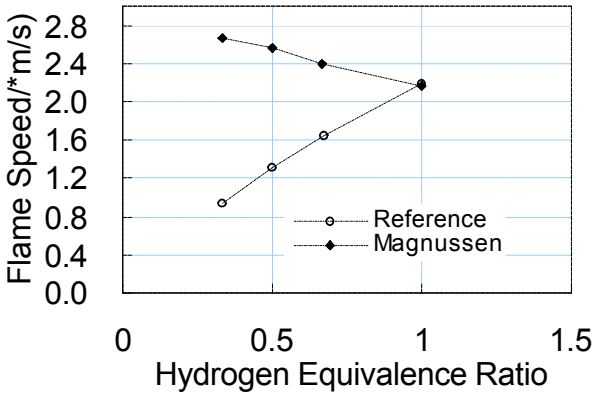

Figure 4-8. Comparison of simulated concentration effect on flame speed with Magnussen Model versus reference data

Figure 4-8 shows the relationship between the calculated (flat range) flame speed and mixture concentration. Compared with the reference data in table 4-1, the simulated result shows a contrary concentration effect.

In traditional gasoline engine, the charge concentration does not change so much as in hydrogen engine due to the narrow flammable range of gasoline. Therefore, the negative concentration effect might not influence too much to the gasoline engine simulation. But it will have significant influence on hydrogen engine

simulation.

Therefore, it is clear that Magnussen Model cannot be used for hydrogen engine simulation.

4.2.4 Turbulence Effect

With Magnussen Model, the calculation result is greatly dependent on Initial Turbulence Condition. Both Initial Turbulence Kinetic Energy and Initial Turbulence Length Scale will directly influence the reaction progress.

Figure 4-9 shows the influence of Initial Turbulence Kinetic Energy on flame speed at different initial Temperature with fixed Initial Turbulence Length Scale of 5e-5m. It is obvious that the reaction speed will increase linearly along with the increase of Initial TKE.

Figure 4-10 shows the influence of Initial Turbulence Length Scale on flame speed at different initial Temperature with fixed Initial Turbulence Kinetic Energy of 0.1 m^2/s^2. It can be seen that the flame speed will decrease linearly along with the natural logarithm of Initial Turbulence Length Scale.

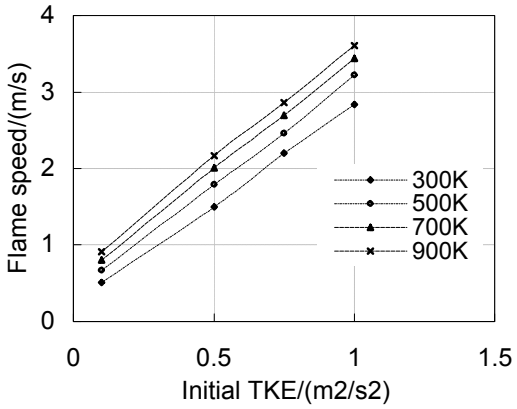

Figure 4-9. Influence of initial TKE on flame speed with Magnussen model

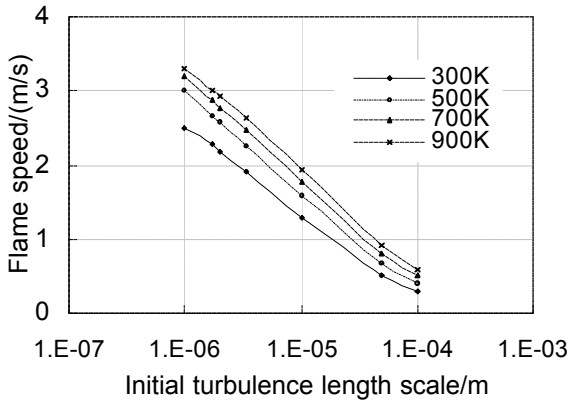

Figure 4-10. Influence of initial turbulence length scale on flame speed with Magnussen model

According to figure 4-9 and 4-10, a rough formula can be summarized to explain to relationship between flame speed, S_t, and Initial Turbulence condition:

$$S_t = aK_0 + b\ln(l_{t0}) + c \tag{4-2}$$

In formula 4-2, K_0 means the Initial Turbulence Kinetic Energy; l_{t0} represents Initial Turbulence Length Scale and *a*, *b*, *c* are Constants

4.2.5 Influence of Geometry

Further study on Magnussen Model reveals that the calculation results will be significantly influenced by the geometry even though all the settings keep the same as in table 4-2.

Table 4-2. Influence of geometry on calculation results

Initial Condition					
Fuel	Mixture	TKE	Length	Pressure	Temperature
Hydrogen	Stoichiometric	0.1m2/s2	2.E-06m	100,000pa	300K
Combustion Parameter					
Model		Factor A		Factor B	
Magnussen		3		0.5	

Figure 4-11 shows the simulated variation of flame radius/position and flame speed with different geometries respectively. It shows that the results are different from each other, but have a rough trend that:

(1). The more expanding dimension the flame has, the lower the calculated flame speed will be. The calculated flame speed with rectangle mesh (1-D) is much more higher as that with other meshes.

(2). The flame position does not move linearly with 1D mesh. There is no flat range on flame speed curve. The flame speed is very high at the beginning of the combustion and reduces gradually with flame propagation.

(3) The flame radius curves for 2D and 3D mesh show quasi-linear trend. Therefore, the flame speed does not vary so violently as that with 1D mesh.

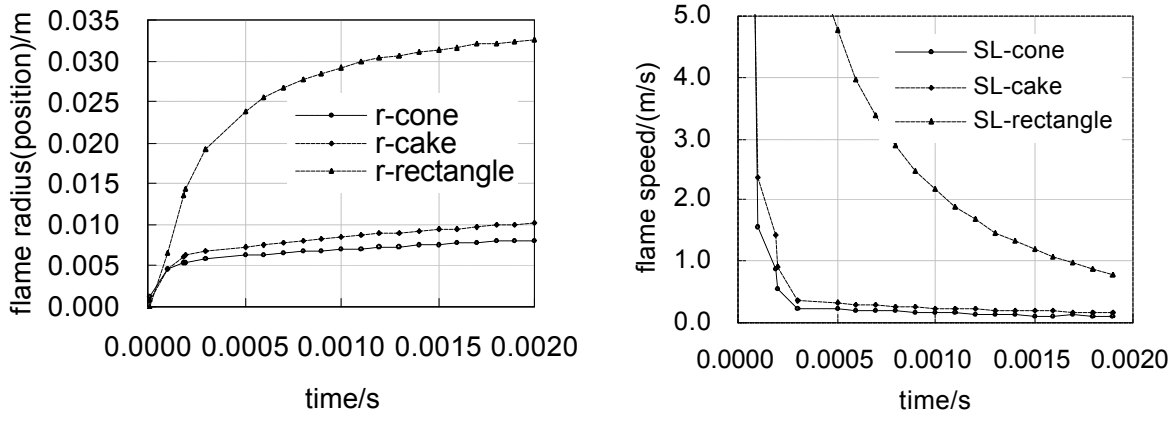

(a). Flame radius/position (b) Flame speed

Figure 4-11. Comparison of flame speed in different geometries with Magnussen model

Figure 4-11 gives a deep impression that the calculation results are definitely geometry dependent when the reaction flow is simulated with Eddy Breakup model.

This phenomenon can be explained by stretch effect, which will be discussed in detail later. The problem is: the stretch effect is too much in Eddy Breakup Model. The calculation result is too much dependent on geometry, which will lead to significant error when the model is use to simulate the combustion performance of hydrogen engines with different geometries.

4.2.6 Influence of time increment

Detailed study proves that the calculation result is greatly dependent on Calculation Time Increment.

Figure 4-12 gives the calculation results with Time Increment of 1e-5s, 2e-5s and 5e-5s separately. It shows that different time increment will get different calculation result.

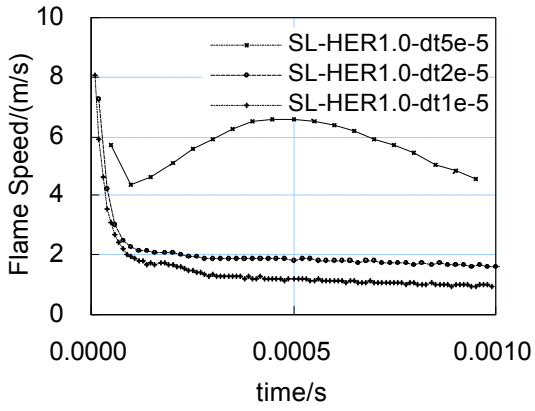

Figure 4-12. Influence of time increments on flame speed

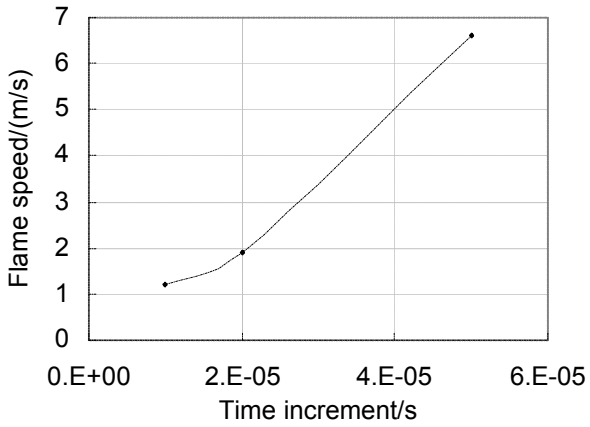

Figure 4-13. Relationship between averaged flame speed and time increment

Figure 4-13 shows the relationship between averaged flame speed (0.4ms~0.6ms) and time increment. It reveals a general trend that the bigger the time increment is, the faster the flame speed is.

Due to the reaction process is intensively influenced by turbulence condition, and the calculated turbulence condition is dependent of time increment (refer to 2.3.3.3), there is no temporal convergence in reaction flow simulation; the simulation result is definitely dependent on time increment.

The same phenomenon will be found with other combustion models. In other words, time increment will influence reaction speed no matter what model is used. Therefore, when the multi-case comparison is carried out, the time increment in all calculations must be the same. Otherwise, the comparison is meaningless.

4.2.7 Conclusion

Summarizing the studies in the section, the following conclusions can be made:

- Magnussen Model is a typical turbulent combustion model. The reaction speed is greatly dependent on Initial turbulence conditions.
- Reaction speed will increase linearly along with the increase of Initial TKE, but decease with the increase of Turbulence Length Scale.
- The model can simulate neither temperature Performance nor fuel concentration performance of Hydrogen combustion.

- Reaction speed is too much geometry dependent.
- Calculation results will also influenced by time increment. The bigger the time increment is, the faster the reaction will be. This conclusion is also applicable to other combustion models.
- Magnussen model can't be used for the general performance study of Hydrogen engine combustion.

4.3 Validation of CFM model

The CFM model assumes that reaction takes place within relatively thin layers that separate the fresh unburned gas from the fully burnt gas. Using this assumption the mean turbulent reaction rate is computed as the product of the flame surface density Σ and the laminar burning velocity S_L via:

$$\overline{rr_{fu}} = -w_L \Sigma \tag{4-3}$$

With ω_L as the mean laminar fuel consumption rate per unit surface along the flame front.

For lean combustion:

$$w_L = r_{fu,fr} S_L \quad \text{with} \quad r_{fu,fr} = r_{fr} y_{fu,fr} \tag{4-4}$$

Where, $\rho_{fu,fr}$ means partial fuel density of the fresh gas; ρ_{fr} is the density of the fresh gas and $y_{fu,fr}$ represents fuel mass fraction in the fresh gas.

4.3.1 Example calculation

An example, with the Pyramid mesh, is carried out to get the general understanding of simulated combustion results with CFM model. The calculation assumes that the initial turbulence kinetic energy is 20 m^2/s^2 with length scale of 0.001 m. The vessel in charged with stoichiometric hydrogen/air mixture at initial temperature of 300K, and initial pressure of 1 atm.

The control parameter in CFM model is set to be 400 1/m for Surface Density and 1.6 for Stretch Factor

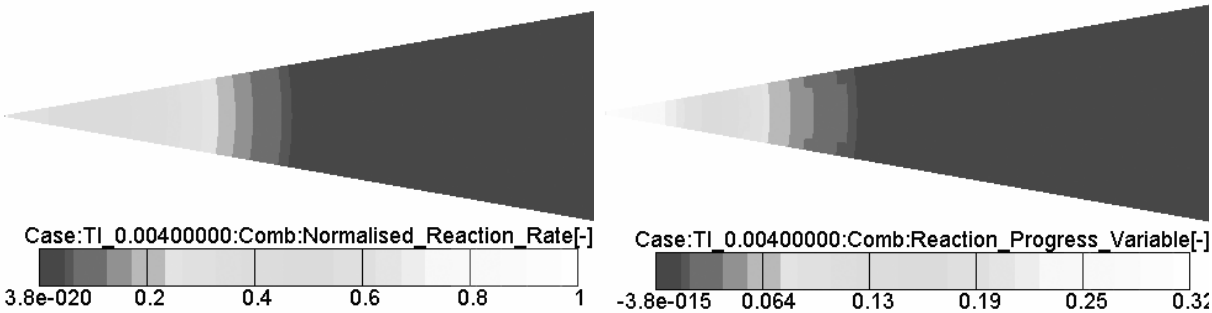

(a). Normalized reaction rate (b). Reaction progress

Figure 4-14. Example distributions with CFM model

Figure 4-14 shows the distribution of Normalized Reaction rate and Reaction

Progress of Hydrogen combustion at 4 ms. It can be seen that there is no obvious combustion surface. The combustion progress is typical turbulent combustion.

In order to make quantitative comparison, formula (A-10) is applied to this simulation, and the equivalent flame surface radius and flame speed are calculated and plotted in Figure 4-15.

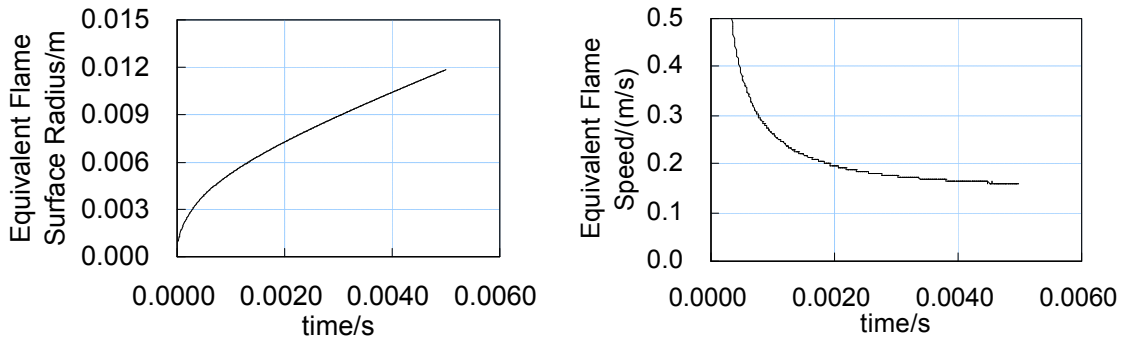

(a) (b)

Figure 4-15. Typical curves of flame surface and flame speed with CFD model

It gives the impression that there is no linear flame propagation. The flame speed will decrease continuously with the development of the flame.

Comparing with reference data in table 4-1, it can be seen that the calculated equivalent flame speed is far slower than hydrogen laminar flame speed even though the initial is set to be very high.

4.3.2 Control Parameter Influence

There are two tunable Parameters in CFM Model, named Stretch factor and Flame Surface Density, which will influence the reaction speed of given charge according to the manual. The recommended values in AVL FIRE 8.1 are:

- Stretch factor: 1~4 (default 1.6)
- Flame surface density: 100~500 1/m (default 300 1/m)

Detailed study is carried out to find the exact influence of these two factors on the reaction speed of hydrogen combustion.

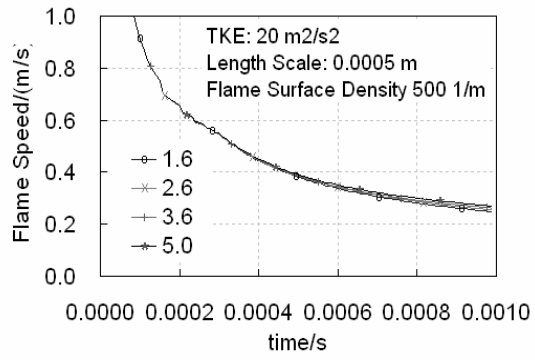

Figure 4-16. Influence of stretch factor on flame speed with CFM model

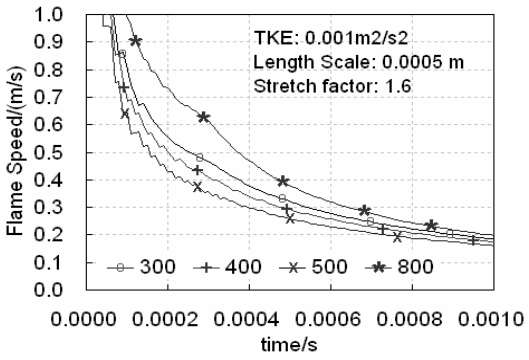

Figure 4-17. Influence of surface density on flame speed with CFM model

Figure 4-16 shows the variations of equivalent flame speed with different Stretch Factor. The initial condition in shown on the figure.

According to the manual, an increase of the stretch factor leads to an intensification of the production of flame surface and hence in a shorter and faster combustion phase. But the calculated results show little difference. In other words, Stretch factor has very little influence on hydrogen-Air reaction speed.

Figure 4-17 shows the variations of equivalent flame speed with different Flame Surface Density.

It can be seen that the calculated equivalent flame speed is obviously influenced by Initial flame surface density at the begging of the combustion. But the influence becomes smaller and smaller with the development of the flame. The calculated equivalent flame will converge to the same value when the flame is fully developed no matter how much the initial flame surface density is.

Further more, the simulated flame speed is too low compared with the reference data in table 4-1 no matter how large the factors are selected. Present CFM model is not capable to simulate hydrogen combustion just from the point of view of reaction speed.

Theoretically, the simulated flame speed range should cover the normal range of hydrogen laminar flame speed, based on formula 4-5. The most possible reason for this shortcoming might be that the present database inside FIRE 8 is not properly set for hydrogen fuel.

Due to the above shortcoming in present FIRE version, other performances, such as temperature effect, pressure effect and concentration effect, will not be reasonable. Further studies on these effects are not necessary.

4.3.3 Influence of Initial Turbulence Conditions

Similar to 4.2.5, both the turbulence effect is studied in both aspects: the influence of Initial TKE and the influence of initial turbulence length scale. This study is just to have a general understanding of the turbulence effect in CFM model.

Table 4-3 Initial conditions for turbulence effect study

case	TKE/ (m^2/s^2)	Length Scale/m	Temperature /K	Pressure /pa	Stretch factor	Initial Flame surface density /(1/m)
TKE effect	0.5-20	0.001	300	100,000	2.6	500
Length effect	20	0.0005-0.01	300	100,000	3.6	400

The initial conditions are for all of the calculations are listed in table 4-3

Figure 4-18 and figure 4-19 present the calculated equivalent flame speed curves

with different initial TKE and different turbulence length scale respectively.

From Figure 4-18, it can be found that the reaction will be accelerated with the increase of initial TKE, but the effect is not as much as that in other Models. Again, the maximum equivalent flame speed is much smaller than the experimental laminar flame speed of hydrogen (2.18 m/s) even if the Initial TKE is as high as 20 m^2/s^2.

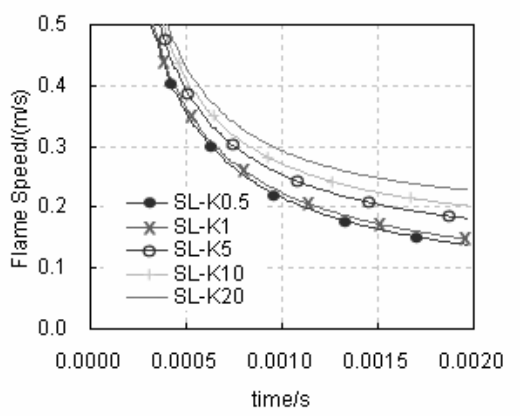

Figure 4-18. Influence of initial TKE on flame speed with CFM model

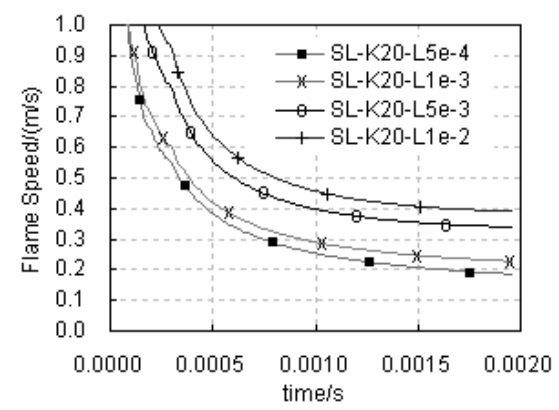

Figure 4-19. Influence of initial turbulence length scale on flame speed with CFM model

From figure 4-19, the following phenomena can be found:

- Being contrary to Magnussen Model, the increase of initial turbulence length scale will accelerate the reaction process in CFM Model.
- The maximum equivalent flame speed is still much smaller than the Laminar flame speed of Hydrogen (2.17m/s) even if the Initial Length scale is set to be 0.01m (20% of the maximum dimension of the object).

4.3.4 Conclusion

The above study on CFM model gives the following impression:

- CFM is a simply turbulence combustion model. It cannot be used to simulate laminar hydrogen combustion.
- Stretch factor has little influence on reaction speed. Increase of Initial flame surface density will obviously enhance the reaction speed during Ignition phase, but the effect will reduce gradually with the development of flame.
- The reaction process is significantly influence by initial turbulence condition. Both Initial TKE and Turbulence length scale have positive influence on reaction speed.
- The present FIRE version cannot simulate high-speed combustion (such as Hydrogen combustion) with CFM Model.

4.4 Validation of PDF model

The Probability Density Function model, takes into account the simultaneous effects of both finite rate chemistry and turbulence, and thus obviates the need for any prior assumptions as to whether one of the two processes is limiting the mean rate of reaction.

In this method, the thermochemistry of the reactive mixture is expressed in terms of reaction progress variable c, the mixture fraction f, and the enthalpy in order to account for non-adiabaticity and bulk compression effects on temperature.

The current method solves a transport equation for the joint probability density function of the mixture fraction f, the reaction progress variable c, and the enthalpy h by means of a Monte Carlo Simulation technique.

4.4.1 Example calculation

The same as previous sections, an example calculation is carried out with PDF combustion model in order to get the general understanding of the calculated results and post-processing procedure.

The Initial condition is set to be 300K at 1 atm with the initial TKE of 20 m^2/s^2 and initial turbulence length Scale of 0.0005 m.

The three control parameters in PDF model are set as following:

- Pre-Exponential Factor: 5.0000E+11 m3/kg/s
- Activation Energy: 1.7000E+08 J/kmol
- Mixing Rate Constant: 5.0

Figure 4-20 shows the reaction rate and temperature distributions of the example calculation at 3.0ms.

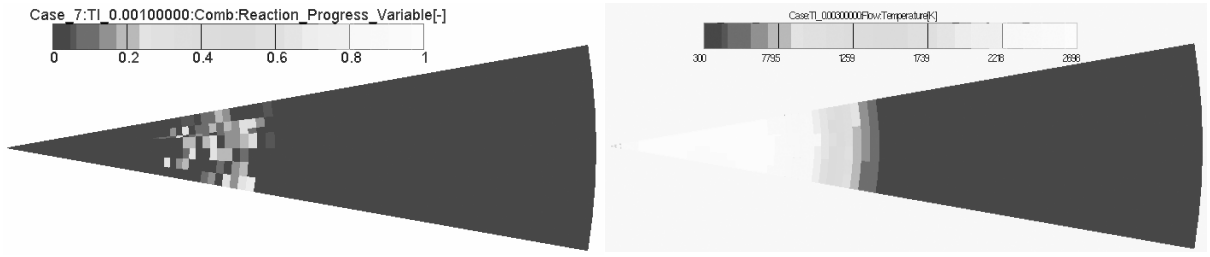

(a) Normalized reaction rate (b). Temperature

Figure 4-20. Example distributions with PDF model

From temperature distribution picture, the combustion surface can be observed obviously. But the reaction rate picture gives clear impression that the reaction takes place in a wide range rather than on a thin surface. The reaction is typical turbulent combustion process with the characteristic of incontinuity, which is resulted by the methodology in PDF model.

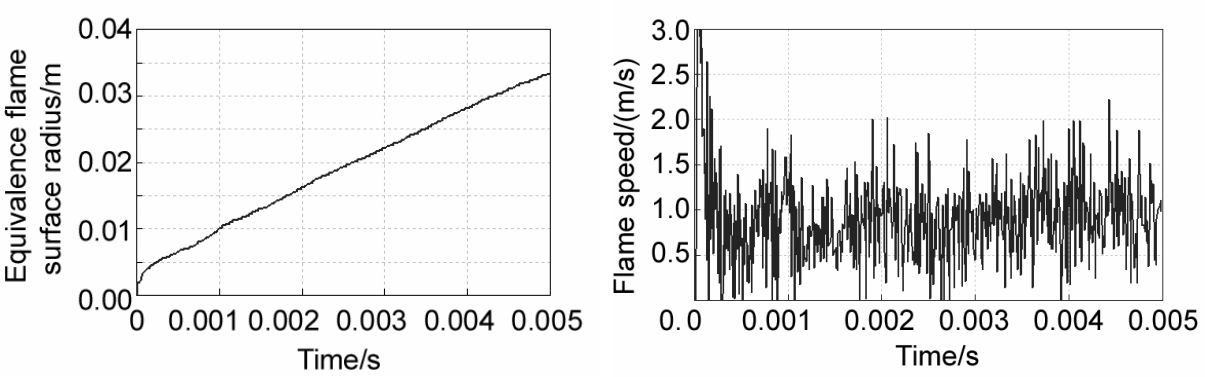

(a) (b)

Figure 4-21. Typical curves of flame surface and flame speed with Magnussen model

Figure 4-21a) shows the variation of the flame radius. Roughly, the increase of flame radius presents linear trend. But the flame speed (figure 4-21b, calculated with formula 4-10) fluctuates violently due to the incontinuity of the combustion process.

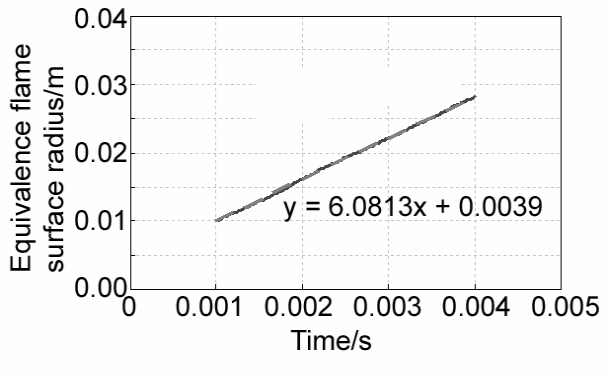

Figure 4-22. Trend line of flame radius curve for flame speed calculation with PDF model

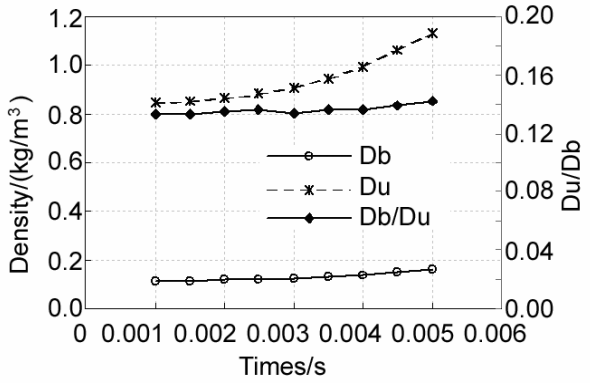

Figure 4-23 Density curves for flame speed calculation with PDF model

In the post-processing PDF results, formula (A-10') will get more smooth flame speed. The procedure is as following:

1). Find the trend line of flame surface radius curve in interested range (1~4ms in Figure 4-22), and get the gradient (dr/dt).

2). Measure the density in burnt zone and density in unburned zone, separately from 3D results and calculate the ratio of D_b to D_u.

Figure 4-23 presents the variation of D_b, D_u and D_b/D_u respectively. It is clear that D_b/D_u keeps almost the same in a wide range (D_b/D_u keeps to be around 0.135 in the example calculation from 1ms to 4ms).

3) Apply formula (4-10') to calculate the mean flame speed in the interested range.

$$St = \frac{D_b}{D_u} dr/dt = 0.135 \times 6.08 = 0.82(m/s)$$

The procedure of the example calculation is listed in table 4-4.

Table 4-4 Flame speed calculation with PDF model

time	Db	Du	Db /Du	Mean	dr/dt	Mean flame speed
s	kg/m3	kg/m3			m/s	m/s
0.0010	0.113	0.850	0.133			
0.0015	0.114	0.855	0.133			
0.0020	0.117	0.867	0.135			
0.0025	0.120	0.886	0.136	0.135	6.080	0.82
0.0030	0.122	0.911	0.134			
0.0035	0.129	0.947	0.136			
0.0040	0.135	0.997	0.136			
0.0045	0.148	1.064	0.139			
0.0050	0.161	1.134	0.142			

All of the flame speeds are calculated in the same way and will not be repeated in the following part of this section.

4.4.2 Turbulence effect

The initial conditions and PDF control parameters are set the same setting as that in the example calculation, but with different initial turbulence kinetic energy.

By giving different initial TKE (from 0.01 to 20 m^2/s^2), a group of results are calculated with PDF model.

By focusing on the interested range of flame surface radius from 0.01m to 0.015m, a group of flame speeds are calculated.

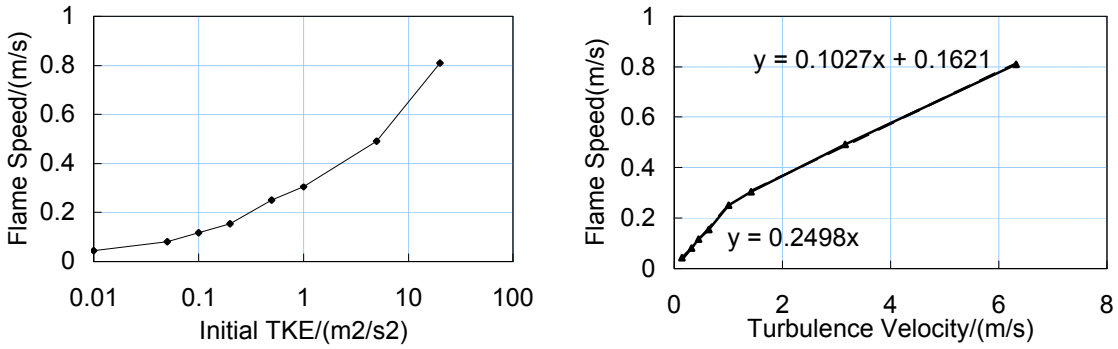

a) b)

Figure 4-24. Turbulence effect on flame speed with PDF model

Figure 4-24a) shows the relationship between initial TKE and calculated flame speed. Figure 4-24b) gives relationship between initial turbulence velocity and flame speed.

The initial turbulence velocity, u_0', is calculated with the following formula:

$$u_0' = \sqrt{2K_0}$$

Figure 4-24b) gives a rough impression that the relationship between u_0' and flame speed is piecewise linear. Initial turbulence intensity has much stronger influence on reaction speed in the range of $0<u_0'<1$ than that in the range of $u_0'>1$.

4.4.3 Concentration effect

With the same initial conditions and PDF control parameter as that in example calculation, the concentration effect is studies by varying the equivalence ratio of the charge.

The calculation results, which are derived by setting different hydrogen concentrations, are plotted and compared with the reference data in Figure 4-25.

The results show that:

(1). In the range of ϕ=0.3 to 1.0, the leaner the mixture is, the slower the flame speed will be.

(2). The variation has the similar tendency as the experiment result in spite that the calculated value of flame speed, which is dependent of initial turbulence conditions and can be adjusted by tuning the parameters of PDF model, is much smaller than the reference value.

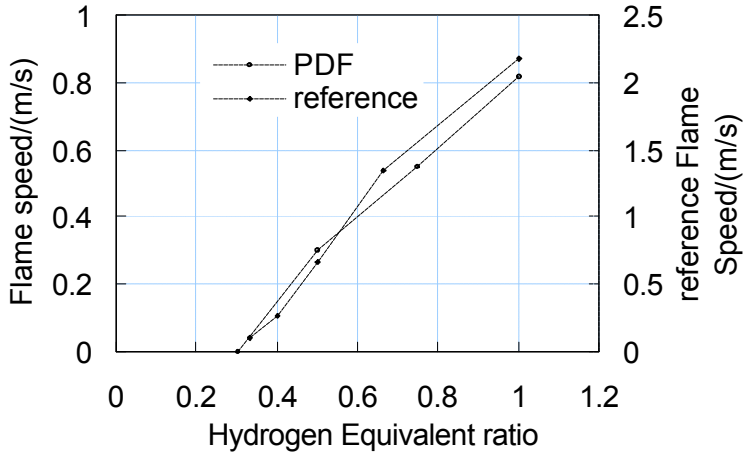

Figure 4-25 Comparison of simulated concentration effect on flame speed with PDF Model versus reference data

4.4.4 Temperature effect

With the initial pressure of 1 atm, Initial TKE of 1 m^2/s^2 and turbulence length Scale of 0.0005 m, the temperature effect for stoichiometric hydrogen/air mixture is studied in this section.

The control parameter in PDF model is set as following:

- Pre-Exponential Factor: 5.0E+11 $m^3/kg/s$
- Activation Energy: 1.6E+08 J/kmol
- Mixing Rate Constant: 5.0

Figure 4-26a gives the variation of D_b/D_u at different initial temperature. It shows that the higher the initial temperature is, the bigger the ρ_b/ρ_u is. That is to say, the higher temperature is, the faster the expansion speed will be in the burnt zone.

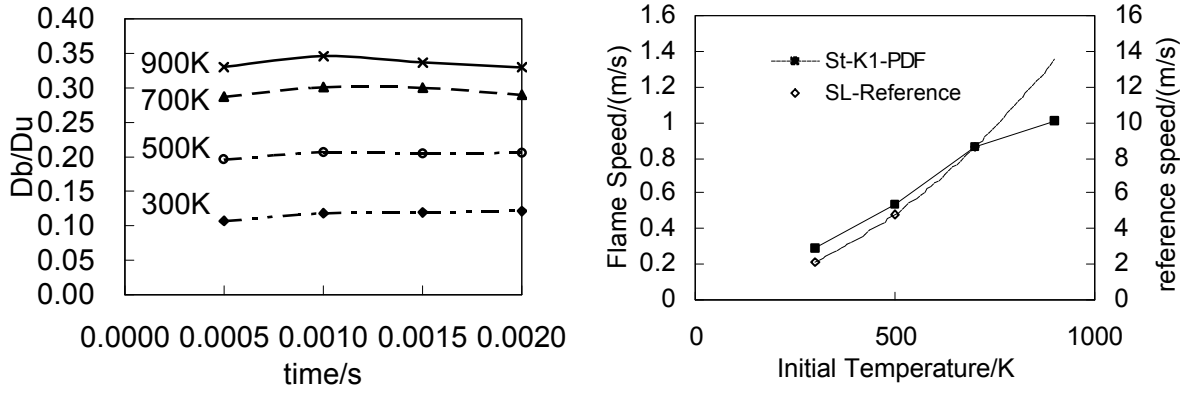

a) b)

Figure 4-26 Comparison of simulated temperature effect on flame speed with PDF Model versus reference data

Figure 4-26b presents the comparison of the calculated turbulence flame speed and the reference data in table 4-1. The two curves show the similar tendency, but the calculated speed is almost an order smaller than the reference data.

This study shows that PDF can simulate the temperature effect with reasonable variation trend.

4.4.5 Pressure effect

With the initial temperature of 300K, Initial TKE of 20 m^2/s^2 and turbulence length Scale of 0.0005 m, the pressure effect for stoichiometric hydrogen/air mixture is studied in this section.

The control parameter in PDF model is set the same as that in 4.4.4

The variation of calculated turbulence flame speed is presented in figure 4-27.

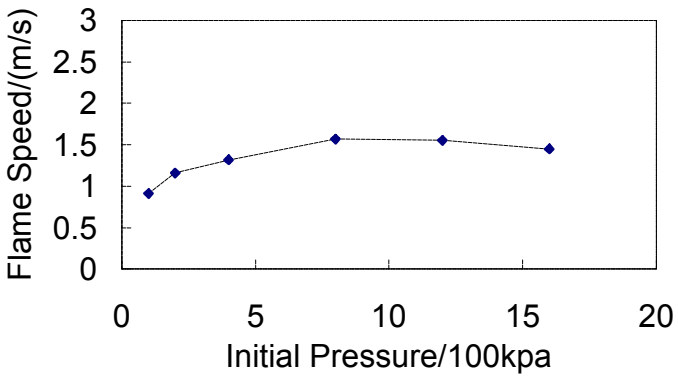

Figure 4-27. Simulated pressure effect on flame speed with PDF Model

The calculation results show that the turbulence flame speed will increase with

the increase of initial pressure in the range of 100-800kpa. This performance is accord with John Manton and B. B. Milliken's theory (refer to 4.5.7). When pressure is higher than 800kpa, there is a slight negative effect.

4.4.6 Comparison of calculation time

In order to compare the CPU time consumptions with different combustion models, comparison calculations are carried out with the same initial setting. Figure 4-28 presents the difference among different models.

Model consumes almost double CPU time as that of other three models. The consumed CPU time is almost the same with Magnussen models, CFM model and TFSC model.

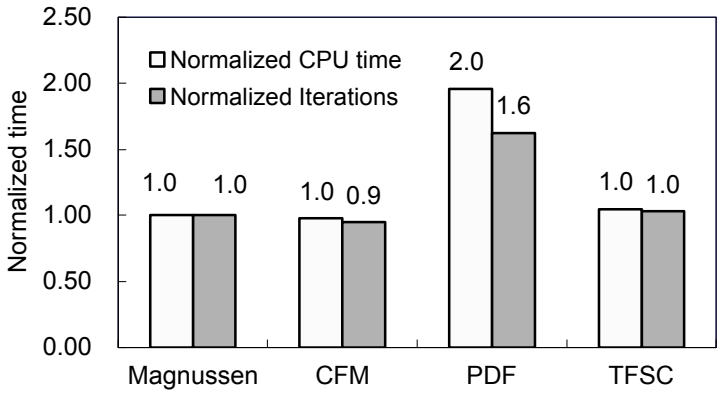

Figure 4-28. Comparison of CPU time and iterations for different combustion models

4.4.7 Conclusion

Up to now, the general impression to PDF model can be summarized:

- PDF model is based on turbulent combustion. The reaction speed is greatly dependent on initial turbulence condition. Therefore, it can't be used to simulate laminar combustion.
- The stronger is the initial TKE, the faster is the reaction speed. When initial TKE is zero, there is no reaction.
- PDF model can correctly reflect temperature and concentration effects in Hydrogen engine combustion. It is a good model for turbulence combustion study.
- PDF model is much more time consuming other models.

4.5 Validation of TFSC Model

The kernel of the Turbulence Flame Speed Closure model is the determination of the reaction rate based on an approach depending on parameters of turbulence, i.e. turbulence intensity and turbulent length scale, and of flame structure like the flame thickness and flame speed, respectively.

The reaction rate can be determined by two different mechanisms via:

- Auto-ignition and
- Flame propagation scheme

The auto-ignition scheme is described by an Arrhenius approach and the flame propagation mechanism depends mainly on the turbulent flame speed. The larger reaction rate of these two mechanisms is the dominant one. Hence, the fuel reaction rate ω_{fuel} can be described using a maximum operator via:

$$\overline{r r_{fu}} = \max\left\{\text{Auto - ignition } w_{AI}, \text{Flame Propagation } w_{FP}\right\} \tag{4-5}$$

The first scheme is only constructed for air/fuel equivalence ratios from 1.5 up to 2.0 and for pressure levels between 30 and 120 [bar], respectively. The auto-ignition reaction rate ω_{AI} can be written as:

$$w_{AI} = a_1 r^{a_2} y_{fuel}^{a_3} y_{O_2}^{a_4} T^{a_5} \exp\left(-\frac{T_a}{T}\right) \tag{4-6}$$

Where a_1 to a_5 are empirical coefficients and T_a is the activation temperature, respectively.

The reaction rate ω_{FP} of the flame propagation mechanism, the second one in this model, can be written as the product of the gas density, the turbulent burning velocity S_T and the fuel mass fraction gradient ∇y_{fuel} via:

$$w_{FP} = r S_T \nabla y_{fuel} \tag{4-7}$$

In order to apply this model also for inhomogeneous charge processes, the fuel mass fraction gradient is replaced by the reaction progress variable gradient multiplied by the stoichiometric mixture fraction as follows:

$$w_{FP} = r S_T \nabla c f_{st} \tag{4-8}$$

This approach can also be used for homogeneous charge combustion and a near-wall treatment of the reaction rate is considered additionally.

The turbulent burning velocity S_T is determined by the following formula:

$$S_T = \left(S_L + \frac{1}{\sqrt{2}} a u'\right)\left(1.0 - Ka^2\right) \quad \text{.....for } 0 < \text{Ka} < 0.5 \tag{4-9}$$

$$S_T = \frac{3}{4} S_L \left(\frac{ab}{2\sqrt{2}} + 1\right) \quad \text{.....for } 0.5 < \text{Ka} < 1.0 \tag{4-9a}$$

$$\text{ST} = 0.0 \quad \text{.....for Ka} > 1 \tag{4-9b}$$

With

$$a = \left(1.0 + \frac{d_L}{l_t}\right)^{b_4} \quad \text{and} \quad b = b_5 \left(\frac{S_L}{u'}\right)^{b_6} \left(\frac{l_t}{d_L}\right)^{b_7} \tag{4-10}$$

Where Ka is the local turbulent Karlovitz number, which is calculated with the following formula:

$$Ka = b_1 \left(\frac{u'}{S_L} \right)^{b_2} \left(\frac{d_L}{l_t} \right)^{b_3} \tag{4-11}$$

In these expressions, δ_L is the laminar flame thickness, S_L as laminar flame velocity, u' represents the turbulence intensity, l_t the turbulent length scale and b_1 to b_7 are constants, respectively. The laminar burning velocity S_L, which is necessary for the determination of the turbulent burning velocity and the flame thickness δ_L, can be expressed via:

$$\left. \begin{matrix} S_L \\ d_L \end{matrix} \right\} = \left(c_1 + c_2 l + c_3 l^2 + c_4 l^3 + c_5 l^4 \right) \times \left(c_6 + \frac{c_7}{c_8 + p} + \frac{c_9}{c_{10} + c_{11} p + p^2} \right) \times \exp\left(c_{12} + \frac{c_{13}}{T} + \frac{c_{14}}{T^2} \right) \tag{4-12}$$

Where, c_1 to c_{14} are empirical parameters.

Hence, the laminar flame speed S_L and flame thickness δ_L, respectively, depend on the air excess λ, pressure p and temperature T.

4.5.1 Example calculation

The initial condition is also set to be 300K at 1 atm, but with very small Turbulence (TKE of 0.001 m^2/s^2 and Length Scale of 0.0005 m).

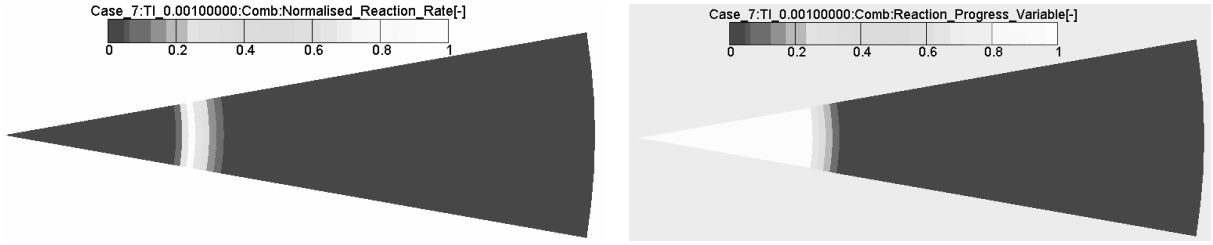

a) b)

Figure 4-29 Example distributions with TFSC model

The only adjustable control parameter $C_{FP,}$ which influences the flame reaction rate, is set to be 3.4 in the example calculation.

Figure 4-29 presents the distribution of normalized reaction rate and reaction progress variable. The pictures show very thin reaction layer, which divides the burnt zone and unburned zone clearly. It appears to be a typical linear combustion phenomenon.

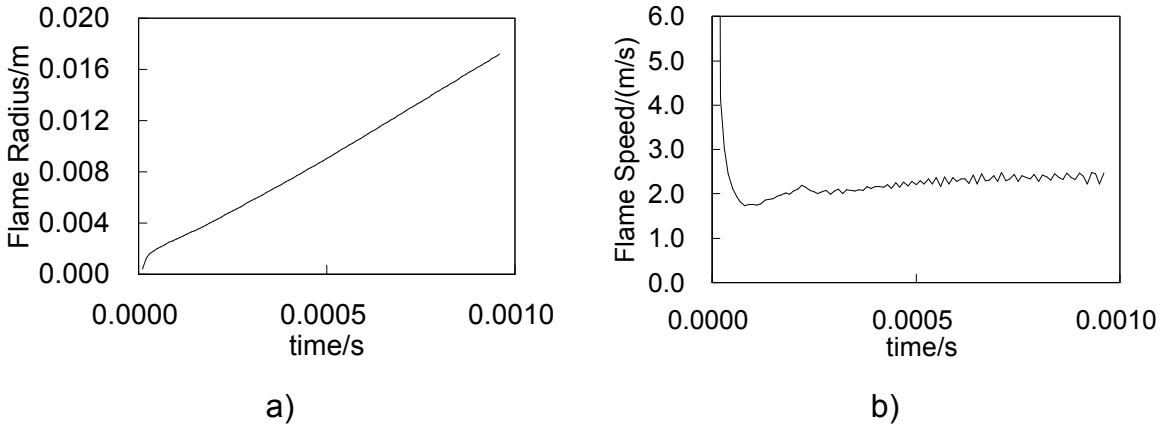

a) b)

Figure 4-30. Typical curves of flame surface and flame speed with TFSC model

The variations of flame surface radius and flame speed are plotted in figure 4-30. The flame surface radius shows a clear liner trend and the flame speed keeps roughly a constant value when there is stable combustion (after 0.6ms or flame radius is bigger than 10 mm). The mean value in the flat range will be treated as the representative flame speed in the later studies in this section.

Previous calculation proves that, when other models (Magnussen, CFM, PDF) are selected, there will be no stable combustion if the initial turbulence kinetic energy is too small, say less than $0.01m^2/s^2$. Therefore, this calculation gives a very prospective signal that TFSC Model is capable to simulate laminar combustion.

4.5.2 Turbulence effect

The turbulence effect is the most important performance for laminar flame speed validation. Therefore, this is effect is studied in the first place. The main purpose of this study is to find the influence of initial turbulence condition on flame speed in order to prove that the TFSC Model can simulate truly laminar combustion.

Similar to 4.2.5, the study is carried out by considering two aspects:

(1). Influence of Turbulence Kinetic Energy. Keeping the initial Turbulence Length Scale to be 0.0005 m, the influence is studied by changing the initial TKE.

(2). Influence of Turbulence Length Scale. Keeping the initial TKE to be $0.001\ m^2/s^2$, the influence is studied by changing the initial Turbulence Length Scale.

All of the calculations have the same initial temperature of 300K and initial pressure of 100kpa. The control parameter, C_{fp}, is set to be 3.4 and the charge is at stoichiometric condition.

Figure 4-32 and Figure 4-33 show the variation of flame speed with initial TKE and initial length scale respectively.

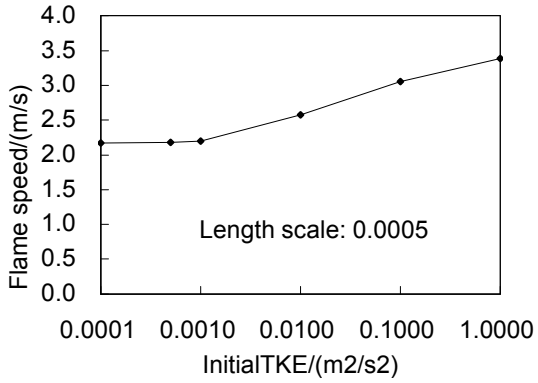

Figure 4-31. Influence of initial TKE on flame speed with TFSC model

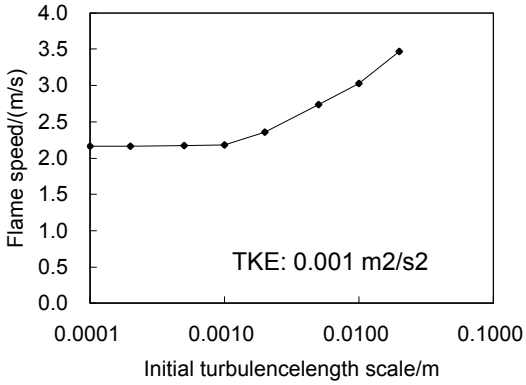

Figure 4-32. Influence of initial turbulence length scale on flame speed with TFSC model

Figure 4-31 shows a clear trend that the calculated Flame speed will decease with the decrease of TKE, until it converge to a fixed value. When TKE is less than 1e-3m^2/s^2, the flame speed is independent of the initial TKE and keep to be the same value as 2.2 m/s.

The same phenomenon appears in figure 4-32. When turbulence length scale is small enough, the calculated flame speed will converge to the same value as that in figure 4-31.

When TKE is close to zero, energy and mass transfers are accomplished mainly by molecular movement; the combustion tends to be laminar, rather than turbulence combustion. When turbulence length scale is less than the dimension of one cell, it means that the eddy Scale is so small that the turbulence effect is similar to that of molecular movement in CFD study.

Therefore, the calculated flame speed is definitely laminar flame speed when TKE and length scale tend to zero.

Further more, the study in this section proves that the pre-conditions for laminar combustion simulation should be:

- Initial TKE is less than 0.001 m^2/s^2
- Initial turbulence scale is less than 0.001 m

Comparing figure 4-31 and figure 4-32 with related figures in other sections, the conclusion can be made that TFSC model is the only model to be able to simulate laminar combustion process.

4.5.3 Constant Cfp influence on Reaction Speed

It is worth emphasizing that TFSC model has only one control parameter, which should be adjusted according to the fuel property. This characteristic makes the application of this model very convenient.

This section is going to study the influence of the control parameter on reaction speed and to find a suitable value of C_{FP} for Hydrogen combustion simulation.

Figure 4-33 presents the relationship between C_{FP} and simulated flame speed.

The calculation results show a clear trend that the flame speed will increase linearly with the increase of C_{fp}. The relationship can be described in the formula:

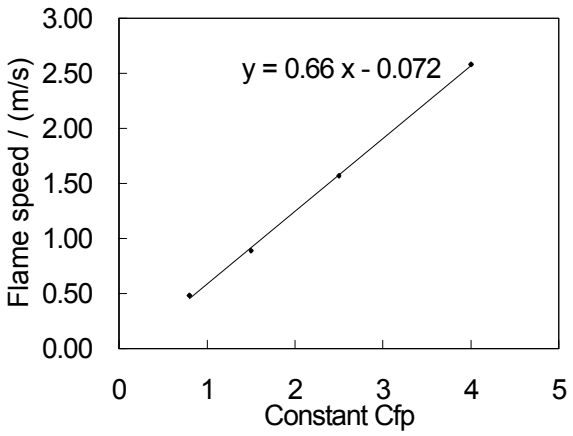

Figure 4-33 relationship between constant C_{fp} and flame speed in TFSC model

$$S_L = 0.66 \times C_{FP} - 0.072 \quad (4\text{-}13)$$

Since the laminar flame speed of Hydrogen is 2.17m/s at 300K/1bar, the Suitable C_{fp} for Hydrogen combustion simulation should be 3.4.

4.5.4 Geometry influence

4.5.4.1 Stretch effect introduction

Before the numerical study, it is necessary to review the stretch effect.

It is well known that stretch, consisting of strain rate and curvature, has a profound effect on the local flame speed through coupled effects of unequal heat and mass diffusion.

The general definition of stretch is[8]:

$$\Gamma = \left(1/A\right) dA/dt \quad (4\text{-}14)$$

When applied to expanding flame:

$$\Gamma = \left(\frac{k}{r}\right) dr/dt \quad (4\text{-}14a)$$

Where A is the area of the flame, r is its radius. k equals to 1 for 2D expansion flame and 2 for 3D expansion flame.

The relationship between stretch and burning velocity in low stretch regime can be expressed as:

$$S_{L,r} = S_L^0 - L\Gamma \quad (4\text{-}15)$$

$$(S_{L,r} - S_L^0)/S_L^0 = \frac{L}{S_L^0} \times \left(\frac{k}{r}\right) dr/dt \quad (4\text{-}15a)$$

Here, $S_{L,r}$ is the flame velocity referred to the reference surface, and S_L^0 is the 1D

flame speed according to its definition. *L* is the Markstein length.

David and his partners investigated the Markstein length for Hydrogen-Air flame, and gave the result as shown in figure 4-34. There is negative stretch effect for lean mixture, and positive effect for rich mixture. With the stoichiometric mixture, the Markstein length is approximate 0.02mm.

From previous simulation, it is known that the speed of flame surface, *dr/dt*, is around 15 m/s in stoichiometric combustion. Therefore, the influence of stretch effect on flame speed can be calculated with formula 4-15a.

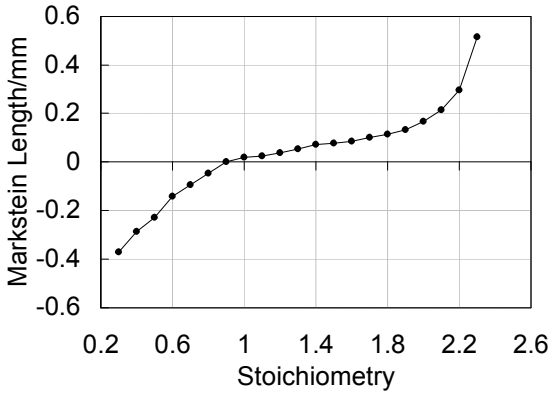

Figure 4-34 Markstein length for hydrogen/air as a function of stoichiometry

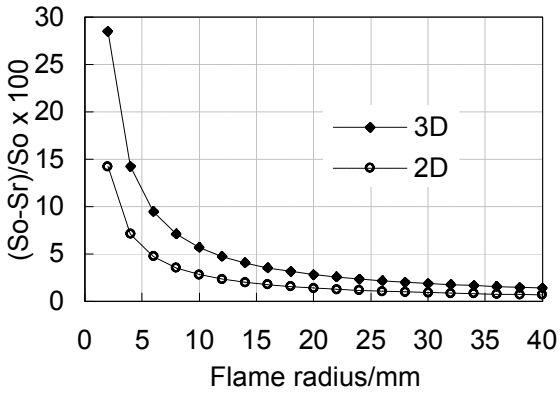

Figure 4-35 Stretch effect on flame speed for stoichiometric hydrogen/air mixture

Figure 4-35 shows the calculated influence of stretch effect on flame speed for stoichiometric Hydrogen/Air mixture. It can be seen that the stretch has significant influence on flame speed when the flame radius is very small. But the influence will reduce rapidly with the increase of flame radius. When flame radius is bigger than 10 mm, the influence will be less than 5%.

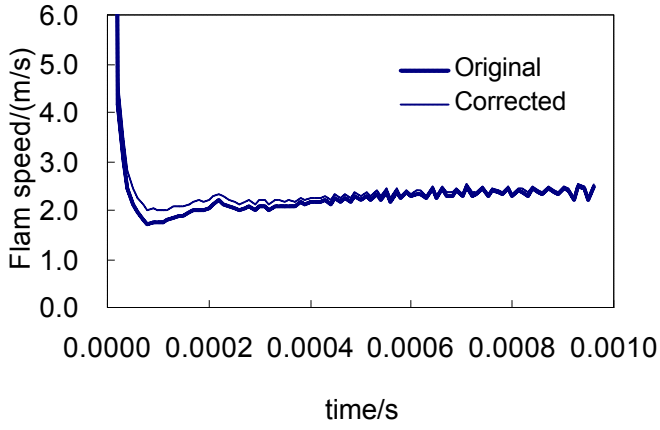

Figure 4-36 Comparison of direct calculated flame speed versus corrected one

Figure 4-36 gives the comparison of the corrected flame speed curve and the original one in example calculation. It can be seen that there is obvious difference at the beginning of the combustion, but the two curves almost overlap

when the flame has fully developed after 0.6ms (r> 10mm).

In fact, the representative flame speed is calculated by averaging the flat rang after 0.6 ms as explained in 4.5.1. Therefore, the stretch effect has no much influence to the calculation of flame speed in this section.

4.5.4.2 Geometry influence with TFSC model

The three typical geometries are adopted to see the geometry influence with TFSC model.

Figure 4-37 shows the comparison of the flame speed in the three geometries.

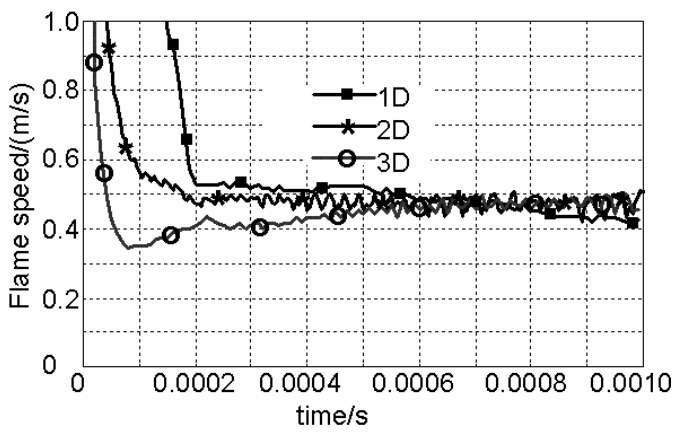

Figure 4-37 Calculated flame speed in different geometries with TFSC model

Here gives a brief analysis of Figure 4-37:

- During 0.2ms to 0.6ms, 1D model has the fastest flame speed; 3D model has the lowest flame speed, and that of 2D model is in the middle. This is obviously because of the flame stretch effect.
- During 0.6ms to 0.8ms, all the three models get almost the same flame speed because the stretch effect becomes smaller and smaller with the increase of the radius of flame ball/cylinder. The flame speed in this period should be the actual value of Hydrogen combustion.
- After 8e-4s, the flame speed of 1D model will decrease, while those of 2D and 3D model will not change significantly. This is because of the rapid pressure increase, consequently the density of unburned mixture increases, in 1D model.

Compared figure 4-37 with figure 4-11b, big difference can be found. The analysis in 4.5.4.1 proves that the stretch effect could not cause so much difference as shown in figure 4-14b. Therefore, the result in figure 4-37 is more reasonable. In other words, TFSC model can uniformly simulate Hydrogen laminar combustion with little influence of geometrical difference.

4.5.5 Effect of initial Temperature

With the initial pressure of 100kpa, Initial TKE of 0.001 m^2/s^2 and turbulence length Scale of 0.001 m, the temperature effect for stoichiometric hydrogen/air mixture is studied in this section.

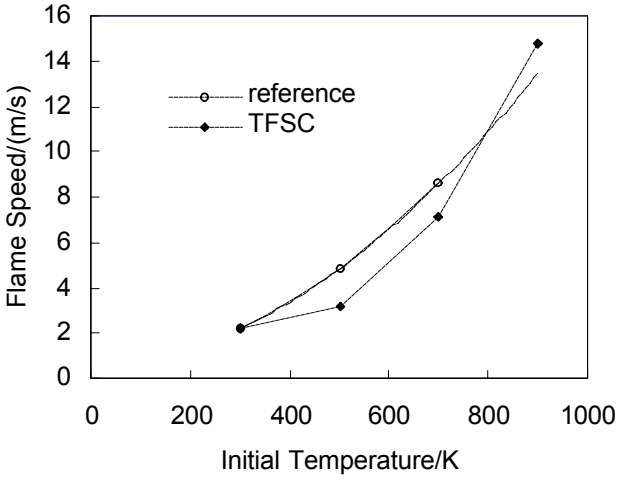

Figure 4-38. Comparison of simulated temperature effect on flame speed with TFSC Model versus reference data

Figure 4-38 shows the variation of flame speed (solid line) with different initial Temperature. The reference data are also given with the trend line up to 900K (dashed line).

Even though there is a little difference, the calculated result shows the same trend as the reference data. When the high temperature range (700K~900K) is focused, which is the actual ignition condition in the real engine, the calculated results will show good consistent with the trend line of the reference data. Therefore, it can be concluded that TFSC model can be used to simulate laminar hydrogen combustion with good temperature effect.

4.5.6 Concentration effect

In the wide range of flammability, the laminar flame speed of hydrogen/air mixture changes considerably. Therefore, concentration effect plays an important role for the performance of hydrogen engine.

4.5.6.1 Result comparison

Figure 4-39 gives a comparison of the calculated result and the reference[9] data at initial Temperature of 300K.

The experimental result (the dashed line) shows that the flame speed reaches its maximum value between 1.5 and 2.0 stoichiometric, and decreases gradually on both sides.

The calculation result shows a strange combustion performance:

- The maximum flame speed is at 1.1 stoichiometric

- In the range of 0.8~1.3 stoichiometric, the curve is quit smooth, but decrease rapidly on both sides.
- The curve turn up sharply when the mixture is leaner than 0.5 stoichiometric.

When the two curves are compared, it gives an impression that only in the range of 0.5~1.0 stoichiometric the calculated result has the same trend with the experiment data. Neither lean (less than 0.5) combustion results nor rich (higher than 1) ones are reasonable!

Figure 4-40 presents the variation of flame speed in the range of 0.5~1.0 stoichiometric with different initial temperature. It shows the similar performance that:

- The richer the mixture is, the faster the reaction will be;
- The higher the temperature is, the faster the flame speed is.

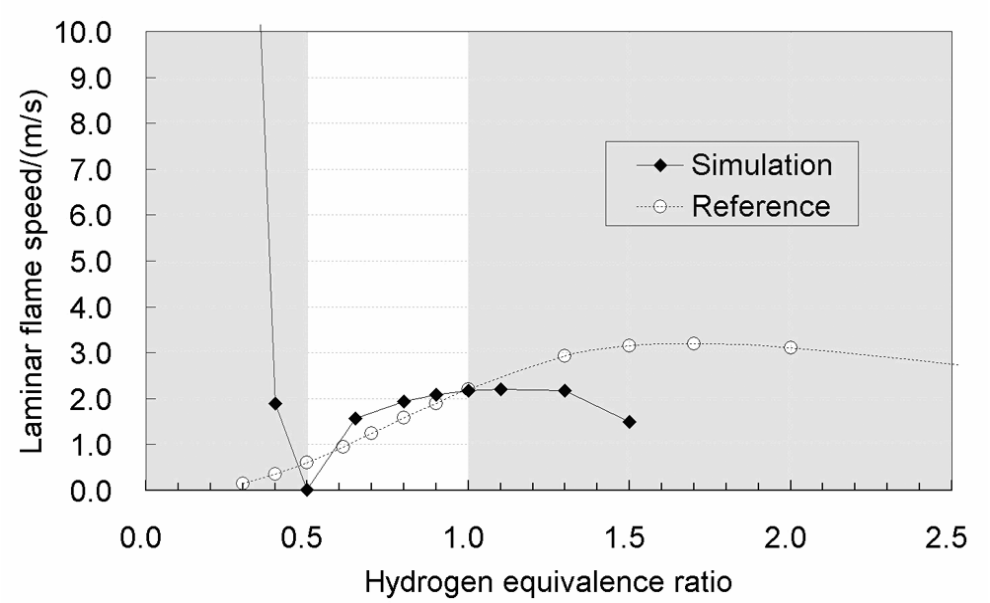

Figure 4-39 Comparison of simulated concentration effect on flame speed with TFSC Model versus reference data

The most satisfying phenomenon is that the concentration-speed curve at high temperature, say at 900K, resembles more the sharp of the experiment curve than that at 300K. Since the initial temperature in hydrogen engine is normally in the range of 700K to 900K, the TFSC model gives reasonable temperature effect under engine condition.

As explained in previous that the main function of simulation is to predict the variation trend of a phenomenon. From this point of view, TFSC model can simulate concentration effect of hydrogen/air with reasonable result in the range of 0.5 to 1.0 stoichiometric.

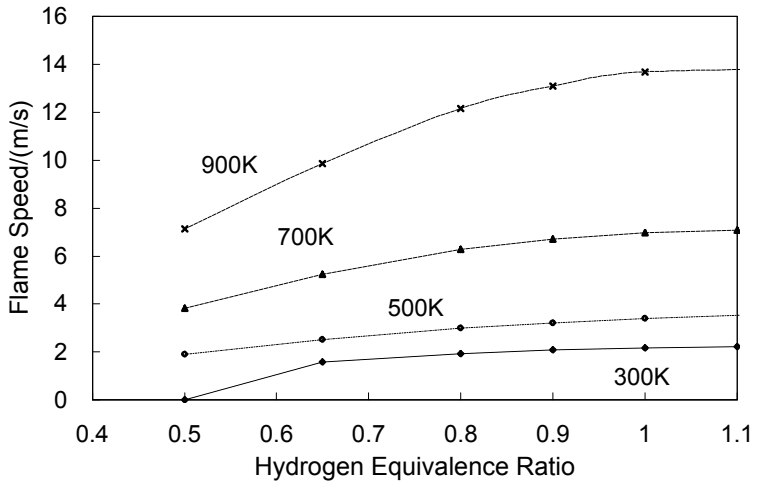

Figure 4-40. Simulated concentration effect on flame speed at different initial temperature with TFSC Model

4.5.6.2 Problems analysis

The strange performance, which is shown in figure 4-42, may be because of the following reasons:

- FIRE 8.11 is compiled mainly for the simulation of Diesel engine and Gasoline Engine. The inside database has not been correctly set for Hydrogen combustion in the present version.
- TFSC Model is the newest combustion model, which is just implemented in the latest version of FIRE. It needs to be improved for hydrogen combustion simulation.

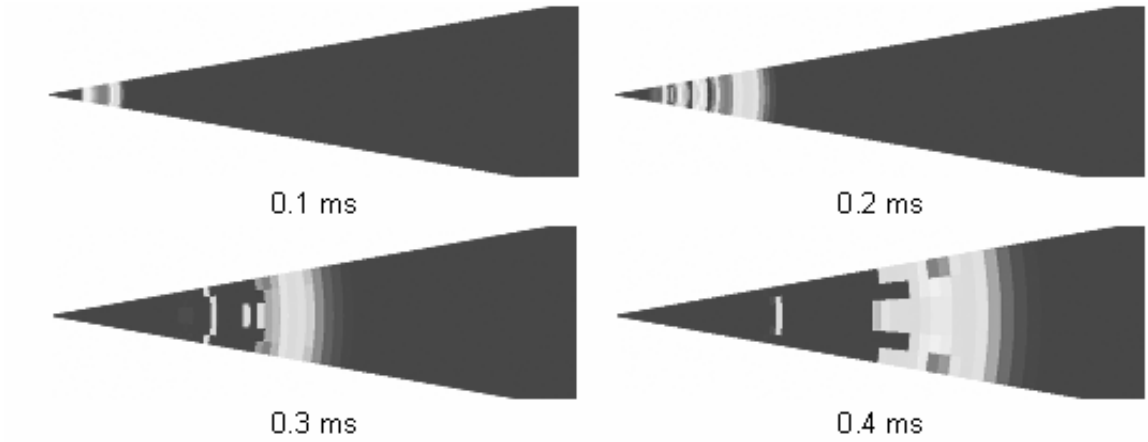

Figure 4-41. Abnormal reaction distribution for lean combustion with TFSC model

Figure 4-41 shows the normalized reaction rate during the ignition (0~0.3 ms) and early flame combustion phase (0.4 ms) with 0.3 stoichiometric. There is no laminar combustion in this case. It is obvious that this is not laminar combustion and the progress is unreasonable. There must be something wrong with the model for very lean (ϕ<0.5) combustion. Therefore, the calculation result of lean (ϕ<0.5) combustion is unreliable.

Figure 4-42 shows the progress and the temperature distribution with 2 stoichiometric Hydrogen-air mixture. First of all, it appears not to be a normal laminar combustion process. Second there are many problems when the scale values are considered:

(1). The reaction progress variable is higher than unit. The reaction progress variable is defined to be the ratio of the mass of combustion products to the theoretical maximum mass of combustion products. Its value is bounded between zero and unit. A value higher than unit means there must be some thing wrong with the reaction mechanism.

(2). The temperature is too high. The maximum combustion temperature should be less than 3000K with initial temperature of 300K[10]. But simulation shows a temperature high than 4000K. This is obviously wrong.

Consequently, the calculation result for rich combustion is unreliable.

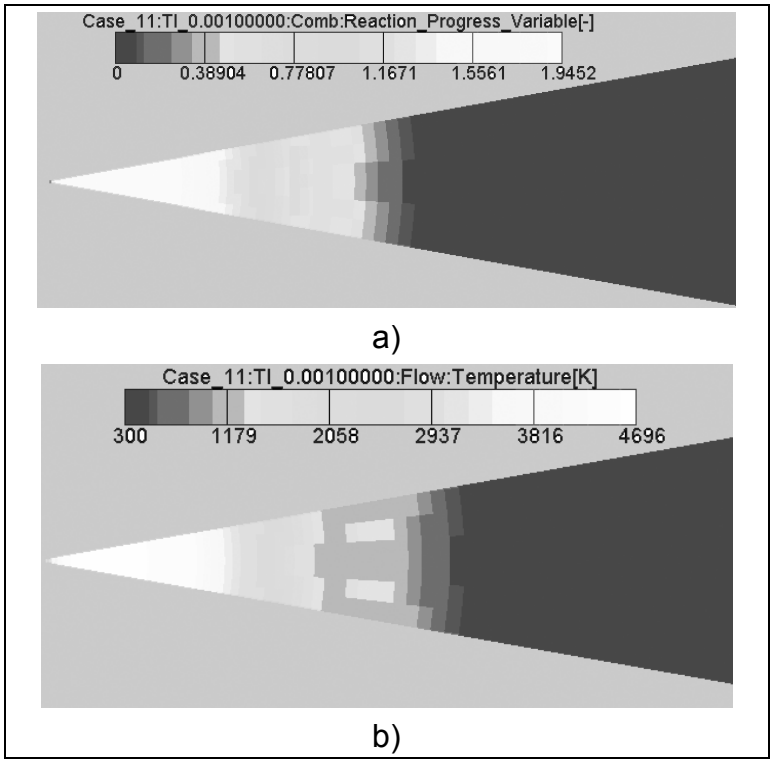

Figure 4-42. Abnormal reaction progress and temperature for rich combustion with TFSC model

Therefore, the conclusions can be made that:

- Present FIRE version has problems in TFSC Model with very lean ($\phi<0.5$) and rich ($\phi>1.0$) Hydrogen combustion.
- It can only be used for the simulation of Hydrogen combustion in the range of $0.5<\phi\leq1.0$.

4.5.7 Effect of initial pressure

Figure 4-43 shows the simulated pressure effect at different initial temperature. The results have the uniform trends:

1) Initial Pressure has negative effect on flame speed. With the increase of Initial pressure, the flame speed will decrease.
2) The negative effect becomes stronger and stronger with the increase of initial temperature.

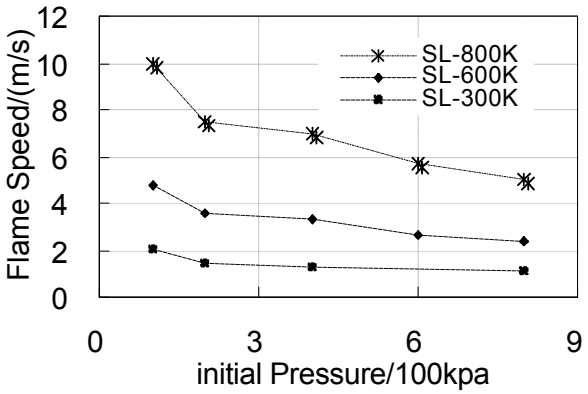

Figure 4-43 Simulated pressure effect on flame speed at different initial temperature with TFSC Model

The phenomenon accords well with formula 4-12. This means that the simulated results seams to be reasonable if the basic theory of the model is correct.

50 year ago, John Manton and B. B. Milliken promoted a formula[11] for the pressure dependence for hydrogen/air mixture:

$$U_L(a) \Big/ U_L(b) = \left(P_a \Big/ P_b \right)^x \tag{4-16}$$

Where $U_L(a)$, $U_L(b)$ represent the Laminar flame speed at initial pressure P_a and P_b respectively. The exponent x is summarized in figure 4-44.

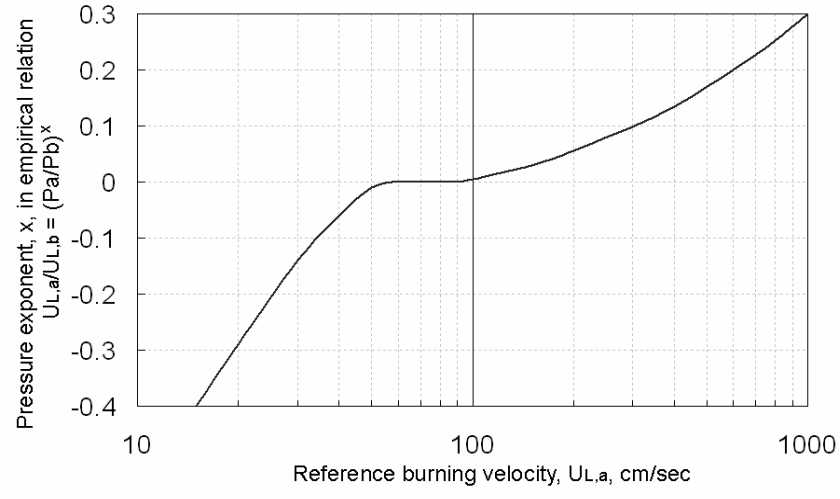

Figure 4-44. Variation of pressure dependence of burning velocity with reference burning velocity

Figure 4-44 shows that the pressure dependence is variable and apparently a function of flame speed. At burning velocities below 50 cm/s, burning velocity varies inversely with pressure; in the range of 50-100cm/s, burning velocity is almost constant with pressure; and from 100cm/s upward, it increases with

pressure.

According to this theory, the calculated pressure effect is reasonable for lean combustion ($\phi<0.5$). For high speed, such as stoichiometric combustion, formula (4-12) should be modified to represent positive pressure effect.

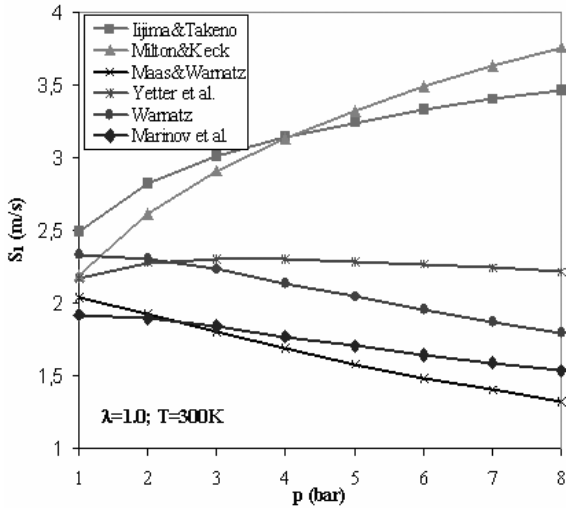

Figure 4-45. Experiment result of pressure effect on flame speed by different persons

Figure 4-45 gives a group of experiment data by different workers[12]. All of these experimental data show large discrepancies. This reflects that the measurements of laminar flame speed at pressures rather than atmospheric are difficult.

Due to lack of authoritative experiment result, the pressure effect of hydrogen/air mixture is still an unsolved problem.

Since the pressure is almost equalizing in the combustion chamber of an Engine, the pressure effect will not significantly influence the reaction distribution, but the overall value. Therefore, the present version can be used for multi-case comparison.

4.5.8 Conclusion

The above study shows that TFSC model is the only model to be able to simulate laminar combustion. This model has the following performances:

- Even though it is based on laminar combustion, this model can also be used to simulate turbulence combustion.
- It can reflect good temperature performance.
- The simulation result has little influence on geometry. Therefore, it can be used to predict the performance of new designed engines.
- The present version is not well developed for rich ($\phi>1$) and very lean ($\phi<0.5$) combustion simulation. In the range of $0.5<\phi\leq1$, the simulation result is relatively reasonable.

4.6 Brief summary

Up to now, all of the available combustion models in FIRE version 8 have been studied in order to carry out reliable simulation of hydrogen engine.

Summarizing the study results, the following conclusions can be achieved:

- Magnussen Model is very simple and easy to be used. But flame speed is significantly influenced by initial turbulence conditions and geometry. Since it is too simple, it can't be used to simulate general combustion performance, such as temperature performance, mixture concentration performance.
- CFM Model can't be used for laminar combustion simulation of hydrogen/air mixture. And the present version is not possible to simulate high-speed combustion, such as hydrogen combustion.
- PDF model is also based on turbulence combustion. Its result is dependent on initial turbulence conditions. The model consumes much more time than other models. But this model involves all of the mixture property effects and is capable for general turbulence combustion research.
- TFSC Model is the only available model in FIRE8.2 for Hydrogen laminar combustion simulation. It can reflect good temperature performance. But the present version is not well developed for rich ($\phi>1$) and very lean ($\phi<0.5$) combustion simulation. It can only be used to simulate hydrogen concentration effect in the range of $0.5<\phi\leq1$.

Since TFSC model is the only model, it will be used for Hydrogen engine combustion study in the next part of this thesis.

---

[1] *Joel Tagalian and John Heywood, 1986.*

[2] *Stefan Pischinger and John Heywood, 1990.*

[3] *Andrei N. Lipatnikov and Jerzy Chomiak, 2003.*

[4] *Sebastian Verhelst and Roger Sierens, 2003.*

[5] *Lt. Herbert "R" Poorman, 1953.*

[6] *Faranak Rahim, 2002.*

[7] *AVL Fire, 2003. Combustion, Version 8. All of the theoretical explanations of the combustion models in this part are from the same source.*

[8] *David R. Dowdy,et al., 1990..*

[9] *David R. Dowdy, et al., 1990.*

[10] *Isadore L. Drell and Frank E. Belles, 1958.*

[11] *John Manton and B. B. Milliken, 1956.*

[12] *Sebastian Verhelst and Roger Sierens, 2003.*

Part V: Research on Hydrogen Engine Combustion

To control pollution emission, reduce fuel consumption and increase specific power output are the ultimate targets for IC engine development. The optimization of the combustion process is always a dream of engine designers.

In order to optimize combustion processes, engine designers have traditionally undertaken manual engine modifications, conducted testing, and analyzed the results. This iterative process is painstakingly slow and costly and does not lend itself to identifying the optimal engine design specifications.

CFD provides a very efficient and economic tool to perform the optimization process. Nowadays, computer-based simulation for prediction of engine performance and exhaust emission has become an integral part of the internal combustion engine design process.

A lot of work has been done to understand the relationship between the engine parameters and the engine performance in the traditional IC engine field. The methodologies for efficient and accurate investigations have been developed for gasoline/diesel engine design.

This part of the thesis will focus on the Hydrogen engine; try to build an effective Simulation method for Hydrogen engine combustion process research. With this method, a few typical parameters will be studied to find their influences on engine performances, and consequently get the idea of optimizing these parameters.

5.1 General Characteristics of combustion process in Hydrogen Engine

5.1.1 Characteristics of Hydrogen fuel[1]

Table 5-1 compares Hydrogen with natural gas and gasoline on their combustion properties[2]. These characteristics make Hydrogen an ideal fuel for IC Engine. Because of its difference from traditional fuels, Hydrogen engine has its distinct characteristics.

Table 5-1 Combustion performances for hydrogen and other fuels

Characteristics	Hydrogen	Natural gas	Gasoline
Lower heating value/(kJ/g)	120	50	44.5
Self-ignition temperature/(°C)	585	540	228-501
Flame temperature/(°C)	2045	1875	2200
Flammability limits in air(vol%)	4-75	5.3-15	1-7.6
Minimum ignition energy in air (uJ)	20	290	240
Diffusion coefficient in air/(cm2/s)	0.61	0.16	0.05

Here gives a brief analysis of these characteristics as well we their influence on engine performances:

(1). Wide range of flammability

Hydrogen has a wide flammability range in comparison with all other fuels. As a result, hydrogen can be combusted in an internal combustion engine over a wide range of fuel-air mixtures. A significant advantage of this is that hydrogen can run on a lean mixture. This is why it is fairly easy to get an engine to start on hydrogen.

Generally, fuel economy is greater and the combustion reaction is more complete when a vehicle is run on a lean mixture. Additionally, the final combustion temperature is generally lower, which will significantly reduce the amount of NOx pollutant in the exhaust. This performance makes hydrogen engine have very good part-load performance.

(2) Low ignition energy

Although hydrogen has a higher auto-ignition temperature than methane, propane or gasoline, its ignition energy (0.02 mJ) is about an order of magnitude lower and is therefore more easily ignitable. This enables hydrogen engines to ignite lean mixtures and ensures prompt ignition.

(3). High auto-ignition temperature

Hydrogen has a relatively high auto-ignition temperature. This has important implications when a hydrogen-air mixture is compressed. The high auto-ignition temperature of hydrogen allows larger compression ratios to be used in a hydrogen engine than in a hydrocarbon engine.

Theoretically, the higher the compression ratio is, the higher the thermal efficiency will be. Therefore, this performance gives the possibility to make the thermal efficiency of a Hydrogen engine be much higher than that of a gasoline engine.

On the other hand, hydrogen is difficult to ignite in a compression ignition or diesel configuration, because the temperatures needed for those types of ignition are relatively high.

(4) Wide range of flame speed

The burning speed of hydrogen is nearly an order of magnitude higher than that of methane or gasoline (at stoichiometric conditions). Thus hydrogen fires burn quickly and, as a result, tend to be relatively short-lived. This means that hydrogen engines can more closely approach the thermodynamically ideal engine cycle.

However, the flame velocity decreases significantly at leaner mixtures. Therefore, the combustion process must be carefully organized for lean combustion to prevent late combustion, which will decrease thermal efficiency and make the exhaust gas too hot.

(5). High diffusivity

Hydrogen has very high diffusivity. This ability to disperse in air is considerably greater than gasoline and is advantageous for two main reasons. Firstly, it

facilitates the formation of a uniform mixture of fuel and air. Secondly, if a hydrogen leak develops, the hydrogen disperses rapidly. Thus, unsafe conditions can either be avoided or minimized.

(6) Very low density

Hydrogen has very low density. This results in two problems when used in an internal combustion engine. Firstly, a very large volume is necessary to store enough hydrogen to give a vehicle an adequate driving range. Secondly, the energy density of a hydrogen-air mixture, and hence the power output, is reduced. Fortunately, the later problem can be solved by Hydrogen direct injection.

5.1.2 Turbulence variation

Initial Turbulence Condition will influence the combustion process significantly. To understand its variation principle in a Hydrogen direct injection engine is important for the understanding of the combustion process, further more, for the modeling of a hydrogen engine simulation.

5.1.2.1 Influence of Initial Condition

Figure 5-1 shows the mesh of the study object, one-twelfth of a cylinder with a 12-hole injector. Hydrogen is injected form the hole with mass flow of 0.75g/s. the injection duration is set to be 1ms.

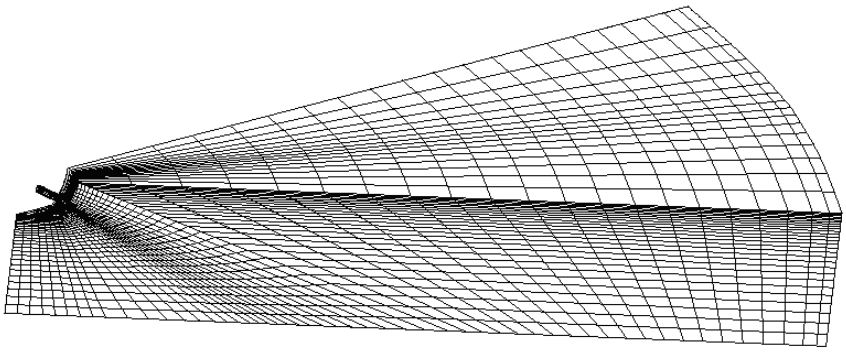

Figure 5-1. Mesh for hydrogen injection simulation

Different initial turbulence conditions are set:

- TKE: 0.001 m2/s2; Turbulence length scale: 0.001m
- TKE: 5.0 m2/s2; Turbulence length scale: 0.001m

Figures 5-2 presents the variation of the mean TKE during and after injection. The mean TKE will increase to the maximum value before the injection is finished, then decrease rapidly. The most interesting phenomenon is that the mean TKE will have approximately the same value at a certain time after the injection finished. In other words, the mean TKE is mainly dependent on the injection performance, and the initial condition has little influence on the variation of TKE during the mixing process. The variation of turbulence length scale shows the similar performance: initial length scale has little influence. The

mean turbulence length scale will always converge to a fixed value after the injection.

This is because Hydrogen is injected into the cylinder with very high speed (about 2000 m/s), which will cause very high turbulence and the initial TKE will almost be submerged. The high-speed stream will also break all the big eddies into small ones.

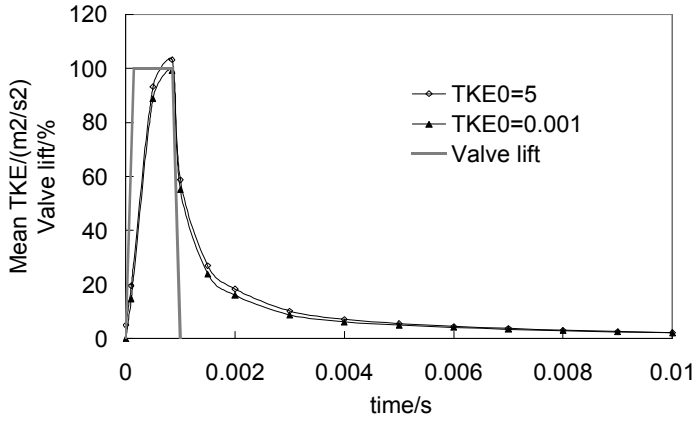

Figure 5-2. Turbulence variation in hydrogen injection engine

Therefore, the combustion simulation can be started just before the beginning of the injection. The intake stroke has little influence on the turbulence magnitude during the combustion process.

5.1.2.2 Influence of Injection parameters

With the same mesh (figure 5-1) but with piston moving, the influence of injection parameters on turbulence in studied in detail.

With the same injection time but different injection mass flow (0.45g/s, 0.6g/s, 0.75g/s, 0.9g/s), different mixture can be obtained. Figure 5-3 shows the variation of inlet total pressure and TKE respectively.

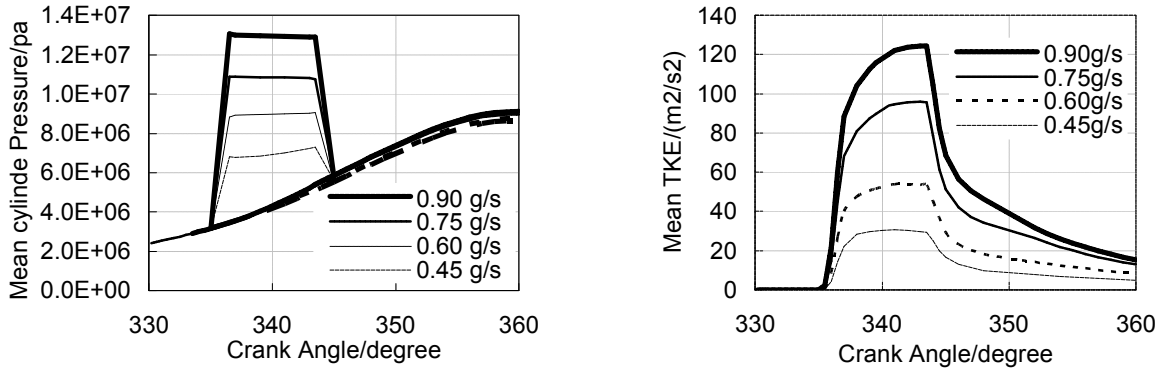

(a) (b)

Figure 5-3. Pressure and TKE variation in hydrogen direct injection engine

With the increase of inlet mass flow (or inlet total pressure), the mean TKE will increase with a linear trend. In other words, the higher the injection pressure is,

consequently the higher the injection speed, the higher the TKE will be.

5.2 Hydrogen engine Simulation Modeling

5.2.1 Study approach

The study in PART IV shows that the TFSC model is suitable for Hydrogen engine combustion simulation. Based on this information, the study process can be explained as in figure 5-4.

Path 1 should be the normal way for Hydrogen engine performance study. This path can be used to study not only the influence of engine parameters, but also the influence of mixture distribution, which can evaluate the mixture formation methods.

But, since the present TFSC model can neither simulate lean mixture nor rich one (refer to figure 4-39), it cannot correctly calculate the combustion propagation in the whole cylinder, where there is big concentration difference caused by in-cylinder Hydrogen injection.

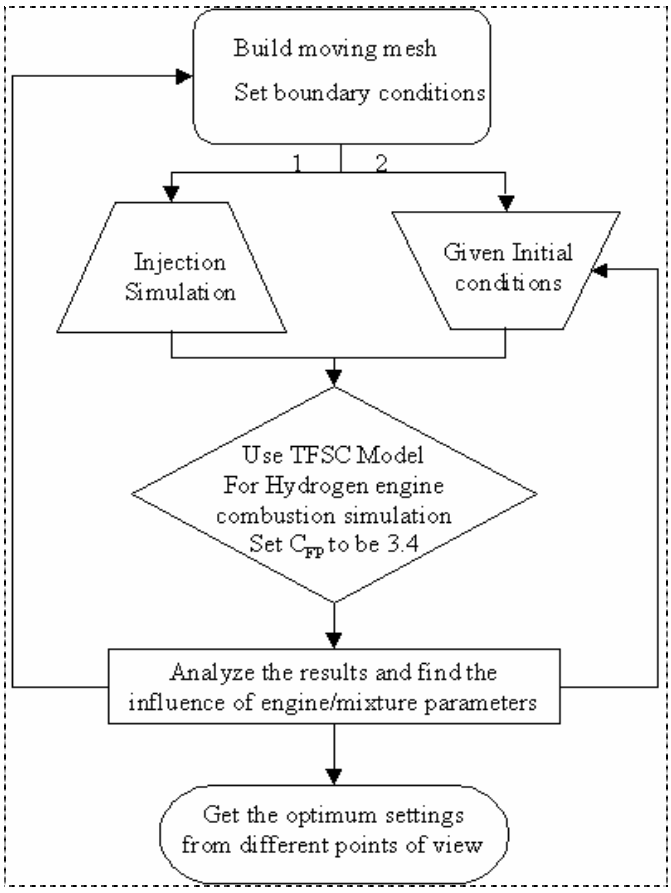

Figure 5-4 Flowchart for hydrogen engine combustion study

Therefore, this thesis has to use path 2 to simulate homogenous mixture. This path will omit the injection and mixture formation process, and study the influence of some parameters to find some general principles of Hydrogen engine combustion.

In its wide range of flammability, Hydrogen's burning speed varies enormously. Figure 5-7 shows the variation of Hydrogen laminar flame speed along with the Hydrogen concentration in air[3] (300K, 1atm). The maximum flame speed could be higher than 3m/s. But, when the mixture becomes very lean, say ϕ=0.3, the flame speed will be as slow as 0.15 m/s (less than 1/30 of the maximum speed).

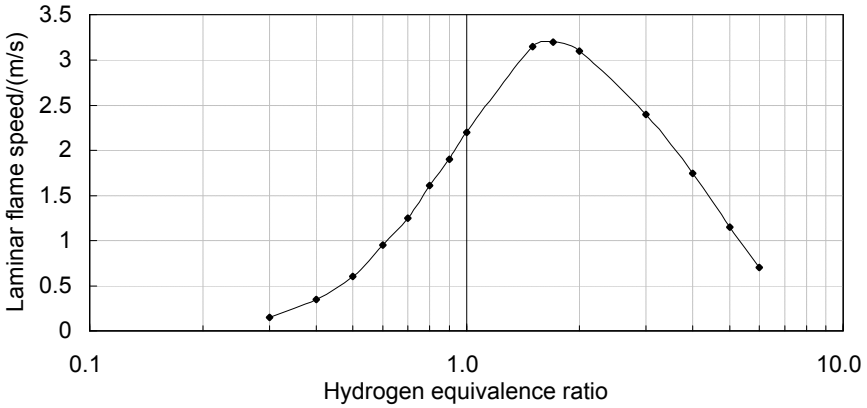

Figure 5-5. Burning velocity of hydrogen/air as a function of stoichiometry

The wide range of flame speed will lead to big difference of the combustion performance in a Hydrogen engine when it runs with different Hydrogen/air mixture.

Therefore, both the lean and "rich" (close to 1) need to be studied in order to get complete understanding of the combustion performance in Hydrogen engine.

Due to the limit of TFSC model in FIRE 8, this thesis will discuss the combustion performance in the range of ϕ=0.5 (represent for lean combustion) to ϕ=1 (represent for "rich" combustion).

NOx emission is calculated with Zeldovish Model.

Due to lack of effective calibration data, this model is not validated in this research. Therefore, the NO emission result can only be used as reference data, which can only reflect the variation trend qualitatively, but not quantificationally.

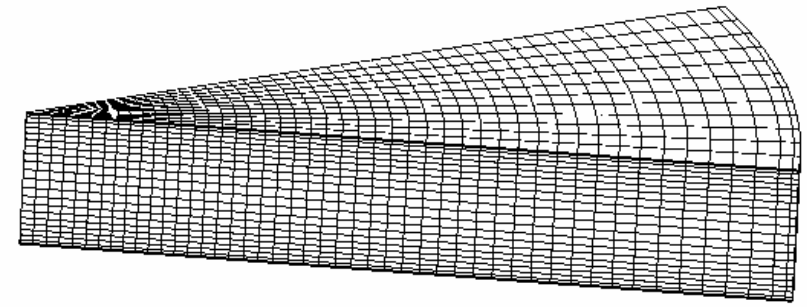

Figure 5-6. Mesh for hydrogen engine combustion simulation

5.2.2 Calculation setting

In order to reduce calculation time, a simple mesh (as shown in figure 5-6), with

moving information, is used for Hydrogen combustion study. The ignition point is set to be the center of the cylinder the in the middle of the clearance.

The geometric data of the object engine is listed in table 5-2.

Table 5-2. Basic data of object engine

	Value/m	Note
Bore	0.085	
Length of con-rod	0.2	
Stroke	0.085	To be changed for "ε" effect study
Clearance distance	0.0055	

The calculation starts from the beginning of the compression stroke with initial TKE of $10m^2/s^2$, which will reduce to around $3m^2/s^2$ before ignition, and initial length scale of 0.0005m.

Assuming the engine is naturally aspirated, the initial pressure is set to be 100kpa and temperature 323.15K(50°C).

5.2.3 example calculations

Before the performance optimization, it is necessary to analyze the characteristics of Hydrogen engine combustion process. Two typical examples will be discussed in this part.

5.2.3.1 "rich" (ϕ=0.8) combustion

Figure 5-7 presents the variation of the main performance parameters in the object engine in compression and expansion stroke. The engine is charged with Homogeneous Hydrogen/air mixture (ϕ=0.8). Ignition angle is set to be 345 CA (15° BTDC).

The results show that Hydrogen engine combustion process, with relatively rich mixture (away from lean), has the following characteristics:

(1). Very short combustion duration

The P-V graph (figure 5-7a) shows that the combustion is a very typical constant Volume combustion process. This is because the high burning speed enables the combustion progress to be finished in very short time. Figure 5-7(b) shows that the combustion process is finished in less than 30 degree, which is approximate 2.5 ms at 2000 r/min.

Since the reaction duration is so short, the ignition timing becomes very important in this case. Later study will show that the combustion performance will be significantly influence by ignition advance. Therefore, the ignition timing should be carefully adjusted to optimize Hydrogen engine performance.

(2) Maximum pressure and maximum temperature points

Normally, the maximum temperature appears a little later after the maximum pressure in a gasoline engine. But these two points could take place at almost the

same time/angle (figure 5-7c) due to the fast reaction progress. This enables Hydrogen engine having more thermal efficiency than gasoline engine.

(3) Maximum NO formation rate arises at the end of the reaction Progress

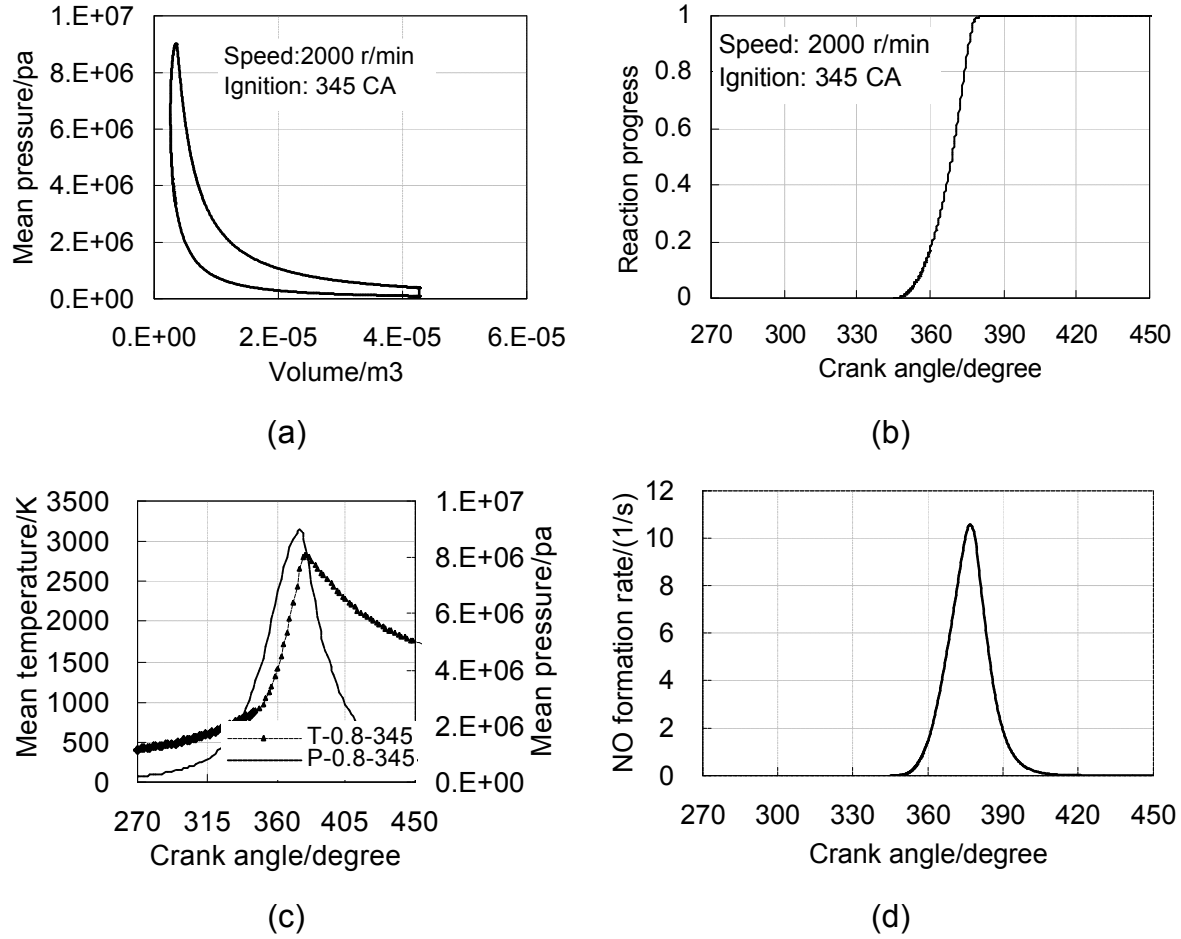

Figure 5-7. Variation of main engine performance parameters in rich combustion

Figure 5-7(d) shows that the maximum NO formation rate occurs at the end of the reaction progress in this calculation. This is because the mixture reaches its maximum temperature at this time, even though the Hydrogen combustion has finished. Therefore, to control the maximum temperature is the key to control NO emission.

5.2.3.2 Lean (ϕ=0.5) combustion

Figure 5-8 gives another group of curves, which are resulted from ϕ=0.5 Hydrogen/Air mixture. These curves show typical lean combustion behaviors in Hydrogen engine.

Comparing figure 5-8 with figure 5-7, big differences will be found, and consequently the characteristics of lean Hydrogen combustion can be discovered:

The reaction duration becomes much longer. It lasts approximately 60 degree (figure 5-8b), equal to 5 ms. This makes the P-V curve (figure 5-8a) be much

fatter than the previous one.

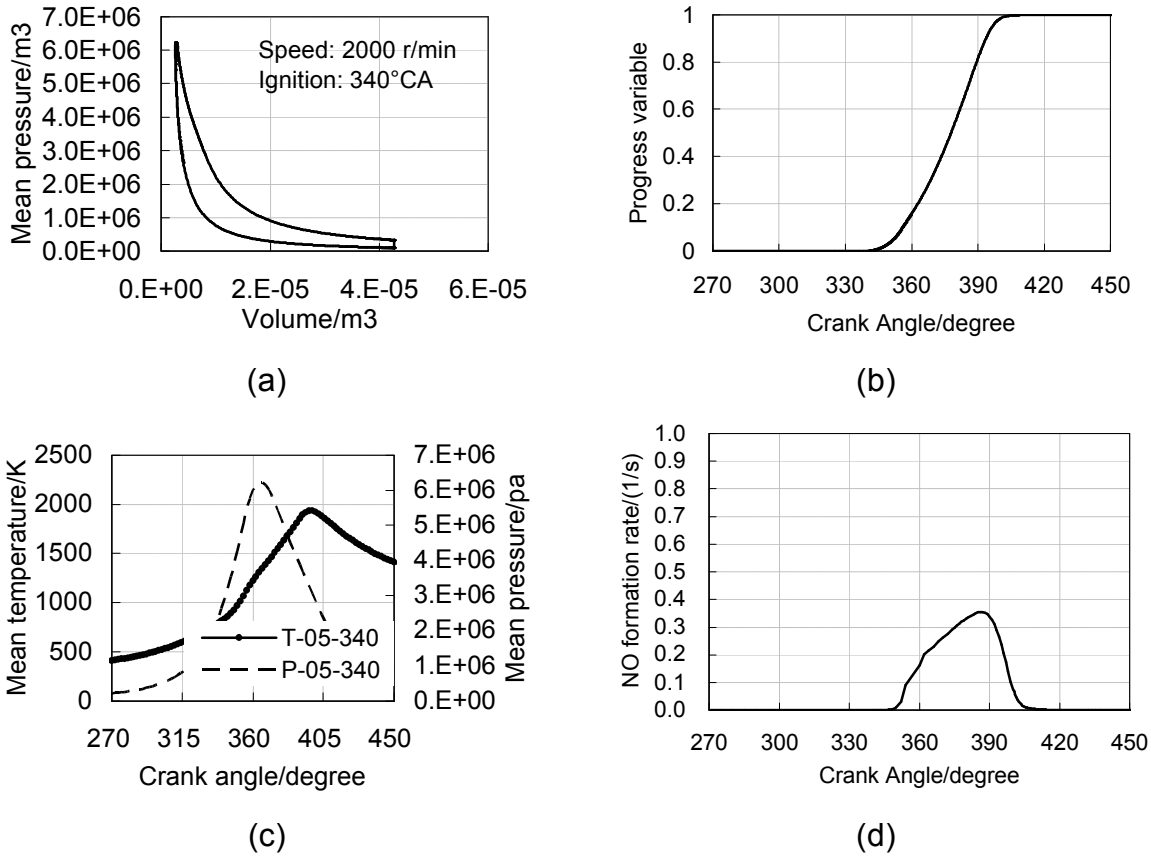

Figure 5-8. Variation of main engine performance parameters in lean combustion

Due to the long reaction duration, the maximum temperature point is obviously later than the maximum pressure point (figure 5-8c). The benefit is that the maximum pressure and the maximum temperature are much lower than that in figure 5-9.

The NO formation rate behaviors much different from “rich” combustion: the whole NO formation process is within the combustion period. Theoretically, the fast NO formation condition is above 2000K[4]. Since the maximum mean temperature is less than 2000K (figure 5-8c), NO can only be produced in the combustion zone, where the local temperature may be higher than 2000K. Therefore, NO formation process must finishes when the Hydrogen combustion finishes.

The No formation rate is much lower than that in “rich” combustion. This make the lean combustion be very attractive for NO emission control.

5.3 Influence of Ignition timing

5.3.1 General effects

Figure 5-7 shows the variation of pressure, temperature, progress and NO formation rate with different ignition angle respectively. Even though these

curves are resulted from "rich" (ϕ=0.8) mixture combustion simulation, they show the general influence of ignition on reaction process.

These curves give very clear trends that, with the increase of ignition advance,

(1). The maximum mean pressure will increase significantly (figure 5-9a),

(2). The reaction progress will advance parallelly (figure 5-9b),

(3). The maximum temperature increases obviously (figure 5-9c).

(4). The NO formation rate will increase exponentially(figure 5-9d).

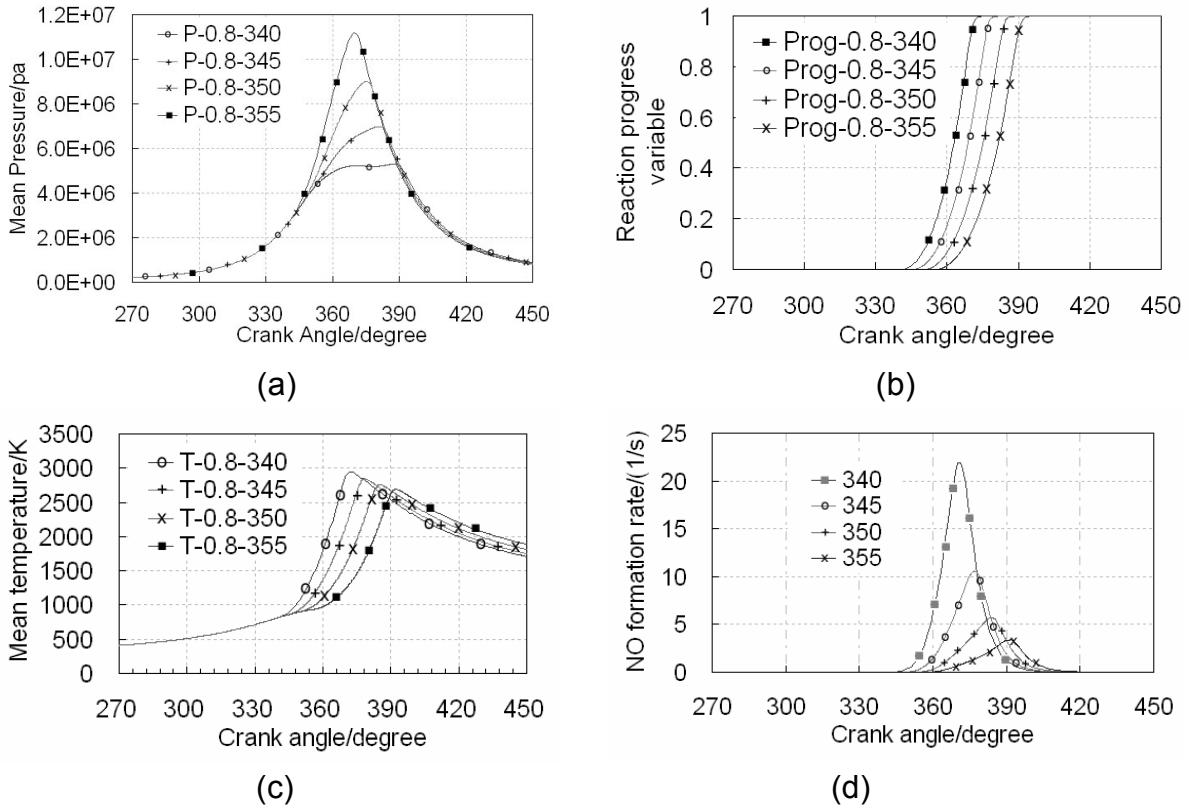

Figure 5-9. Ignition influence on the Variation of main engine performance parameters

Figure 5-10 presents further information of the influence of Ignition advance on NO emission and thermal efficiency.

Figure 5-10(a) shows the NO emission, which is deduced from the raw results and expressed in g/kWh. This result seems to be too high for an IC engine. But the variation trend is reasonable. It again gives the trend that the total NO emission will increase exponentially with the increase of ignition advance. This is easy to be understood because the NO formation rate will increase exponentially with the increase of temperature as shown in Formula 5-1[5].

$$d[NO]/dt = \frac{A}{\sqrt{T}} \exp\left(-\frac{E_a}{RT}\right) \times [N_2] \times [O_2] \qquad (5\text{-}1)$$

Where, [ ] means concentration, E_a is the activation energy, A is pre-exponential factor.

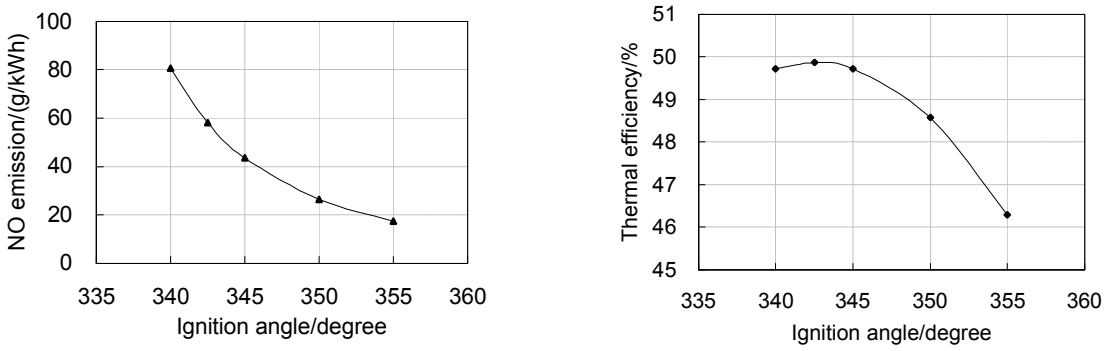

(a) (b)

Figure 5-10. Variation of NO emission and thermal efficiency as a function of ignition angle

Figure 5-10(b) presents the variation of the deduced thermal efficiency. With the increase of ignition advance, the thermal efficiency will be increased because the burnt gas gets more expansion. But further increase of the ignition advance will reduce the thermal efficiency since too early combustion will consume much more energy for the compression and increase wall heat transfer due to increased temperature.

5.3.2 Optimum Ignition timing

Four cases (ϕ=0.5, 0.65, 0.8 and 1.0 respectively) are studied to get more information on the influence of ignition.

Figure 5-11 presents the influence of ignition timing on maximum pressure and thermal efficiency respectively.

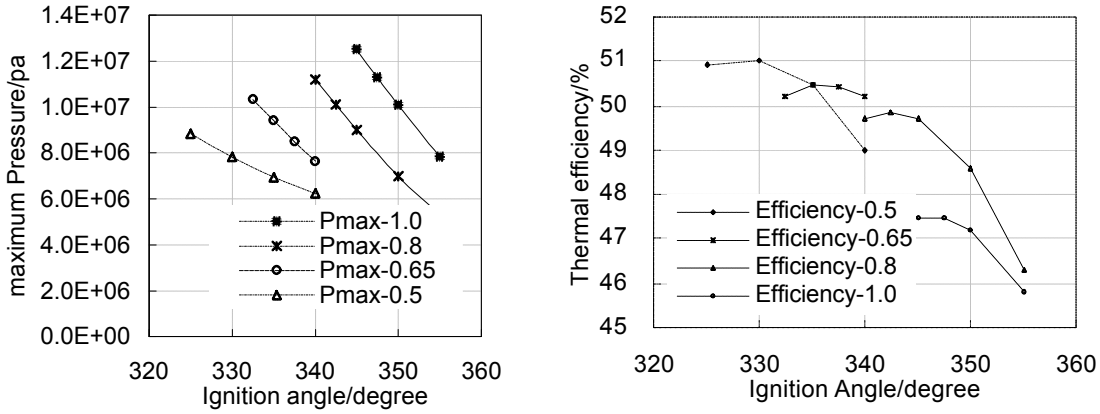

(a) (b)

Figure 5-11. Influence of ignition timing and concentration on maximum pressure and thermal efficiency

The ignition influence on combustion temperature is shown in figure 5-12.

Here is a brief analysis of the results:

(1). The higher the mixture concentration is, the steeper the maximum pressure curve will be (figure 5-11a). This is because richer mixture has higher flame

speed, and consequently shorter reaction duration, which makes the combustion performance more sensitive to the ignition timing.

(2). The higher the hydrogen concentration is, the higher the maximum temperature (Figure 5-12). The higher flame speed of richer mixture leads to higher heat release, and consequently, cause the higher maximum temperature.

(3) The leaner the mixture is, the higher the maximum thermal efficiency will be. In addition, the curve is much more flatter with leaner mixture than that of richer mixture. The lower thermal efficiency at "rich" combustion is due to the higher Wall Heat Transfer (figure 5-13) during the expansion stroke (this phenomenon needs to be verified by experiment) and more energy is consumed for the dissociation of combustion product at high temperature.

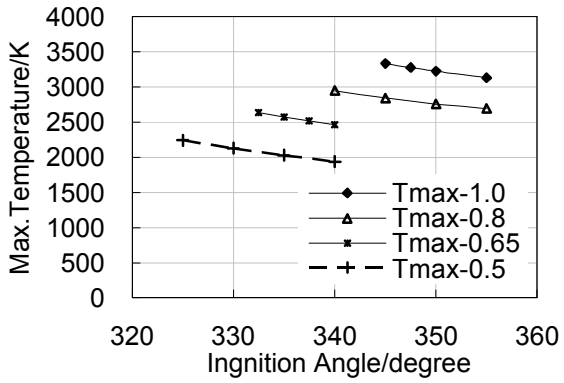

Figure 5-12 Maximum temperature with different Ignition timing and concentration

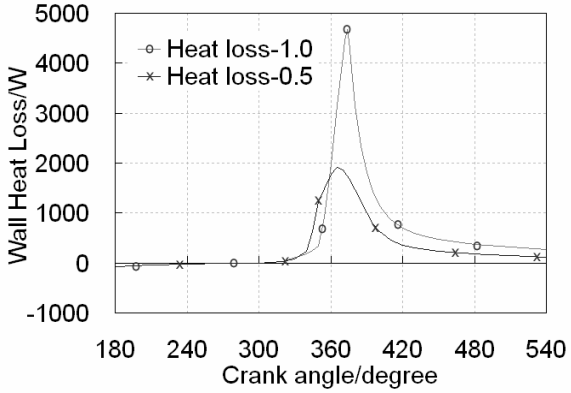

Figure 5-13. Wall heat transfer with different mixture Concentration

The optimum ignition angle, at which the engine can get the maximum thermal efficiency, can be selected through figure 5-11(b) for every kind of mixtures. Put the pressure and Progress variable curves of the optimum combustion cases together, figure 5-14 can be formed.

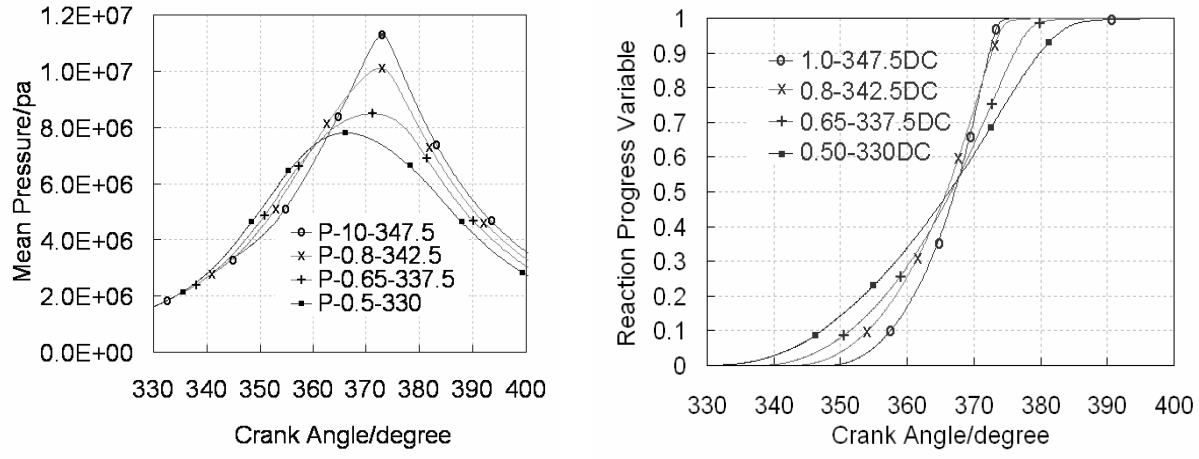

(a) (b)

Figure 5-14. Variations of mean pressure and reaction progress with optimum ignition timing

By analyzing figure 5-14, the general conditions for optimum ignition timing can be summarized:

(1). “Rich” combustion

The combustion should meet both of the following conditions:

- The optimum ignition should make the maximum pressure point take place at 373° (13° after TDC).
- 50% of the mixture has combusted up to 367° (7° after TDC)

(2). Lean Combustion

Due to the slow burning speed, the maximum pressure point cannot be postponed too much, but a little after the TDC. The leaner the mixture is, the smaller the maximum pressure angle will be. Therefore, the optimum ignition condition can’t be judged by maximum pressure angle, but the combustion progress (figure 5-14b). That is:

- 50% of the mixture has combusted up to 367° (7° after TDC)

Synthesizing the above analysis, the optimum ignition timing for best thermal efficiency should meet the uniform condition that: 50% of the mixture has combusted up to 367° (7° after TDC).

5.4 Influence of Mixture Concentration

Figure 5-15 shows the Hydrogen engine performance with different mixture concentrations. All the calculations have been adjusted to optimum conditions in order to make the results be comparable.

The following information can be obtained from figure 5-15:

(1). NO emission

Lean combustion will greatly reduce NO emission. This is because the maximum temperature is significantly reduced due to extra air.

With the increase of Hydrogen density, the NO emission will increase dramatically, when the mixture is leaner than 0.95 (Figure 5-15a).

With stoichiometric mixture, NO emission is dramatically reduced even though the maximum temperature is higher than other cases. The most possible reason for this phenomenon could be that Hydrogen is much more easier than Nitrogen to reacted with Oxygen. When the hydrogen combustion is finished, all the Oxygen is consumed. There is no Oxygen available to react with Nitrogen.

(2). Power output

The same as gasoline engine, higher fuel density will get higher mean effective pressure (figure 5-15c). But, the increase of power is not proportional to the increase of Hydrogen equivalence ratio because the thermal efficiency will reduce at richer combustion (figure 5-15b).

(3). Maximum mean pressure and temperature

The maximum mean pressure and temperature will increase almost linearly along with the increase of mixture concentration (figure 5-15d).

The higher the maximum pressure is, the higher structural strength is required. This will result the engine to be heavy and bulky.

The increased maximum temperature will meet the similar problem: the engine must have higher hot strength to tolerate the high temperature (much higher than gasoline engine). The cooling system may also be enhanced to maintain the engine to run properly.

When the extra power loss on cooling system as well the mechanical efficiency reducing, due to the high maximum pressure, are considered, the effective thermal efficiency at rich combustion will become even lower.

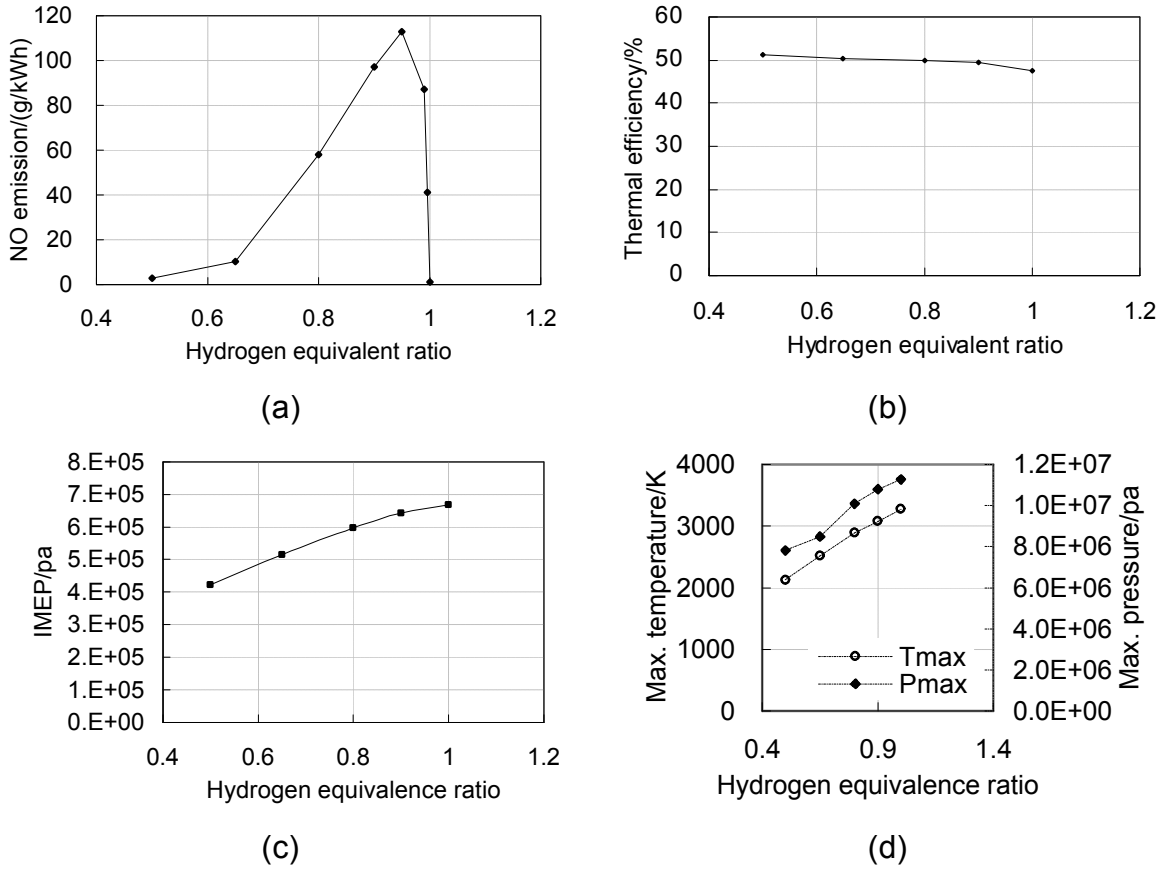

Figure 5-15. Main performance parameters as a function of concentration

5.5 Other parameter study

5.5.1 Compression ratio

The influence of compression ratio is studied by changing the clearance volume with the same Hydrogen concentration (ϕ=0.65). Figure 5-16 presents the main performances with compression ratio of 13.14, 16.45 and 18.

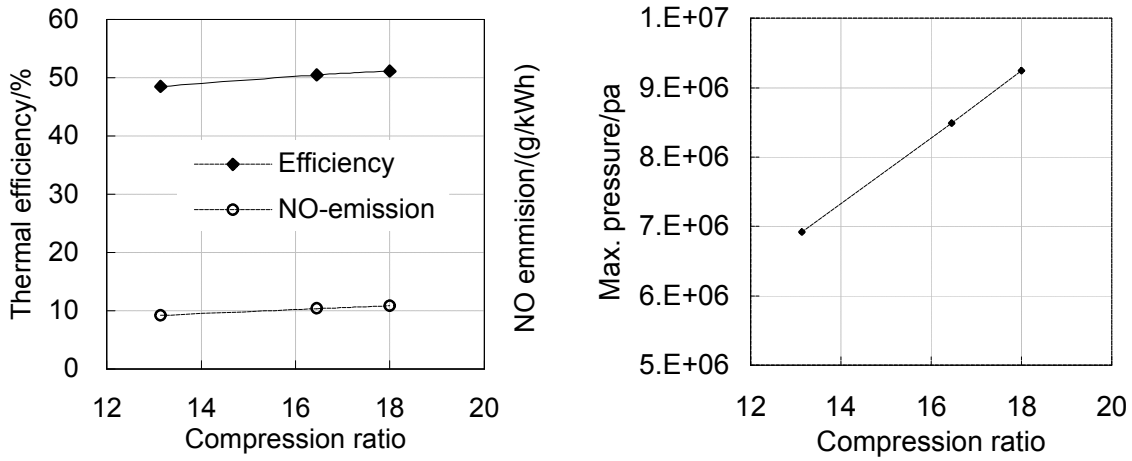

(a) (b)

Figure 5-16. Main performance parameters as a function of compression ratio

The simulated results give clear ideas that with the increase of compression ratio:

(1). Thermal efficiency will increase quasi-linearly (solid line in figure 5-16a). In this study, the thermal efficiency increases 5.5% when compression ratio increases from 13.14 to 18.

(2). NO emission will also increase (dashed line in figure 5-16a). But, comparing with figure 5-14a, it can be seen that the influence of compression ration on NO emission is far less than that of concentration.

(3). Maximum pressure will increase significantly (figure 5-16b) with the increase of compression ratio, which will require stronger engine structure. Therefore, the increase of compression ratio will be limited by engine strength. Certainly, hydrogen self-ignition temperature should another limit at the same time.

5.5.2 Intake Temperature

Intake temperature has little influence on NO emission, but obviously influences power output.

Table 5-3 Comparison of main performances with different intake temperature

Intake temperature /K	303.15		323.15		343.15		363.15	
	Value	Difference /%	Value	Difference /%	Value	Difference/ %	Value	Difference /%
Efficiency/%	51.9	1.7	51.0	-	50	-1.7	49.4	-3.1
imep/Mpa	0.46	8.5	0.42	-	0.39	-7.4	0.36	-13.8
NO-emission /(g/kWh)	2.4	-15.1	2.9	-	3.0	4.6	2.9	0.1
Tmax/K	2088	-1.8	2126	-	2158	1.5	2193	3.2
Pmax/Mpa	8.1	3.2	7.8	-	7.5	-3.5	7.3	-6.6

Note: “Difference” is calculated by $(Value_{curent}-Value_{323.15})/Value_{323.15}\times 100\%$

Table 5-3 gives the comparison of the main simulation results. All of the four cases have the same mixture concentration of 0.5, but with intake temperature of 303.15K, 323.15K, 343.15K and 363.15K respectively.

Figure 5-17 gives the visual explanation of the relationships between intake temperature and engine performance parameters.

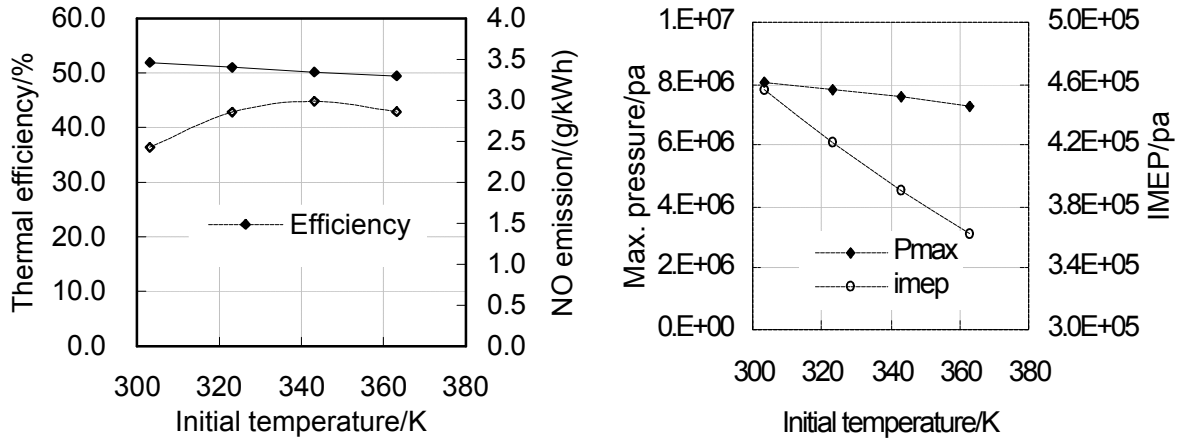

(a) (b)

Figure 5-17 relationship between engine performances and intake temperature

The calculation results show the following trends:

(1). Intake temperature has little influence on NO emission (dashed line in figure 5-17a).

Theoretically, intake temperature will influence NO formation in two directions: on the one hand, lower intake temperature will get lower maximum **mean** temperature, which is good for constraint of NO formation; on the other hand, lower intake temperature will get higher mixture density, more heat release in unit volume, and will cause higher **local** temperature, which will furtherance NO formation. Therefore, the influence of intake temperature on NO emission is a balanced result of these two functions.

(2). Thermal efficiency will increase when intake temperature is reduced. The lower the intake temperature is, the less energy will be transferred to the wall, consequently, the higher the thermal efficiency will be.

(3). Maximum pressure and imep increase when intake temperature is reduced.

This phenomenon is easy to understand. Since the total mass of the charge is increased with the decrease of intake temperature, the total heat release is increased. This could be the main reason, besides the increase of thermal efficiency, for the increase of maximum pressure and imep.

As for naturally aspirated engine, the intake temperature will not change in a wide range. Considering the intensive influence of other parameters (mixture concentration, EGR, etc), the influence of initial temperature can be neglected. The results can only be used as reference when the influence of environment

temperature is considered.

When the engine is supercharged, the intake temperature should be well controlled in order to get good efficiency, high imep and low maximum pressure.

5.5.3 EGR

(1) EGR can effectively reduce NO emission with little decrease of thermal efficiency.

The relationship between NO emission and EGR percentage is show in Figure 5-18 (a). Since EGR can efficiently control the maximum combustion temperature, NO emission will decrease exponentially with the increase of EGR percentage.

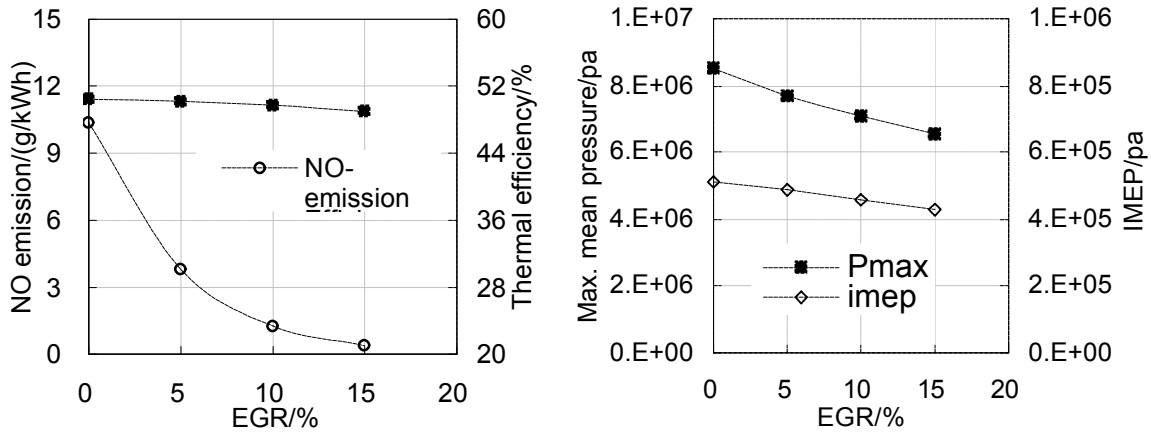

(a) (b)

Figure 5-18. EGR effect on engine performance

There is a little decrease of thermal efficiency with the increase of EGR percentage. With 15% of EGR, approximately 1% of thermal efficiency will be lost. Comparing with the intensive improvement of NO emission, the sacrifice of thermal efficiency is worthwhile.

(2) EGR will reduce power output

The penalty is proportional loss of power output with the increase of EGR percentage.

EGR will displace the cylinder volume, the effective swept volume is consequently reduced and the mean effective pressure reduced. Figure 5-18(b) shows that the loss of power output is almost proportional to EGR percentage.

Based on this performance, the engine output can be adjusted by giving different EGR percentage.

Generally speaking, the optimum EGR percentage should be the balance of power reduction and NO emission improvement.

5.6 Optimum design of hydrogen engine

Since the combustion speed is dependent on turbulence condition and the turbulence is mainly dependent on the injection characteristics, the combustion simulation in hydrogen direct injection engine can be started from the beginning of the injection, rather than from the beginning of intake stroke as in gasoline engine.

Detailed simulations show that:

(1). Optimum Ignition Timing varies in a wide range according to hydrogen concentration due to the wide flame speed range of hydrogen/air mixture. The ignition timing can be optimized in the way that 50% of the mixture has combusted up to 367°CA (7° after TDC)

(2). Hydrogen concentration will influence the combustion performance the most. With the decrease of hydrogen concentration, NO emission will reduce dramatically and thermal efficiency will increase at the same time. When hydrogen engine runs with stoichiometric mixture, the NO emission will also be significantly reduced.

(3). With the increase of compression ratio the thermal efficiency can be improved, but with the penalty of increased maximum pressure.

(4). Since EGR can efficiently control the maximum combustion temperature, NO emission will decrease exponentially with the increase of EGR percentage.

(5). The lower the intake temperature, the higher the thermal efficiency and power output.

Based on the above conclusions, the general concepts for optimum design on hydrogen engine can be figured out:

1). Ignition timing

The ignition timing can be optimized in the way that 50% of the mixture has combusted up to 367°CA (7° after TDC)

2). Compression ratio

Under the strength limit of the engine and the limit of self-ignition, the compression ratio should be as high as possible in order to increase thermal efficiency.

3). Intake temperature

Intake temperature should be well controlled, mainly for supercharged engine, in order to increase thermal efficiency and power output.

4) Power control strategy

In order to control NO emission, hydrogen engine should avoid running with middle-high concentration mixture (0.7-0.9). That is to say:

- At partial load, engine should run with lean mixture (less than 0.7), and

the power is tuned by varying mixture density and/or varying EGR percentage.

- At heavy load, engine should run with stoichiometric mixture, and the power is tuned by varying EGR percentage.

---

[1] *http://www.ott.doe.gov/otu/field_ops/hydrogen_class.html*

[2] *Bellona Report, 2002.*

[3] *David R. Dowdy, David B. Smith, Simon C. Taylor, Alan Williams, 1990.*

[4] *J.B. Heywood, translated by Tang Kaiyuan, 1992*

[5] *AVL Fire, 2003. Combustion, Version 8.*

Part VI: Main Conclusions

Up to now, the following conclusions can be made from the previous study.

6.1 Hydrogen engine will be prospective at least in near future

The environmental problem, especially the greenhouse effect, gives extreme pressure on the traditional engines. The oil crisis is going to dig the grave for fossil fueled engines.

Hydrogen, the most abundant elements in the universe, is an idea energy carrier to build a clean, recycle energy economy.

Hydrogen engine, with its extra clean combustion property and high thermal efficiency, will give the traditional engine a new life.

6.2 FIRE is capable for hydrogen injection simulation

CFD simulation is an effective tool for hydrogen engine performance study. The only problem is how to make reliable simulations with present CFD codes.

Verification and Validation are fatally important to carry out valuable CFD research. All the relative aspects, such grid convergence and Iterative Convergence, should be carefully studied before practical simulation.

FIRE is proved to be an effective tool for supersonic flow calculation and be capable to simulate hydrogen injection and mixture formation process in hydrogen engine with satisfied accuracy.

6.3 Hydrogen injection and Mixture formation

Hydrogen direct injection engine, with its good safety and high power output, is the most sophisticated type among all types of hydrogen engines.

Injector is the most important part for mixture formation process in the cylinder. With the same injection pressure and the same total injection section area, more holes will accelerate the mixture formation process and give better mixture distribution.

Since the injection speed is very high, engine speed and initial swirl have little influence on the injection and mixture formation process.

Due to non-homogenous distribution, ignition position and ignition timing should be carefully designed in order to organize successful ignition and stable flame propagation. Side located spark plug shows obvious advantages over central located one from the points of view of stream blockage and flammability of the charge.

6.4 Combustion models study

Combustion simulation lies on the combustion model. The FIRE version 8 has four available combustion models for Spark Ignition Engine simulation, but

none of them has been used for hydrogen engine combustion simulation before. Therefore, the combustion models have to be carefully calibrated and selected to make reliable combustion simulations in hydrogen engine.

The research in part III shows that:

(1). Magnussen Model is very simple and easy to be used. But flame speed is significantly influenced by initial Turbulence conditions and geometry. Since it is too simple, it can't be used to simulate general combustion performance, such as temperature effect, concentration effect.

(2). CFM Model can't be used for hydrogen laminar combustion simulation. And the present version is not possible to simulate high-speed combustion, such as stoichiometric hydrogen combustion.

(3). PDF model is also based on turbulence combustion. Its result is dependent on initial turbulence conditions. The model consumes much more time than other models. But it involves all of the property effects and is capable for general turbulence combustion research, but not for laminar combustion study.

(4). TFSC Model is the only available model for Hydrogen laminar combustion simulation. It can reflect good temperature performance. But the present version is not well developed for rich ($\alpha>1$) and very lean ($\alpha<0.5$) combustion simulation. It can only be used to simulate hydrogen concentration effect in the range of $0.5<\alpha\leq1$.

6.5 Optimization of Hydrogen engine combustion

Since the combustion speed is dependent on turbulence condition and the turbulence is mainly dependent on the injection characteristics, the combustion simulation in hydrogen direct injection engine can be started from the beginning of the injection, rather than from the beginning of intake stroke as in gasoline engine.

After careful research, the general concepts for optimum design on hydrogen engine have been figured out:

(1). Ignition timing

The ignition timing can be optimized in the way that 50% of the mixture has combusted up to 367°CA (7° after TDC)

(2). Compression ratio

Under the strength limit of the engine and the limit of self-ignition, the compression ratio should be as high as possible in order to increase thermal efficiency.

(3). Intake temperature

Intake temperature should be well controlled, mainly for supercharged engine, in order to increase thermal efficiency and power output.

(4) Power control strategy

In order to control NO emission, hydrogen engine should run with lean mixture, and avoid running with middle-high concentration mixture (0.7-0.9). Figure 6-1 gives a rough concept of the control strategy:

- At idle and part load, engine should run with very lean mixture $ø_0$, and throttle adjustment should be used to control engine power output. Since too lean mixture will get very low combustion speed, the recommended value for $ø_0$ should be in the range of 0.3 to 0.5. the actual value of $ø_0$ should be determined by real engine experiment.
- At medium load, mixture concentration should be adjusted in the range of $ø_0$ to 0.7, with wide open throttle. In other words, the power is tuned by varying mixture density.
- At heavy load, engine should run with stoichiometric mixture, and the power is tuned by varying EGR percentage.

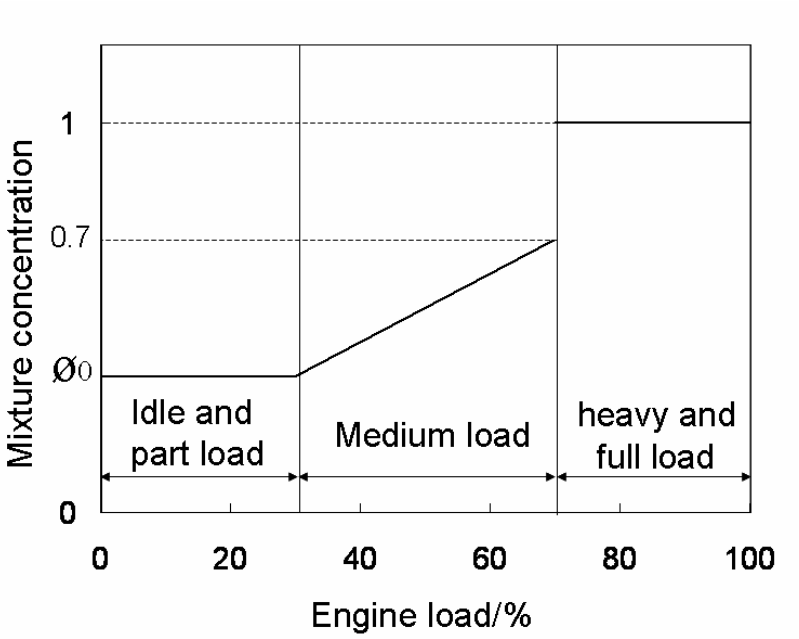

Figure 6-1

Appendix I: Flame Speed Calculation

A1.1 Flame surface radius calculation

A1.1.1 Pyramid Geometry

Figure A-1 shows the flame propagation in spherical vessel. R is the radius of the spherical vessel and r is the radius of the burnt zone. P_b and D_b represent the pressure and density in the burnt zone. P_u and D_u represent the pressure and density in the unburned zone.

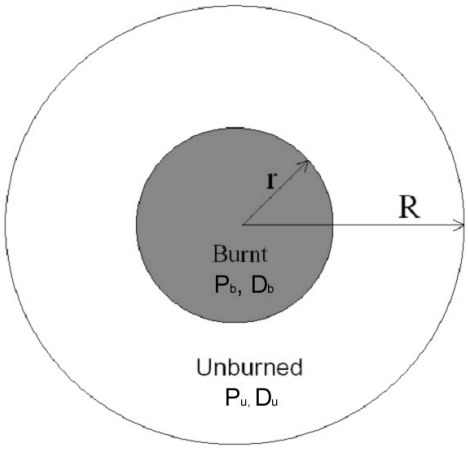

Figure A-1. Diagram for flame radius calculation

The mass of unburned mixture, m_u, is:

$$m_u = D_u \frac{4}{3} p (R^3 - r^3) = D_u V_0 (1 - \frac{r^3}{R^3}) \tag{A-1}$$

Since the Progress variable c is define as:

$$c = \frac{m_{pr}}{m_{pr,\infty}} = \begin{cases} \frac{m_{f,b}}{m_f} \ldots\ldots\ldots\ldots a \le 1 \\ \frac{a \times m_{f,b}}{m_f} \ldots\ldots\ldots a > 1 \end{cases} \tag{A-2}$$

Here,

m_{pr}: mass of combustion products;

$m_{pr,\infty}$: theoretical maximum mass of combustion products;

$m_{f,b}$: mass of burnt fuel;

m_f: mass of total fuel;

V_0: Total volume of the spherical vessel.

α: Fuel equivalence ratio

Formula (A-2) can be reformed as:

$$m_{f,b} = \begin{cases} c \times m_f \ldots\ldots\ldots\ldots a \le 1 \\ c \times m_f / a \ldots\ldots\ldots a > 1 \end{cases} \quad \text{(A-2a)}$$

Or:

$$m_{f,u} = \begin{cases} (1-c) \times m_f \ldots\ldots\ldots\ldots a \le 1 \\ (1-c/a) \times m_f \ldots\ldots\ldots a > 1 \end{cases} \quad \text{(A-2b)}$$

Since:

$$m_T = (a + S) \times m_f \quad \text{(A-3)}$$

Put formula (A-2b) into (A-3):

$$m_u = \begin{cases} m_T \times (1-c) = V_0 D_0 (1-c) \ldots\ldots\ldots\ldots\ldots a \le 1 \\ m_T \times (1-c/a) = V_0 D_0 (1-c/a) \ldots\ldots\ldots a > 1 \end{cases} \quad \text{(A-4)}$$

S: Stoichiometric Air to Fuel ratio

m_T: Total mixture mass

Put formula (A-1) and (A-4) together:

$$(r/R)^3 = \begin{cases} 1-(1-c)\dfrac{D_0}{D_u} \ldots\ldots\ldots\ldots a \le 1 \\ 1-(1-c/a)\dfrac{D_0}{D_u} \ldots\ldots\ldots a > 1 \end{cases} \quad \text{(A-5)}$$

On the assumption that the unburned mixture is compressed with constant entropy, then:

$$D_0/D_u = \left(P_0/P_u\right)^{\frac{1}{k}} \quad \text{(A-6)}$$

Here:

Po: Initial Pressure

Pu: Pressure of unburned mixture

k: isentropic exponent, k=1.4 for H2 and air mixture

Normally, the pressure in the vessel does not vary significantly. In other words, the Pressure in unburned zone (P_u) can be replaced by the mean pressure P_t at time t. Therefore, given the reaction progress and mean pressure, the radius of the flame surface at given time cane be calculated by;

$$r = \begin{cases} R \times \left[1 - (1-c)\left(P_0 / P_t \right)^{\frac{1}{k}} \right]^{\frac{1}{3}} \quad \ldots\ldots\ldots\ldots a \le 1 \\ R \times \left[1 - (1 - c/a)\left(P_0 / P_t \right)^{\frac{1}{k}} \right]^{\frac{1}{3}} \quad \ldots\ldots\ldots a > 1 \end{cases} \tag{A-7}$$

A1.1.2 Cake Geometry

In the similar way, the radius of the flame surface in cake geometry, r_{2D}, can be deduced:

$$r_{2D} = \begin{cases} R \times \left[1 - (1-c)\left(P_0 / P_t \right)^{\frac{1}{k}} \right]^{\frac{1}{2}} \quad \ldots\ldots\ldots\ldots a \le 1 \\ R \times \left[1 - (1 - c/a)\left(P_0 / P_t \right)^{\frac{1}{k}} \right]^{\frac{1}{2}} \quad \ldots\ldots\ldots a > 1 \end{cases} \tag{A-7a}$$

A1.1.3 Rectangle Geometry

The flame surface position in rectangle geometry, x_{1D}, will be:

$$x_{1D} = \begin{cases} L \times \left[1 - (1-c)\left(P_0 / P_t \right)^{\frac{1}{k}} \right] \quad \ldots\ldots\ldots\ldots a \le 1 \\ L \times \left[1 - (1 - c/a)\left(P_0 / P_t \right)^{\frac{1}{k}} \right] \quad \ldots\ldots\ldots a > 1 \end{cases} \tag{A-7b}$$

In formula A-7b, L represents the Length of the geometry.

A1.2 Laminar flame speed calculation

The Laminar burning velocity is defined[1] as the velocity at which unburned gas of given composition, pressure, and temperature flows into a flame in a direction normal to the flame surface.

According to the definition, the laminar burning velocity can be calculated with formula (1)[2]:

$$S_L = \frac{dm_{f,b}/dt}{A_f . r_{f,u}} \tag{A-8}$$

A_f *is* the Area of flame surface

A1.2.1 Pyramid geometry

From formula (A-2a) and (A-3):

$$dm_{f,b}/dt = \begin{cases} \frac{m_T}{(S+a)} dc/dt = \frac{4/3 pR^3 D_0}{S+a} dc/dt \ldots\ldots\ldots a \le 1 \\ \frac{m_T}{a(S+a)} dc/dt = \frac{4/3 pR^3 D_0}{a(S+a)} dc/dt \ldots\ldots\ldots a > 1 \end{cases} \quad \text{(A-9)}$$

Therefore:

$$S_L = \begin{cases} \frac{R^3}{3r^2}\left(\frac{P_0}{P_u}\right)^{\frac{1}{k}} dc/dt \ldots\ldots\ldots\ldots a \le 1 \\ \frac{R^3}{3ar^2}\left(\frac{P_0}{P_u}\right)^{\frac{1}{k}} dc/dt \ldots\ldots\ldots\ldots a > 1 \end{cases} \quad \text{(A-10)}$$

Given Reaction Progress Variable, c, and Pressure of Unburned zone, P_u, the Radius of Flame Surface, r, and Flame Speed, S_L, can be calculated with formula (A-7) and (A-10).

Get derivatives in both sides of Formula (A-5).

$$\frac{3r^2}{R^3} dr/dt = \begin{cases} \frac{D_0}{D_u} dc/dt + \frac{(1-c)}{D_u^2} dD_u/dt \ldots\ldots\ldots\ldots a \le 1 \\ \frac{D_0}{aD_u} dc/dt + \frac{(1-c/a)}{D_u^2} dD_u/dt \ldots\ldots\ldots a > 1 \end{cases}$$

In the spherical vessel, the density variation of unburned zone, $d\rho_u/dt$, is very small when r/R is less than 0.2. In this case, the above equation can be written as:

$$dr/dt = \begin{cases} \frac{R^3}{3r^2}\frac{D_0}{D_u} dc/dt \ldots\ldots\ldots\ldots a \le 1 \\ \frac{R^3}{3r^2}\frac{D_0}{aD_u} dc/dt \ldots\ldots\ldots a > 1 \end{cases} \quad \text{(A-11)}$$

Or:

$$dc/dt = \begin{cases} \frac{3r^2}{R^3}\frac{D_u}{D_o} dr/dt \ldots\ldots\ldots\ldots a \le 1 \\ \frac{3r^2}{R^3}\frac{aD_u}{D_0} dr/dt \ldots\ldots\ldots a > 1 \end{cases} \quad \text{(A-11a)}$$

Put formula (A-11a) and (A-6) into formula (A-10):

$$S_L = \begin{cases} \frac{D_b}{D_u} dr/dt \ldots\ldots\ldots\ldots a \le 1 \\ \frac{D_b}{aD_u} dr/dt \ldots\ldots\ldots\ldots a > 1 \end{cases} \quad \text{(A-10')}$$

With formula (A-7) and (A-10'), the Flame Speed can also be calculated when the density of both burnt zone and unburned zone are given. Formula (A-10') is very useful when the variation of Progress Variable, c, is not smooth (eg: when PDF model is selected).

Formula (A-10') can also be applied for 2D and 1D geometries.

A1.2.2 Cake geometry

$$S_{L,2D} = \begin{cases} \frac{R^2}{2r}\left(\frac{P_0}{P_u}\right)^{\frac{1}{k}} dc/dt \ldots\ldots\ldots\ldots a \le 1 \\ \frac{R^2}{2ar}\left(\frac{P_0}{P_u}\right)^{\frac{1}{k}} dc/dt \ldots\ldots\ldots\ldots a > 1 \end{cases} \quad \text{(A-10b)}$$

A1.2.3 rectangle geometry

$$S_{L,1D} = \begin{cases} L\left(\frac{P_0}{P_u}\right)^{\frac{1}{k}} dc/dt \ldots\ldots\ldots\ldots a \le 1 \\ \frac{L}{a}\left(\frac{P_0}{P_u}\right)^{\frac{1}{k}} dc/dt \ldots\ldots\ldots\ldots a > 1 \end{cases} \quad \text{(A-10c)}$$

---

[1] *Drell I.L. and Heap M.P. "Survey of hydrogen combustion properties". Technical report 1383, NACA, 1957*

[2] *John. B. Heywood, Internal Combustion Engine Fundamental (Chinese Translation by Kaiyuan Tang, Xian Jiaotong University).*

Appendix II: Nomenclature

A_f: area of flame surface
BDC: Bottom Dead Center
c: progress variable
CFM: coherent flame model
CH_4: Methane
CO: Carbon monoxide
CO_2: Carbon Dioxide
$C_{FP:}$ Constant in TFSC Model
C_{fu}, C_{Pr}: empirical coefficients
D_b: mixture density in burnt zone
D_u: mixture density in unburned zone
EGR: exhaust gas recycling
H_2: Hydrogen
H_2O: water
k: isentropic exponent
K_0: initial turbulence kinetic energy
Ka: turbulent Karlovitz number
l_t: turbulent length scale
l_{t0} : initial turbulence length scale
m_f: mass of total fuel
$m_{f,b}$: mass of burnt fuel
m_{pr}: mass of combustion products
$m_{pr,\infty}$: theoretical maximum mass of combustion products
m_T: total mixture mass
m_u: mass of unburned mixture
P: pressure
P_b: pressure in burnt zone
P_o: initial pressure
P_t: mean pressure at time t
P_u: pressure in unburned zone
PDF: probability density function
r: flame radius
R: radius of the spherical vessel

SI:	Spark Ignition
S_L:	laminar flow velocity
S:	stoichiometric air to fuel ratio
S_T:	turbulent burning velocity
t_F:	time scale of the laminar flame
t_k:	Kolmogorov time scale
T:	temperature
T_0:	initial temperature
TDC:	Top Dead Center
TFSC:	turbulence flame speed closure
TKE:	turbulence kinetic energy
V_0:	total volume of the spherical vessel.
x_{1D}:	flame surface position in rectangle geometry
y_{fu}:	fuel mass fraction
y_{Ox}:	oxygen mass fraction;
y_{Pr}:	products mass fraction
$y_{fu,fr}$:	fuel mass fraction in the fresh
ϕ:	fuel equivalence ratio
$\rho_{fu,fr}$:	partial fuel density of the fresh charge
ρ_{fr}:	density of the fresh charge
τ_R:	turbulent mixing time scale
∇y_{fuel}:	fuel mass fraction gradient
ω_L:	mean laminar fuel consumption rate per unit surface along the flame front
ω_{fuel}:	fuel reaction rate
ω_{AI}:	auto-ignition reaction rate
ω_{FP}:	reaction rate of the flame propagation
υ:	characteristic kinematic viscosity
ε:	dissipation rate
δ_L:	laminar flame thickness
u':	turbulence intensity
u_0':	initial turbulence velocity
λ:	air excess
$\overline{rr_{fu}}$:	mean reaction rate

Acknowledgements

In the first place I would like to thank my promoter Prof. Dr.-Ing. Peter Berg for his stimulation and the freedom he gave me to explore the interested subjects. I also thank for his many useful suggestions for improving the thesis. Without his advice and support I could not possibly have achieved as much as I was able to in so short a period of time.

I should express my great appreciations to Dr. Gunther Elsaesser in BMW for his kind help in the CFD study on Hydrogen injection, Dr. Norbert Brehm for his appreciation on my CFD work and gave my the opportunity to carry out the BMW projects, which lead me to enter the Hydrogen engine research field and sponsored me to finished my doctor program.

I appreciate the cooperation with AVL Company and the support from Mr. Ingolf Tiehle Ms. Hongshu and other experts in AVL.

I am particularly grateful to my colleague Mr. Micheal Prinzler for his friendly assistance during my work and live in Cottbus, and my colleagues Mr. Guido Rabe, Mr. Frank Schlag, Mr. Stefan Ahlinda, Mr. Marian Block and Mr. Oleksiy Antoshkiv for their kind help.

Many thanks to my Chinese friends Dr. Jianqi Shen, Dr. Jinsheng Feng, Mr. Feng Liu, Ms. Linbo Zhu, Ms. Haizhen Tian, Mr. Lili Wu, for their help and assistant in my research work.

I want to express my special thanks to my former wife Chunfang Liu and my son Yadong Liu for their understanding, support and encouragement in my struggle in the research work.

At last, please extend my thanks once again, for your continued support and patronage, to all of you!

Resume

28.03.1964	Born in Hebei Province, China
09.1979—05.1986	Study in Department of Vehicle Engineering, Beijing Institute of Technology
07.1983	Bachelor of Science in Engineering
06.1986	Master of Science in Engineering
05.1986—10.2000	Work in the Chair of Internal Combustion Engine, Beijing Institute of Technology
10.2000—12.2003	Work in the Chair of Combustion Engines and Flight Propulsion, Brandenburg Technical University of Cottbus

Reference

R1 Articles

AIAA, 1998. Guide for the Verification and Validation of Computational Fluid Simulations. Published by AIAA.

Alcock, J. L.; Shirvill, L. C.; Cracknell, R. F.: 2001. Compilation of Existing Safety Data on Hydrogen and Comparative Fuels.

Anderson, John D. JR.: 2002. Computational Fluid Dynamics, Tsinghua University Press & McGraw-Hill, Beijing

Appel, Christoph; Mantzaras, John; Schaeren, Rolf; Bombach, Rolf; Inauen, Andreas: 2002. Catalytic Combustion of Hydrogen-Air Mixtures over Platinum: Validation of Hetero/homogeneous Chemical Reaction Schemes, Int. J. of Environmental Combustion Technologies.

AVL Fire, 2002. Species Transport, Version 8.

AVL Fire, 2003. Combustion, Version 8.

AVL Fire, 2003. Primer, Version 8.

AVL Fire, 2003. Theory, Version 8.

Bellona Foundation: 2002. Bellona Report 6:02, Hydrogen-Status and possibilities.

Ben-Yakar, A.; Kamel, M.R.; Morris, C.I.; Hanson, R.K.: 1998. Hypersonic Combustion and Mixing Studies Using Simultaneous OH-PLIF and Schlieren Imaging, AIAA Paper 98-0940, 36th AIAA Aerospace Sciences Meeting and Exhibit, Reno, NV

Ben-Yakar, Adela; Kamel, Michel; Morris, Christopher; Hanson, Ronald K: 1997. Experimental Investigation of H2 Transverse Jet Combustion in Hypervelocity Flows, AIAA Paper 97-3019, 33rd AIAA/ASME/SAE/ASEE Joint Propulsion Conference, Seattle, WA.

Berckmüller, M.; Rottengruber, H.;. Eder, A; Brehm, N.; Elsässer, G.; Müller-Alander, G.; Schwarz, C.: 2003, Potentials of a Charged SI-Hydrogen Engine, SAE2003-01-3210, BMW AG, Advanced Powertrain Development, München, Germany

Blarigan, Peter Van: 2000. Advamced Internal Combustion Engine Research, Sandia National Laboratories, Livermore. Proceedings of the 2000 DOE Hydrogen Program Review, NREL/CP-570-28890.

Bludszuweit, S.; Jungmichel, H.; Buchholz, B.: 1999. Today's Targets & Technologies for Reducing Emissions from Large Marine Diesel Engines, Motor Ship Conference 1999, Athens.

Bombach, R: Hubschmid, W.; Inauen, A.; Käppeli, B.: 2000. Simultaneous Raman and Lif Measurements in a Catalytic Burner. Proceedings 22nd IEA Task Leaders Meeting 2000

Campbell, C. J.; 1996. The Twenty First Century The World's Endowment of Conventional Oil and its Depletion.

Cant, R. S.; Pope, S. B.; Bray, K. N. C.: 1990. Modeling of Flamelet Surface-to-Volume Ratio in Turbulent Premixed Combustion, Twenty-third Symposium on Combustion, France, 1990, pp. 809-816.

Cha, Chong M.: 2002. Transported PDF modeling of turbulent premixed combustion, Center for Turbulence Research, Annual Research Briefs 2002, pp. 77-89.

Cha, Chong M.: 2002. Transported PDF Modeling of Turbulent Premixed Combustion, Center for Turbulence Research, Annual Research Briefs 2002.

Chen, J.-Y.: 1997. Development of Reduced Mechanisms for Numerical Modeling of Turbulent Combustion, Workshop on “Numerical Aspects of Reduction in Chemical Kinetics”, CERMICS-ENPC Cite Descartes - Champus sur Marne, France.

Chen, Jacqueline H.; IM, Hong G.: 1998. Correlation of Flame Speed with Stretch in Turbulent Premised Methane/AIR Flames, Twenty-Seventh Symposium (International) on Combustion/The Combustion Institute, 1998/pp. 819–826.

Choudhuri, Ahsan R.; Gollahalli, S. R.: 2000. Effects of Isothermal Mixing Process on the Stability of Hydrogen-hydrocarbon Blend Turbulent Jet Diffusion Flames, Proceedings of 2000 International Joint Power Generation Conference Miami Beach, Florida.

Chow, A.; Wyszynski M. L.: 1999. Thermodynamic modelling of complete engine systems - a review, Proceedings of the IMechE, Part D: J. Automobile Engineering, 213, D, 403 - 415. ISSN: 0954-4070.

Cosner, Raymond R.: 2001. The AIAA Committee on Standards for CFD, Presented at the QNET-CFD Conference Athens, Greece May 10-11, 2001.

Cuenot, B.; Egolfopoulos, F.N.; Poinsot, T.: 1999. Direct Numerical Simulation of Stagnation-Flow Premixed Flames: Transition from Planar to Bunsen Flames and the Direct Measurement of Laminar Flame Speeds, In Institute The Combustion, editor, Western Section States Fall Meeting, Irvine, USA.

Daw, C. S.; Kennel, M. B.; Finney, C. E. A.; Connolly, F. T.; 1998. Observing and modeling nonlinear dynamics in an internal combustion engine, Physical Review, March 1998 Volume 57, Number 3.

Daw, C.S.; Finney, C.E.A.; Kennel, M.B.; Connolly, F.T.; 1997. Cycle-by-

Cycle Combustion Variations in Spark-Ignited Engines. Proceedings of the Fourth Experimental Chaos Conference, Boca Raton, Florida USA, ISBN 981-02-3743-X: 329-340.

De Lataillade, A.; Dabireau, F.; Cuenot, B.; Poinsot T.: 2002. Flame / wall interaction and maximum wall heat fluxes in diffusion burners, In 29th Symp. (Int) on Combustion, Saporo, Japan, 2002. The Combustion Institute.

DeCicco, John M.: 2003. Systems Analysis of Low CO2 Emission Designs for Cars and Light Trucks, Environmental Defense, California Air Resources Board International Vehicle Technology Symposium Sacramento

Dowdy, David R.; Smith, David B.; Taylor, Simon C.; Williams, Alan: 1990. The Use of Expanding Spherical Flames to Determine Burning Velocities and Stretch Effects in Hydrogen/Air Mixtures, Twenty-third Symposium on Combustion, France, 1990, pp. 325-332.

Drell, Isadore L.; Belles, Frank E.: 1958. Survey of Hydrogen Combustion Properties, report 1383, Supersedes NACA Research Memorandum E57D24.

Dunn, Seth: 2000. The Hydrogen Experiment, WORLD WATCH Magazine, November/December 2000.

Ec¸ a L.; Hoekstra M.: 2000. On the Application of Verification Procedures in Computational Fluid Dynamics. 2nd MARNET workshop, Kopenhagen.

Ec¸ a L.; Hoekstra M.: 2001. On the Application of the Moment Error Estimate to Error quantification in CFD. 3rd Marnet-CFD Workshop, Creete.

Edmondson, Harry; Heap, Michael Peter: 1971. The Burning Velocity of Hydrogen-Air Flames, Combustion and Flame, 16, 161-165.

Egolfopoulos, F. N.; Law, C. K.: 1990. An Experimental and Computational Study of the Burning Rates of Ultra-lean to Moderately-rich H2/O2/N2 Laminar Flames with Pressure Variations, Twenty-third Symposium on Combustion, France, 1990, pp. 333-340.

Fissore, Davide; Marchisio, Daniele L.; Barresi, Antonello A.: 2002. On the Comparison between Probability Density Function Models for CFD Applications, The Canadian Journal of Chemical Engineering, Volume 80, August 2002.

Floyd, J.E.; Baum, H.R.; McGrattan, K.B.: 2001. A Mixture Fraction Combustion Model for Fire Simulation Using CFD, International Conference on Engineered Fire Protection Design. Proceedings. June 11 – June 15, 2001, San Francisco, CA. Society of Fire Protection, Engineers, Bethesda, MD, pp279-290

Gitay, Habiba; Suarez, Avelino; Watson, Robert T.; 2002. Climate Change and Biodiversity, Intergovernmental Panel on Climate Change.

Golovichev, V.I.: 2001. Revising “Old” Good Models: Detailed Chemistry

Spray Combustion Modeling Based on Eddy Dissipation Concept, Paper presented at the 5th International Conference “Internal Combustion Engines” Capri-Naples, Italy.

Gülder, Ö. L.; Smallwood, G. J.; Wong, R.; Snelling, D. R.; Smith, R.; Deschamps, B.M.; Sautet, J. –C.: 2000. Flame Front Surface Characteristics in Turbulent Premixed Propane/Air Combustion, Combustion and Flame 120: pp407-416.

Haworth, D. C.: 2000. A probability density function/flamelet method for partially premixed turbulent combustion, Center for Turbulence Research, Proceedings of the Summer Program 2000.

Heywood, J.B. (translated by Tang, Kaiyuan): 1992. Internal Combustion Engine Fundamental (Chinese Version), McGraw-Hill, ISBN: 007028637X

Hirasawa, T.; Sung, C. J.; Joshi, A.; Yang, Z.; Wang, H.; Law, C. K.: 2002. Determination of Laminar Flame Speeds Using Digital Particle Image Velocimetry: Binary Fuel Blends of Ethylene, n-Butane, and Toluene, twenty-Ninth Symposium (International) on Combustion and for publication in the Proceedings of the Combustion Institute, Volume 29.

Hyslop, P.; Gaston, M.J.; Houwing, A.F.P.: 1999. Computational fluid dynamical modelling of supersonic combustion and comparisons with experiments in a free piston shock tunnel, Japanese Symposium on Shock Waves, Aoyama Gakuin University, Tokyo.

Ierardi, James A.: 1999. A Computer Model of Fire Spread from Engine to Passenger Compartments in Post-Collision Vehicles, A Thesis Submitted to the Faculty of the Worcester Polytechnic Institute in partial fulfillment of the requirements for the Degree of Master of Science in Fire Protection Engineering.

Igot, Forsythia: 2002. Internal Combustion Engine versus the Hydrogen Fuel Cell, Montgomery College Student Journal of Science & Mathematics, Volume 1 September 2002.

IM, Hong G.; Chen, Jacqueline H.: 2000. Effects of Flow Transients on the Burning Velocity of Laminar Hydrogen/ Air Premixed Flames, Proceedings of the Combustion Institute, Volume 28, 2000/pp. 1833-1840.

IPCC Report, Climate Change 2001, 2001.

IPCC Report, Climate Change 2002, 2002.

Javoy, S.; Naudet, V.; Abid, S.; Paillard, C.E.: 2002. Elementary Reaction Rate Constants of Interest in H2 Supersonic Combustion by ARAS, AIAA-2002-5246.

Johnson, Norman L.: 1997. Review of Numerical Methods, CFD 97- Fifth

Annual Conference of the Computational Fluid Dynamics Society of Canada, University of Victoria.

Kailasanath, K.; Boris, E. Oran ad J.: 1982. A Theoretical Study of the Ignition of Premixed Gases, Combustion and Flame 47: pp173-190.

Kamienski, Paul; Kaldor, Andrew: 2002. Current Fuels and Advanced Fuel - Vehicle Systems, Interfaces 2002, Budapest, Hungary.

Kaneko, Makoto; Morikawa, Koji; Itoh, Jin; Saishu, Youhei: 2001. Study on Homogeneous Charge Compression Ignition Gasoline Engine, The Fifth International Symposium on Diagnostics and Modeling of Combustion in Internal Combustion Engines (COMODIA), Nagoya.

Kemp, René: 2002. Zero Emission Vehicle Mandate in California. Misguided Policy or Example of Enlightened Leadership? Paper submitted for publication in Environment and Planning C: Government and Policy, MERIT and TNO-STB.

Kruse, Bjørnar; Grinna, Sondre; Buch, Cato, 2002. Hydrogen, Published by The Bellona Foundation.

Kumar, R.K.; Koroll, G.W.; Heitsch, M.; Studer, E.: 2000. Carbon Monoxide – Hydrogen Combustion Characteristics in Severe Accident Containment Conditions, Final report, Nuclear Energy Agency Committee on the Safety of Nuclear Installations, NEA/CSNI/R(2000)10.

KUWAHARA, Kazunari: 2003. In-Cylinder Phenomena Diagnostics for Gasoline Engine Development, Technical Review, 2003, No. 15

Kyritsis, Dimitrios C.; Santoro, Vito S.; Gomez, Alessandro: 2002. Quantitative Scalar Dissipation Rate Measurements in Vortex Perturbed Counterflow diffusion Flames, Twenty-Ninth Symposium (International) on Combustion, Sapporo, Japan.

Lanz, Andre; Eng. P.; Heffel, James; Messer, Colin: 2001. Hydrogen Fuel Cell Engines and Related Technologies, College of the Desert, Palm Desert, CA, USA.

Lee, J. T.; Kim, Y. Y.; Lee, C. W.; Caton, J. A.: 2002. An Investigation of a Cause of Backfire and Its Control Due to Crevice Volumes in a Hydrogen Fueled Engine, ASME JOURNAL OF ENGINEERING FOR GAS TURBINES AND POWER, Vol. 123, JANUARY 2001, pp. 204-210.

Leuckel, W.; Nastoll, W.; Zarzalis, N.: 1990. Experimental Investigation of the Influence of Turbulence on the Transient Premixed Flame Propagation Inside Closed Vessels, Twenty-third Symposium on Combustion, France, 1990, pp. 729-734.

Li, G.; Sapsford, S.M.; 2000. CFD Simulation of HSDI Engine Combustion

Using VECTIS, Ricardo Consulting Engineer’s Ltd., Shoreham-by-Sea, UK.

Lipatnikov, Andrei N.; Chomiak, Jerzy: 2003. Premixed Turbulent Flame Theory and Simulations of Combustion in SI Engines:Connection, Discrepanies, and Practical Solusion, 13th International Multidimensional Engine Modeling User's Group Meeting.

Louch, D. S.: 1999. Progress towards a large eddy simulation of premixed turbulent combustion in stagnating turbulence, Center for Turbulence Research, Annual Research Briefs 1999, pp. 109-128.

Luo, Tiqian; Cheng, Zhaoxue: 1999. Fluid Dynamics (in Chinese), CMP, Beijing.

Marinov, N.M.; Westbrook, C.K.; Pitz, W.J.: 1996. Detailed and Global Chemical Kinetics Model for Hydrogen, in Transport Phenomena in Combustion, Volume 1 (SH Chan, edited), Talyor and Francis, Washington, DC.

Mayer, Harald F.; Tabatabai, Behnam: 1993. Visualizing Results of Transient Flow Simulations, Proceedings of IEEE Visualization ´93, pp. 406-409, IEEE Computer Society Press.

Mosbacher, D.; Wehrmeyer, J.; Pitz, R. Sung, C. –J.; Byrd J.; 2002. Experimental and Numerical Investigation of Premixed Cylindrical Flames, AIAA 2002-0481.

Mott, David R.; Oran, Elaine S.: CHEMEQ2, 2001. A Solver for the Stiff Ordinary Differential Equations of Chemical Kinetics, Naval Research Laboratory, NRL/MR/6400—01-8553.

National Energy Policy Development Group: 2002. Reliable, Affordable, and Environmentally Sound Energy for America’s Future, ISBN 0-16-050814-2.

Nelson, E. M.; Eppley, K. R.; Petillo, J. J.; Levush, B.: 2001. Particle Tracking on Unstructured Grids, Proceedings of the 2001 Particle Accelerator Conference, Chicago.

Njapha, Delani; Neomagus, Hein; Everson, Raymond: 2002. The determination of the kinetics of combustion and gasification of low-ranked South-African coal using a thermogramivetric analyzer, Poster presentation at the 5th European gasification conference.

Oberkampf, William L.; Trucano, Timothy G.: 2002. Verification and Validation in Computational Fluid Dynamics, SANDIA REPORT SAND2002-0529, Unlimited Release Printed March 2002.

Oberkampf, William L.; Trucano, Timothy G.; Hirsch, Charles: 2002. Verification, validation, and Predictive Capability in Computational Engineering and Physics, Foundations for Verification and Validation in the 21st Century Workshop, Johns Hopkins University/Applied Physics Laboratory Laurel,

Maryland.

Ogink, Roy; Golovitchev, Valeri: 2002. Gasoline HCCI Modeling: An Engine Cycle Simulation Code with a Multi-Zone Combustion Model, Licentiate Thesis, Chalmers University of Technology, Gothenburg, Sweden.

Partanen, Jatta: 2003. Modelling of Combustion Processes, Final Report, Technology Programme Report 4/2003, Helsinki.

Peterson, Eric L.: 1999. The effect of Aerators on the Benthic Shear Stress in a Pond, PhD Thesis, , James Cook University, Australia, p228.

Pischinger, Stefan; Heywood, John: 1990. A model for Flame Kernel Development in a Spark-ignition Engine, 23rd Symposium on Combustion, pp. 1033-1040.

Plessing, T.; Kortschik, C.; Peters, N.; Mansour, M. S.; Cheng, R. K.: 2000. Measurements of the Turbulent Burning Velocity and the Structure of Premixed Flames on a Low-swirl Burner, Proceedings of the Combustion Institute, Volume 28, 2000, pp. 359-366.

Pointsot, T.; Veynante, D.; Candel, S.: 1990. Diagrams of Premixed Turbulent Combustion Based on Direct Simulation, Twenty-third Symposium on Combustion, France, 1990, pp. 613-620.

Poorman, Hezbert R.: 1953. Some Experimental Studies of Laminar Burning Velocity, in partial fulfillment of the requirements for the Degree of Aeronautical Engineer, California Institute of Technology

Pope, S. B.: 1985. PDF Methods for Turbulent Research Flows, Sibley School of Mechanical and Aerospace Engineering, Cornell University, Ithaca, U.S.A., Prog. Energy Combust. Sci. 1985, Vol, pp. 119-192.

Pope, S. B.: 1990. Computations of Turbulent Combustion: Progress and Challenges, Twenty-third Symposium on Combustion, France, 1990, pp. 591-612.

Prechtl, P.; Mayinger, F.; Zeilinger, K.; Woschni, G.; Vogel, C.: 2000. Directly Injecting Hydrogen Diesel Engine Development of a new combustion process, 4. Internationales Symposium für Verbrennungsdiagnostik.

Preschern, Horst; Engeljehringer, Kurt: 2001. Traffic, Transportation and Environment, Emission Legislation and Test System Requirements, AVL LIST GmbH.

Priesching, P.; Wanker, R.; Cartellieri, P.; Tatschl, R.: 2003. Detailed and Reduced Chemistry CFD Modeling of Premixed Charge Compression Ignition, Engine Combustion International Multidimensional Engine Modeling User's Group Meeting 2003, Advanced Simulation Technologies, AVL List GmbH, A-8020 Graz, Austria.

Rahim, Faranak: 2002. Determination of Burning Speed for Methane/ Oxidizer/Diluent Mixtures, A Thesis Presented to The Department of Mechanical, Industrial and Manufacturing Engineering in partial fulfilment of the requirements for the degree of Doctor of Philosophy In the field of Mechanical Engineering, Northeastern University, Boston, Massachusetts, May 2002.

Rehm, Werner: 2001. Innovative CFD Methoden für Studien zur Wasserstoff-Sicherheit mit High-Performance Supercomputing (HPSC) - Weiterentwicklung, Validierung und Performance Analyse, Juli 2001, Kurzfassungsbericht über EU/HGF-CFD/DDT Projekte, Shaker Verlag.

Renou, B.; Boukhalfa, A.; Puechberty, D.; Trinite M.: 1999. Experimental Study of Freely-propagating Premixed Low-turbulent Flame Response to Local Stretch Influence of Lewis Numbers, Soumis pour le 17th Int. Colloquium on the Dynamic of Explosions and Reactive Systems (ICDERS), Heidelberg, Allemagne, 25-30 juillet 1999.

Ronney, Paul D.; Wu, Ming-Shin; Pearlman, Howard G.; Weiland, Karen J.: 1998. Structure of Flame Balls at Low Lewis-number (SOFBALL): Preliminary Results from the STS-83 Space Flight Experiments, AIAA Journal, Vol. 36, pp. 1361-1368, 1998.

Rottengruber, Hermann; Wiebicke, Ulrich; Woschni, Gerhard; Zeilinger, Klaus: 2000. Hydrogen Diesel Engine with Direct Injection, High Power Density and Low Exhaust Gas Emissions, Part 3: Engine Testing and Calculations, MTZ Motortechnische Zeitschrift 61.

Rutland, C. J.; Ferziger J.H.; El Tahry, S. H.: 1990. Full Numerical Simulation and Modeling of Turbulent Premixed Flames, Twenty-third Symposium on Combustion, France, 1990, pp. 621-628.

Shamim, T.: 2002. Effect of Lewis Number on Radiative Extinction and Flamelet Modeling. Proceedings of the Meeting of the Central States Section of the Combustion Institute, Knoxville, TN.

Sierens, R.; Verhelst, S.: 2001. Experimental Study of a Hydrogen-Fueled Engine, Journal of Engineering for Gas Turbines and Power, January 2001, Vol.123, pp. 211-216.

Simmie, John M.: 2003. Detailed chemical kinetic models for the combustion of hydrocarbon fuels, Progress in Energy and Combustion, SCIENCE 2003, 29:6, pp. 599-634.

Singhal, Ashok K.: 2000. An Industrial Perspective on Modern Trends in Heat Transfer, Lectures/Seminars Presented at Pan American Advanced Studies Institute Universidad Autónoma de San Luis Potosí San Luis Potosí, SLP, Mexico.

Sjöberg, Magnus: 2001. The Rotating Injector as a Tool for Exploring DI Diesel Combustion and Emissions Formation Processes, Doctoral Thesis Department of Machine Design, Royal Institute of Technology, SE-100 44 Stockholm, Sweden.

Sone, Kazuo: 2001. Unsteady Simulations of Mixing and Combustion in Internal Combustion Engines, In Partial Fulfillment of the Requirements for the Degree Master of Science in Aerospace Engineering, Georgia Institute of Technology.

Soyhan, H.S.; Løvås, T.; Mauss, F., 2001. A Stochastic Simulation of an HCCI\ Engine using an Automatically Reduced Mechanism, 2001-ICE-416, ICE-Vol. 37-2, 2001 Fall Technical Conference, ASME.

Spalding, D. B.: 1979. Combustion and Mass Transfer, translated into Chinese by Chang Hongzhe, Zhang lianfang, etc. National Defense Industry Press, China.

Steiger A.; Gonzalo A. B.; Grützmacher K.; Rosa M. I.; Steiger M., 2001. Mapping of the Atomic Hydrogen Density in Combustion Processes at Atmospheric Pressure by two-Photon Polarization Spectroscopy. AIP Conference Proceedings Vol 559(1), pp. 199-201.

Stephenson, P. L.; Taylor, R. G.: 1973. Laminar Flame Propagation in Hydrogen, Oxygen, Nitrogen Mixtures, Combustion and Flame 20, pp. 231-244.

Stern, Fred; Wilson, Robert V.; Coleman, Hugh W.; Paterso, Eric G.; 1999. Verification and Validation Of CFD Simulations, IIHR Report No. 407, Iowa Institute of Hydraulic Research College of Engineering, The University of Iowa.

Tagalian, Joel; Heywood, John B.: 1986. Flame Initiation in a Spark-Ignition Engine, Combustion and Flame 64, pp.243-246.

Taut, C.; Correa, C.; Deutschmann, O.; Warnatz, J.; Einecke, S.; Schulz C.; Wolfrum, J.; 2000. Three-dimensional Modelling with Monte Carlo-parobability Density Function Methods and Laser Diagnostics of the Combustion in a Two-stroke Engine, Interdisziplinäres Zentrum für Wissenschaftliches Rechnen, Physikalisch-Chemisiches Institut Universität Heidelberg, Proceedings of the Combustion Institute, Volume 28, 2000, pp. 1153-1159.

Trautwein, S. E.; Grudno, A.; Adomeit, G.: 1990. The Influence of Turbulence Intensity and Laminar Flame Speed on Turbulent Flame Propagation Under Engine Like Conditions, Twenty-third Symposium on Combustion, France, pp. 723-728.

Verhelst, Sebastian; Sierens, Roger: 2003. A Laminar Burning Velocity Correlation for Hydrogen/Air Mixtures Valid at Spark-ignition Engine Conditions, Proceedings of ICES03, 2003 Spring Technical Conference of the ASME Internal Combustion Engine Division, Salzburg, Austria.

Wang, B.L.; Rehm, W.: 2001. Numerical Studies of Shock Reflection and Ignition, Proc. Intern. Conference on Explosions and Dynamics, Seattle, USA

Weller, H. G.; Marooney, C. J.; Gosman, A. D.: 1990. A New Spectral Method for Calculation of the Time-Varying Area of a Laminar Flame in Homogeneous Turbulence, Twenty-third Symposium on Combustion, France, 1990, pp. 629-636.

Wenzel, Holger: 1998. Direct numerical simulation of the G-equation in the laminar amelet and the thin reaction zone regime, 7th International Conference on Numerical Combustion, York 30th March - 1st April 1998

Wierse, Monika; Echtle, Harald; Gosman, A. David: 1999. Internal Combustion Engines on MPP. Fifth European SGI/Cray MPP Workshop, Bologna, Italy.

Yu, G.; Li, J. G.; Chang, X. Y.; Chen, L.H.; Sung, C.J.; 2001. Investigation of Kerosene Combustion Characteristics with Pilot Hydrogen in Model Supersonic Combustors. Journal of Propulsion and Power 17 (6), pp. 1263-1272.

Zabetta, E. Coda; Kilpinen, P.; Pokela, H.: 2002. CFD Testing of an Improved Model for Simulating NOx in Internal Combustion Engines, in Åbo Akademi Process Chemistry Group series, ISSN 1457-7895, Report 02-1, ISBN 952-12-0971-2, Åbo Akademis tryckeri, Turku, Finland.

Zepter, Klaus; Hustad, Johan E.: 2001. Combustion and Emission Studies, in a Porous Inert Media Burner, 1st Biennial Meeting of the Scandinavian-Nordic Section of the Combustion Institute, Gothenburg, April 2001

Zhou, Longbao; Liu, Yijun; Gao, Zongying: 1999. Internal Combustion Engine (in Chinese), CMP, Beijing.

R2 Websites

http://www.druglibrary.org/schaffer/Misc/driving/s1p4.htm (Transportation and Society - The Role of Values)

http://www.hydrogen.org/Wissen/pdf/ireland2002.pdf (The prospects for a hydrogen economy based on renewable energy)

http://library.iea.org/dbtw-wpd/textbase/nppdf/free/2000/weo2000.pdf (World energy outlook 2000)

http://h50146.www5.hp.com/solutions/ crossindustry/hptc/pdfs/auto2.pdf (High Performance Computing in European Manufacturing: Status and Trends.)

http://my.dreamwiz.com/sungbhan/ (Heat Engine Laboratory, Induk Institute of Technology)

http:// www.iea.org (International Energy Agency)

http://ca-homes.com/science/tsuge-8/node1.html (Shunichi Tsugé: The Kolmogorov turbulence theory in the light of six-dimensional Navier-Stokes'

equation)

http://geography.uoregon.edu/shinker/geog101/lectures/lec02/lec02_figs/human-caused-air-pollution-and-sources-fig3-10.gif

http://gtalumni.org/StayInformed/magazine/fall91/hydrogen.html (James E. Kloeppel: A New Hydrogen Economy?)

http://people.hofstra.edu/geotrans/eng/ch8en/conc8en/ch8c2en.html (Transportation and Energy)

http://students.bath.ac.uk/en1wros/Government.htm

http://www.bellona.no/en/energy/hydrogen/report_6-2002/22852.html (Hydrogen technologies)

http://www.druglibrary.org/schaffer/Misc/driving/s1p4.htm (Patricia F. Waller: Transportation and Society - The Role of Values)

http://www.dwv-info.de/indexe.htm (German Hydrogen Association)

http://www.ford.com/en/innovation/engineFuelTechnology/hydrogenInternalCombustion.htm (Hydrogen Internal Combustion)

http://www.fortunecity.com/silverstone/lancia/58/article/tech_history/tech_history.htm (Technology development during the past 100 years Technology development during the past 100 years)

http://www.grc.nasa.gov/WWW/wind/valid/homepage.html (NPARC Alliance, CFD Verification & Validation)

http://www.isanet.org/noarchive/softing.html (Guri Bang Softing: Climate Change Policymaking in Germany and the USA)

http://www.mpcfaculty.net/mark_bishop/combustion_analysis.htm (Obtaining Empirical and Molecular Formulas from Combustion Data)

http://www.oilcrisis.com/,(The Coming Global Oil Crisis)

http://www.ott.doe.gov/otu/field_ops/hydrogen_class.html

http://www.ovl.co.uk/tax_company2.htm(Data for this graph come from Tax Issues - Reform of Company Car Tax)

http://www.rmi.org/images/other/HCSynArt-Hydrogen_Nov01.pdf (Hydrogen The ultimate clean fuel of the future)